July 2021

Neuromuscular Control Strategy during Object Transport while Walking: Adaptive Integration of Upper and Lower Limb Movements

Ahyoung Song

NEUROMUSCULAR CONTROL STRATEGY DURING OBJECT TRANSPORT WHILE WALKING: ADAPTIVE INTEGRATION OF UPPER AND LOWER LIMB MOVEMENTS

A Dissertation

Submitted to the Graduate Faculty of the
Louisiana State University and
Agricultural and Mechanical College
in partial fulfillment of the
requirements for the degree of
Doctor of Philosophy

in

The School of Kinesiology

by
Ahyoung Song
B.Sc. Korea University 2010
M.Sc. Korea University 2012
August 2021

ACKNOWLEDGEMENTS

To my advisors, Dr. Nikita A. Kuznetsov and Dr. Michael J. MacLellan, I would like to express my deepest appreciation from the bottom of my heart. Thanks for their guidance and support during my studies in the School of Kinesiology at Louisiana State University. Without their persistent help, this dissertation would not have been possible. Thank you for always pushing me to be a better researcher. I would like to thank Dr. Sara A. Winges (at the University of Northern Colorado) for being my co-advisor for the first two years and providing a valuable mentorship for my career.

I would like to thank my committee members, Dr. Jan M. Hondzinski, Dr. Todd Monroe, and Dr. Laura H. Ikuma; their constructive feedbacks and comments throughout my dissertation have always inspired me to improve myself as a researcher. I would like to thank professors in the Kinesiology department, Dr. Arend Van Gemmert, Dr. Marc Dalecki, and Dr. Emily Marcinowski.

I would like to thank my parents and friends at LSU, Erika Garcia Mora, Marcelline Dechenaud, Shijun Yan, Eunhan Cho, Matthew Yeomans, Reuben N. Addison, for their encouragement and support. I also would like to thank Zheng Wang, Charlend K Howard, and Kelley Burger for their help during my last semester. Without their help, it would not have been possible to finish my last study. I thank all undergraduate students at LSU who helped with my data collection.

Lastly, I thank the School of Kinesiology and College of Human Sciences and Education for providing funding support through a department assistantship. I would like to thank Ellen Albarado, Darlene Ainsworth, Donna Smith, and Ellen Cummings for always kindly helping me with administrative works.

TABLE OF CONTENTS

LIST OF TABLES

LIST OF FIGURES

LIST OF NOMENCLATURE

3D: Three-dimensional

AD: Anterior Deltoid

ANOVA: Analysis of Variance

AP: Anterior-posterior

BALL LF: Holding a cup with a ball while looking forward

BALL LO: Holding a cup with a ball while looking at the cup and a ball

BB: Biceps Brachii

BOS: Base of Support

BR: Brachioradialis

BW: Body Weight

CA: Coupling Angle

CNS: Central Nervous System

CoG: Center of Gravity

CoM: Center of Mass

CPG: Central Pattern Generator

D-NOBJ: Dominant arm-positioning without an object

D-OBJ: Holding an object in the dominant arm

DOF: Degrees of Freedom

DP: Distal Phalanx

DR: Damping Ratio

ECU: Extensor Carpi Ulnaris

EDC: Extensor Digitorum Communis

EDL: Extensor Digitorum Longus

EHL: Extensor Hallucis Longus

EMG: Electromyography

FCR: Flexor Carpi Radialis

FDS: Flexor Digitorum Superficialis

GF: Grip Force

GM: Gastrocnemius

GRF: Ground Reaction Force

GTO: Golgi Tendon Organ

HF: Horizontal Force

IC: Initial Contact

IF: Inertial Force

ISW: Initial Swing

LD: Latissimus Dorsi

LF: Load Force

LR: Loading Response

MCP: Metacarpophalangeal

MEP: Motor Evoked Potentials

ML: Mediolateral

MLR: Mesencephalic Locomotor Region

MST: Mid-stance

MSW: Mid-swing

MVC: Maximal Voluntary Contraction

ND-NOBJ: Non-dominant arm-positioning without an object

ND-OBJ: Holding an object in the non-dominant arm

NNMF: Non-negative Matrix Factorization

NOBALL LF: Holding a cup while looking forward

NOBALL LO: Holding a cup while looking at the cup

PCA: Principal Component Analysis

PD: Posterior Deltoid

PM: Pectoralis Major

PSW: Pre-swing

PT: Peroneus Tertius

RMSE: Residual Mean Square Error

SCI: Spinal Cord Injury

SD: Standard Deviation

SICI: Short-latency Intracortical Inhibition

SLR: Subthalamic Locomotor Region

SLS: Single Limb Support

SSE: Sum of Squared Errors

SST: Total Sum of Squares

SYN: Synergy

TA: Tibialis Anterior

TB: Triceps Brachii

TMS: Transcranial Magnetic Stimulation

TRAP: Trapezius

TST: Terminal Stance

TSW: Terminal Swing

TW: Treadmill walking without any object or instructed arm-positioning

UCM: Uncontrolled manifold

VAF: Variance Accounted for

WA: Weight Acceptance

ABSTRACT

When carrying an object while walking, a significant challenge for the central nervous system (CNS) is to preserve the object's stability against the inter-segmental interaction torques and ground reaction forces. Studies documented several strategies used by the CNS: modulation of grip force (GF), alterations in upper limb kinematics, and gait adaptations. However, the question of how the CNS organizes the multi-segmental joint and muscle coordination patterns to deal with gait-induced perturbations remains poorly understood. This dissertation aimed to explore the neuromuscular control strategy utilized by the CNS to transport an object during walking successfully. Study 1 examined the inter-limb coordination patterns of the upper limbs when carrying a cylinder-shaped object while walking on a treadmill. It was predicted that transporting an object in one hand would affect the movement pattern of the contralateral arm to maintain the overall angular momentum. The results showed that transporting an object caused a decreased anti-phase coordination, but it did not induce significant kinematic and muscle activation changes in the unconstrained arm. Study 2 examined muscle synergy patterns for upper limb damping behavior by using non-negative matrix factorization (NNMF) method. Four synergies were identified, showing a proximal-to-distal pattern of activation preceding heel contacts. Study 3 examined the effect of different precision demands (carrying a cup with or without a ball) and altered visual information (looking forward vs. looking at an object) on the upper limb damping behavior and muscle synergies. Increasing precision demand induced stronger damping behavior and increased the electromyography (EMG) activation of wrist/hand flexors and extensors. The NNMF results replicated Study 2 in that the stabilization of proximal joints occurred before the distal joints. The results indicated that the damping incorporates tonic and phasic muscle activation to ensure object stabilization. Overall, three experiments showed that the CNS adopts a similar

synergy pattern regardless of task constraint or altered gaze direction while modulating the amount of muscle activation for object stabilization. Kinematic changes can differ depending on the different levels of constraint, as shown in the smaller movement amplitude of the shoulder joint in the transverse plane during the task with higher precision demand.

CHAPTER 1. INTRODUCTION

Walking while transporting a grasped object is one of the most common dexterous tasks individuals perform every day, such as when carrying a cup of coffee, a cell phone, or a bag of groceries. A significant challenge for the central nervous system (CNS) in this task is to preserve the grasped object's stability when it is perturbed by the inter-segmental interaction torques and reaction forces arising from the interaction of the foot and the ground. One may question how the CNS organizes the multi-segmental joint and muscle coordination patterns to deal with gait-induced perturbations?

Previous studies have reported that predictive and continuous control of grip force (GF) is required to counterbalance gait-induced inertial forces (IFs) throughout the gait cycle (Diermayr et al., 2008; Gysin et al., 2003a; Gysin et al., 2008). In addition to maintaining a secure grasp through the anticipatory adjustment of GF on the transported object, synchronized vertical displacement of the trunk and transported object achieved by coordinated movement of upper limb contributes to upper limb damping behavior to maintain the stability of the carried object (Gysin et al., 2003a).

However, previous studies on object transport tasks during walking mainly focused on the kinematic aspects of object transport and emphasized GF kinetics. Little is known how the CNS coordinates upper limb movements and muscle activations in object transport tasks while walking, which contribute significantly to the observed kinematics and kinetics. Therefore, this dissertation aimed to evaluate how healthy young adults integrate their upper limb movements into their walking patterns while carrying objects in hand using kinematic and muscle activation analyses. Three studies were conducted for this dissertation. Study 1 examines the kinematic patterns of arm swing coordination during object transport. Study 2 identifies the neuromuscular strategy in terms

of muscle synergies formed across major upper limb muscles involved for object stabilization during object transport while walking. Study 3 examines the effect of different levels of task constraints and relative contributions of visual information (central vs. peripheral) to object stabilization and upper limb muscle synergies. Altogether, these studies explain how CNS coordinates the interaction between upper limbs and regulates muscular activations to perform this asymmetrical and functional task of carrying an object in one hand while walking. This dissertation provides a foundation and reference data for future studies on characterizing muscle synergies underlying upper limb control during object transport in populations with neurological pathologies that affect muscle function.

CHAPTER 2. REVIEW OF RELEVANT LITERATURE

BIOMECHANICS OF HUMAN LOCOMOTION

Definition of gait and gait cycle

Walking is one of the most basic forms of human locomotion in which the alternating of two lower limbs provides both support and propulsion. Upright bipedal walking is the most common human locomotion method, characterized by a repeating and continuous sequence of limb movements through complex neural control to translate the body forward (Perry & Burnfield, 2010; Saunders et al., 1953). The term 'gait' in the literature refers typically to the pattern or manner of walking during which the displacement of the center of gravity (CoG) occurs, resulting in a transfer of the body from one position to the other (Perry & Burnfield, 2010; Schiehlen & García-Vallejo, 2011). The gait cycle is defined as a set of repeatable sequences of joint angle variation and muscle activity within one stride of the same limb. Although any gait event can be utilized, heel strike is generally selected to define the start of the gait cycle. A typical gait cycle can be divided into two main periods based on lower limbs' motions: stance and swing (Figure 2.1). The stance phase occurs when the reference foot is in contact with the ground, while the swing phase describes the period when the reference foot is airborne in preparation for the next foot contact. Stance phase accounts for approximately 62 % of a normal gait cycle (Ayyappa, 1997) and is mainly responsible for weight acceptance (WA) and single limb support (SLS). The stance phase can be subdivided into three separate phases: two double limb supports and one single-limb support. Double limb support, when both feet are in contact with the ground, occurs at the beginning and end of the stance phase. Single-limb stance occurs when only one foot is in contact with the ground between

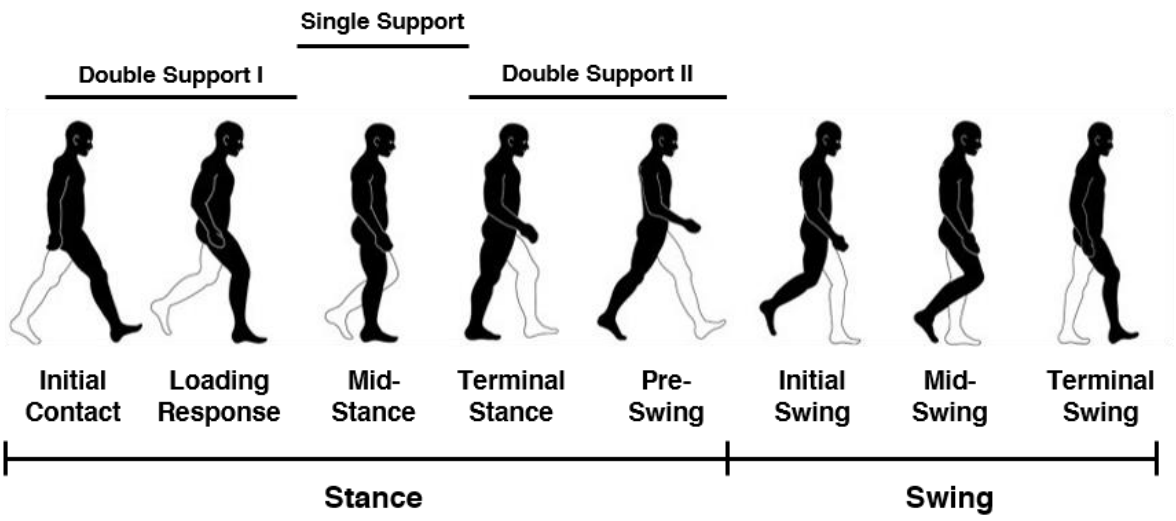

Figure 2.1. Classification of the gait cycle (adapted from Perry & Burnfield, 2010).

double limb support phases. And these three phases can be further divided into five functional sub-phases in the following sequences: initial contact (IC), loading response (LR), mid-stance (MST), terminal stance (TST), and pre-swing (PSW) (Figure 2.1). IC involves floor contact with the heel and is followed by a foot flat on the ground. This phase is mainly responsible for decelerating the impact caused by the heel contact with the ground and preparation of body weight (BW) transfer. LR phase is the period when BW is transferred onto the reference limb, and knee flexion during this phase contributes to shock absorption (Perry & Burnfield, 2010). As the contralateral foot starts the swing phase, MST for the stance limb begins and corresponds to full BW support. TST starts with the heel-rise of the stance limb and ends when the contralateral foot contacts the ground. In this phase, the BW is transferred to the forefoot to progress the body's center of mass (CoM) forward and prepare for IC on the contralateral limb. CoM is defined as a single point at which all the body's mass is concentrated (Ruina & Pratap, 2002). PSW begins at contralateral IC, and during this phase, BW gradually moves to the other limb and ends with the toe-off preparing the position of the limb for swing. Therefore, PSW corresponds to the second double limb support of the gait

cycle. The swing phase, accounting for about 38 % of the gait cycle, can also be further subdivided into three sub-phases: initial swing (ISW), mid-swing (MSW), and terminal swing (TSW). ISW, the first phase of the swing, begins at toe-off and continues until the knee joint of the reference limb reaches the maximum flexion. In this phase, the trunk moves laterally towards the supporting limb. ISW is followed by MSW in which the swing limb advancement occurs. MSW beings with the maximum knee flexion of the reference limb and ends when the shank segment reaches vertical orientation with respect to the ground. During this phase, the hip joint reaches its maximum flexed position in the gait cycle. As the knee and hip joints on the reference side begin extension, the final sub-phase of swing, TSW, is completed when the swing foot strikes the floor. During this phase, the swing limb completes its forward advancement and is ready for the next stance phase. As described above, each of the eight gait sub-phases has its functional purpose, and this sequence of events achieves three principal tasks: WA, SLS, and swing limb advancement (Perry & Burnfield, 2010). Furthermore, each phase is functionally related to the generation of appropriate ground reaction forces (GRFs) (Racic et al., 2009).

Typical walking involves simultaneous reciprocal motions of upper and lower limbs in all three anatomical planes of the body: sagittal, frontal, and transverse (Figure 2.2). Although the major movements during walking take place in the lower limbs, mainly along the sagittal plane, motions of the torso, pelvis, and upper extremity in the other two planes also play an essential role in maintaining the dynamic stability as they contribute to the reduction of angular momentum and displacement of CoG throughout the gait cycle (Della Croce et al., 2001; Saunders et al., 1953; Stokes et al., 1989). To fully understand the kinematics and kinetics of natural walking, therefore, the analysis of human locomotion should be conducted and interpreted in all three planes together so that it can provide necessary information on how body segments interact with each other and

what is the functional significance of individual motions and gait events (Eng & Winter, 1995; Perry & Burnfield, 2010; Vaughan et al., 1999).

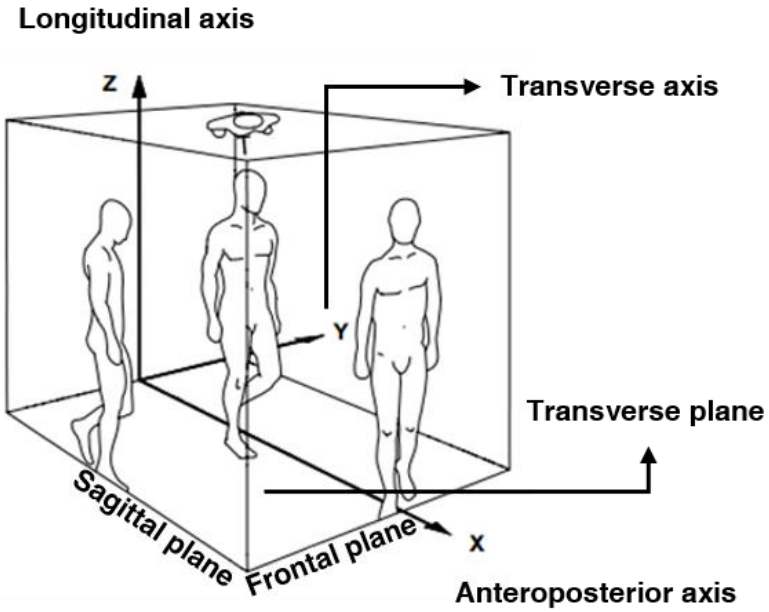

Figure 2.2. Three principal axes and planes of the walking subject (adapted from Inman et al., 1981).

Center of mass (CoM) motion during walking

One valuable and convenient way to obtain fundamental knowledge regarding human gait is by observing and analyzing the displacement pattern using the CoM as a reference point. The acceleration of the CoM serves as an indirect measure of the external forces acting on the body during locomotion. In natural walking, the CoM follows a smooth sinusoidal curve in the vertical and horizontal planes (Figure 2.3). In each gait cycle, the CoM generally displays oscillating lateral displacement moving from left to right in accordance with the supporting limb in the frontal plane and rhythmic biphasic vertical oscillation in the sagittal plane, showing peaks at 25 and 75 % of the gait cycle and the lowest level during the second double limb support of the stance phase (about 50%) (Saunders et al., 1953). When forward velocity is subtracted, and composite motion of horizontal and vertical displacement of CoM is projected on the frontal plane, the path has a closed

figure-eight shape with upward concave while walking at preferred speed (Tesio & Rota, 2019) (Figure 2.3C). As walking speed increases, the size of the CoM path in both frontal and transverse planes decreases and presents a U-shaped pattern in the frontal plane (Figure 2.4A-F), which is associated with the minimization of metabolic energy expenditure and maximization of energy exchange between the kinetic and potential energy of the CoM (Tesio & Rota, 2019; Tesio et al., 2010).

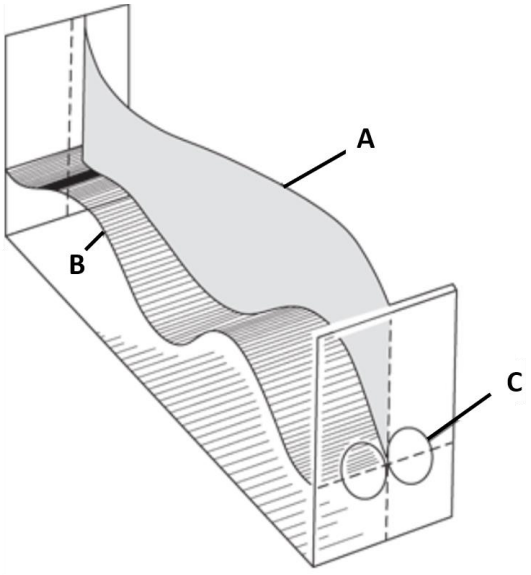

Figure 2.3. Displacement of CoM during walking: A. horizontal displacement, B. vertical displacement, and C. a figure "8" seen from anterior-posterior view as a result of a sum of both displacements (Inman et al., 1981).

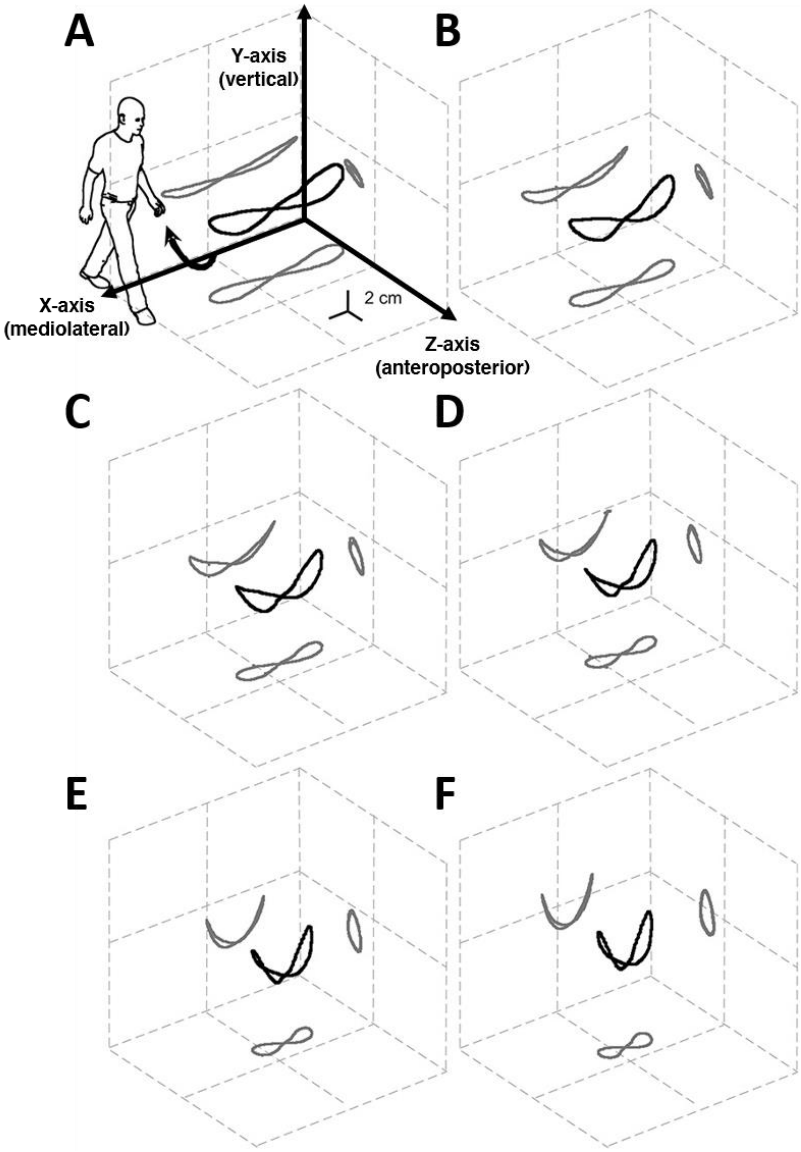

Figure 2.4. 3D displacement of CoM throughout the gait cycle in different walking speeds (A: slowest, F: fastest, ranged from 0.3 to 1.4 m/s). The curves (figure "8" shape) indicate the 3D displacement of the CoM and their projections to the three planes (adapted from Tesio et al., 2010).

Six determinants of human gait

Saunders, Inman, and Eberhart (1953) introduced six major determinants of human locomotion, which act together to minimize the excessive vertical and lateral displacement of the CoM, resulting in smooth gait pattern and conservation of energy expenditure (Saunders et al.,

1953) (Figure 2.5). The six determinants are pelvis rotation, pelvic tilt, lateral pelvic displacement, knee flexion in the stance phase, and co-variation mechanisms between the knee and ankle joints. A gait pattern generated by only flexion and extension of the hip joint—so-called 'compass gait'—results in more significant vertical displacement of the CoM in a circular arc determined by the leg length. During walking, the pelvis rotates about a vertical axis with approximately 4° on each side, allowing a greater step length and radius for the hip joint arcs, smoothing the pathway of the CoM compared to compass gait. Pelvic lowering (pelvic tilt) on the swing side also contributes to flattening of the CoM path as the swing leg moves forward when the elevation of the hip and pelvis are necessary to clear the foot from the ground. Similarly, ankle plantarflexion and knee flexion during the initial stance phase help to flatten the arcs, avoiding abrupt CoM inflections. Lateral displacement of the pelvis during locomotion is reduced by the influence of a tibiofemoral angle and hip joint adduction, avoiding excessive lateral displacement. By these determinants, energy cost during locomotion can be reduced effectively, and therefore, the bipedal walking of humans

Figure 2.5. The theory of six determinants during gait suggests that a set of kinematic features such as knee flexion and pelvic rotation contributes to reducing the vertical and lateral displacement of the body CoM, smoothing and minimizing the CoM trajectory (Saunders et al., 1953).

can maintain a stable and smooth transition effect (Saunders et al., 1953).

Ground reaction forces throughout the gait cycle

Kinetics are also a crucial component of the gait analysis in order to investigate the forces acting on the human body which cause movements. The principle of gait kinetics is based on Newton's three laws of motion (first: low of inertia, second: law of acceleration, and third: law of action-reaction), with the third law providing a basis for the estimation of the forces that the human body generates by relating the forces between the foot and the supporting floor (Perry & Burnfield, 2010). As each foot applies a load to the ground, the ground reacts with forces of equal magnitude but in the opposite direction (Oatis, 2017; Perry & Burnfield, 2010). GRF can be directly measured via force plates embedded in the walking surface. Through the GRF, one can understand the net forces acting on the lower limb and on the body as a whole, leading to the understanding of the acceleration of the whole body's CoM according to Newton's second law ($F = ma$, m: mass, a: acceleration). The magnitude and direction of the GRF continuously change throughout the stance phase. Since the GRF is a vector, it can be resolved into its components orthogonal to each other along with a three-dimensional (3D) coordinate system: horizontal (anterior-posterior, AP), side to side (medial-lateral), and vertical (Hamill & Knutzen, 2006).

Figure 2.6 shows the pattern of GRF during the gait cycle. The vertical GRF generated by one stance foot is typically characterized by a double-humped curve (Oatis, 2017). These two peaks increase above 100% of BW and occur when the body's CoM accelerates in an upward direction (Oatis, 2017). As the heel strikes the ground, transfer of the bodyweight to the stance limb begins. To deal with the impact force induced by the contact with the ground, the foot and leg function together as shock absorbers (Perry & Burnfield, 2010). As the foot fully contacts the ground and BW is gradually transferred to the supporting limb during the LR phase, the vertical

GRF increases to its first vertical peak (F1) between LR and MST (12% of the gait cycle) (Perry & Burnfield, 2010). During the MST, there is a trough in the vertical GRF (F2). In this phase, the stance limb supports the whole-body weight and acts like an inverted pendulum providing a stable base for the rotation of the rest of the body over the ankle (Ayyappa, 1997). The decrease of the GRF below the body's weight occurs due to the decelerated CoM's upward motion as it approaches the highest point. This deceleration of upward motion of the whole body generates a dip in the vertical force pattern, with the typical value of 0.7 times the person's BW. Then, the increase in vertical GRF to third peak F3 occurs during the TST phase when the bodyweight moves to the forefoot as the heel-rise begins by the push of ankle plantar flexor muscles against the ground (Perry & Burnfield, 2010). Lastly, vertical GRF decreases during the PSW phase and falls to zero

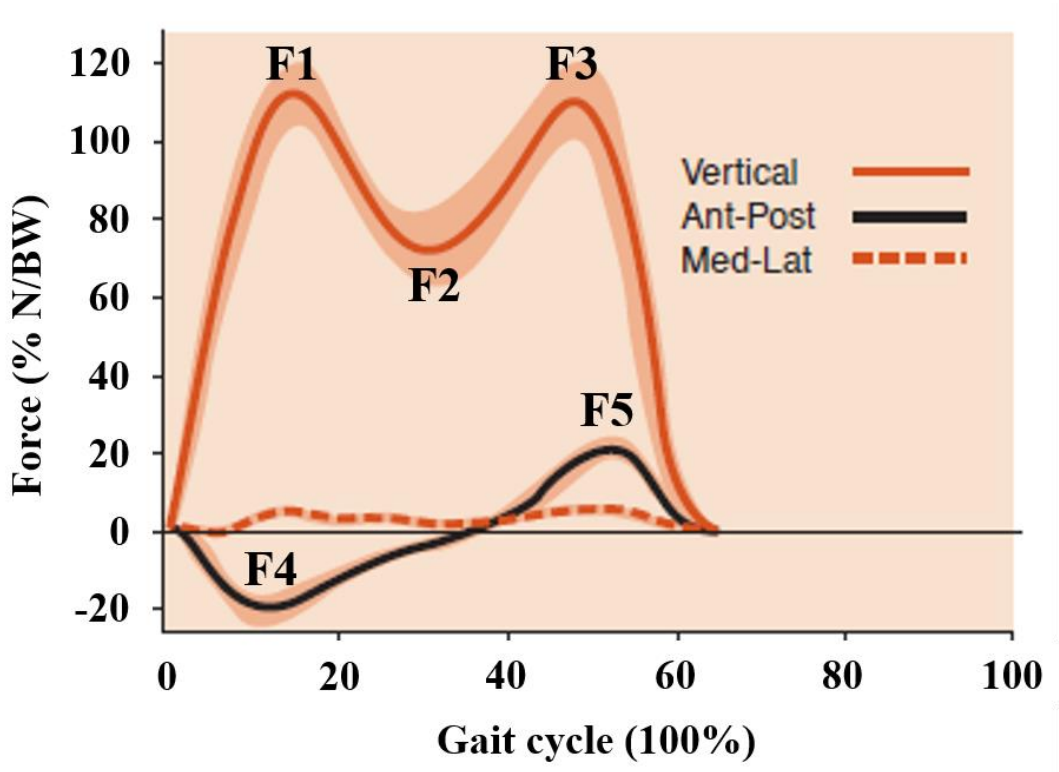

Figure 2.6. Ground reaction force (GRF) during normal walking (Rose & Gamble, 1994). N: newton, BW: body weight.

at the end of the toe-off phase (Figure 2.6).

The magnitude of AP shear components of the GRF is smaller compared to the vertical component but shows a consistent pattern throughout the gait cycle. Similar to the vertical GRF, there are two peaks in an AP shear component in early and late stance, respectively (F4 and F5 in Figure 2.6). In an early stance, the ground exerts a posteriorly directed force onto the foot to decelerate the body's CoM, and this negative portion is known as the braking phase (Hamill & Knutzen, 2006). As the body moves over the ankle, the AP GRF component reaches a minimum at the crossover point. At this point, the body is placed above the foot (around 55% of the stance phase), and this point is usually matched with the dip in the vertical force pattern. As the push-off occurs in late stance, plantar flexor activity leads anteriorly directed GRF acting on the foot, contributing to the forward propulsion of the body. This positive period is called the propulsion phase (Hamill & Knutzen, 2006).

The medial-lateral shear components of the GRF indicate the forces related to the shift of the body from side to side between the supporting feet. These components are more variable than the vertical or AP shear components, and there is no typical pattern. However, there is a generally a laterally directed GRF during the loading phase after heel strike, followed by medially directed force throughout the rest of the stance phase. Sometimes, there is another laterally directed GRF component during the push-off. It has been reported that the medial-lateral shear components of the GRF are associated with foot placement (forefoot adduction and abduction) (Simpson & Jiang, 1999), footwear, and orthoses (Nester et al., 2003).

LOWER LIMB DURING WALKING

Sagittal plane kinematics

In the sagittal plane, the pelvis is maintained in anterior pelvic tilt throughout the gait cycle

and presents two cycles of a sinusoidal wave for one complete gait cycle (Figure 2.7A) (Murray et al., 1984; O'Neill et al., 2015). A relative posterior pelvic tilt occurs during SLS as the trunk is in an erect position over the stance leg and during the ISW as the other leg begins its early SLS phase (Perry & Burnfield, 2010). Anterior pelvic tilt occurs during TST as the limb reaches its maximal hip extension for the trailing limb posture and during the TSW as the trunk leans forward toward the stance limb (Perry & Burnfield, 2010). The total excursion of pelvic tilt is relatively small, approximately 2° to 5° (Kadaba et al., 1990; Murray et al., 1964). In this plane, the motion of the hip has two arcs: hip joint motion is transitioned from flexion to extension during stance and from extension to flexion during swing (Figure 2.7D). The reported values for the normal range of hip motion during gait vary in the literature depending on gait speed (Fukuchi et al., 2018). For a comfortable walking speed, the range of motion at the hip is approximately 40° with maximal flexion of 30° and maximal extension of 10° (Dettmann et al., 1987; Gore et al., 1975; Johnston & Smidt, 1969; Kadaba et al., 1989; Murray et al., 1964). The knee joint motion mainly occurs in the sagittal plane with a full range of motion of about 60° (Figure 2.7G). The knee flexion has two primary peaks: the smaller first one found at the transition between the LR and MST responsible for shock absorption at the knee joint, and the larger one occurring during the ISW to clear the foot from the ground (Chao et al., 1983; Eberhart, 1954; Györy et al., 1976; Inman et al., 1981; Kettelkamp et al., 1970; Murray et al., 1964). The major motions at the ankle joint are primarily observed in the sagittal plane (Figure 2.7J). At IC, the ankle joint is in a neutral position and slowly places the foot flat to the ground by plantar flexion. As the entire BW moves onto the one stance foot and the tibia rotates over the stationary foot, the ankle position is transitioned into dorsiflexion by eccentric control of the ankle plantar flexors. Once PSW and second double limb stance begins, there is a rapid transfer of BW to the forward limb, and then the ankle of the trailing limb starts

plantarflexion to push off, followed by the toe-off (Perry & Burnfield, 2010). At the ISW, ankle dorsiflexion starts for foot clearance from the ground to avoid a dragging foot, and as the limb continues traveling forward shortly before the next heel contact, the ankle joint returns to its neutral position to prepare for the next stance phase.

Frontal plane kinematics

In the frontal plane, the pelvis shows one cycle of movement throughout the gait cycle. At IC, the pelvis is approximately in the neutral position. During WA, a pelvic drop of the contralateral side is observed around 20% of the gait cycle, showing an average of 4° so that the hip on the swing side falls when compared to the stance side (Figure 2.7B), making the trajectory of the center of the pelvis flatter by compensating for the higher position of the pelvis on the stance side (Levangie & Norkin, 2011; Saunders et al., 1953). Conversely, the ipsilateral pelvic drop of 4° occurs as the opposite leg begins the LR phase (Levangie & Norkin, 2011; Saunders et al., 1953). In this plane, the hip shows a small amount of adduction and abduction (Figure 2.7E). At the IC, the hip is in an approximately neutral position in this plane, but adduction increases to about 10° by the end of the LR period as the bodyweight is transferred to the supporting limb due to the contralateral pelvic drop and displacement of the femur (Perry & Burnfield, 2010). As SLS begins, the hip returns to its neutral position, and there is an increase in abduction as it prepares the swing, reaching a maximal abduction of 5° right after toe-off. During the rest of the swing phase, it remains in a neutral position. Although the amount of motion is relatively small, abduction and adduction of the knee joint are also observed in this plane (Figure 2.7H) (Dyrby & Andriacchi, 2004), showing the greatest angle of about 4° of abduction during WA and peak adduction of 2° during MSW (Perry & Burnfield, 2010). Due to the anatomical alignment of dual obliquity of the ankle axis, ankle flexion motions are generally complemented by inversion and eversion motions

at the sub-talar joint, with approximately 15° of range of motion (Figure 2.7 L) (Nordin & Frankel, 2001; Perry & Burnfield, 2010). Ankle plantarflexion is accompanied by inversion, which is also called ankle supination, and dorsiflexion occurs with ankle eversion that is also called ankle pronation (Perry & Burnfield, 2010). At heel strike, ankle inversion occurs with mild plantar flexion of the ankle joint and progresses to eversion during MST phase accompanied with the ankle dorsiflexion as the shank rotates over the joint. As the heel rises and the foot begins rotating about the forefoot resulting in an increase in plantar flexion, the ankle inversion also increases with the peak around toe-off. As the ankle remains in a dorsiflexed position by MSW, the ankle displays eversion and then transitions to inversion as the joint prepares the next heel strike with a slight plantar flexion (Nordin & Frankel, 2001).

Transverse plane kinematics

In the transverse plane, the pelvis rotates with a total range of 10° (5° internal and 5° external). Maximal internal rotation of the pelvis occurs during IC and TSW phase, and maximal external rotation is observed during the TST phase (Figure 2.7C). The rotations of the pelvis in this plane contribute to longer step length and greater radius of the arcs of the hip joint, and therefore a smooth trajectory of the CoM (Murray et al., 1964; Saunders et al., 1953). Also, the reciprocal rotation of the thorax and pelvis contribute to a decrease in angular momentum of the body and dampen the movement of the pelvis, making the smooth pattern of gait trajectory (Stokes et al., 1989). In this plane, the peak internal rotation of the hip occurs at the end of the LR, and maximal external rotation is observed at the beginning of the swing phase (Figure 2.7F) (Levens et al., 1948). Although there can be great variability between individuals and among the different gait laboratories, summation of the transverse rotation of the pelvis, which is approximately 7.7°, and the total range of thigh rotation, which is about 8°, results in the total hip rotation of 15° on

average (Perry & Burnfield, 2010), contributing to lengthening the step length. Variability in these measurements may relate to factors such as subject's gender, walking speed, and pelvis angle definition (for example, we can define pelvis motion with respect to the horizontal or with respect to the thigh). Figure 2.7I shows the internal and external rotation of the tibia relative to the femur bone during the gait cycle. In the IC, the tibia shows external rotation relative to the femur locking the knee joint, but the internal rotation is rapidly accelerated during the LR (Perry & Burnfield, 2010). As the single-leg phase begins, the tibia starts rotating externally to lock the knee joint for limb stability as the entire BW is loaded on the stance limb. During the TST and PSW phases, the knee starts rotating internally so that the knee joint can be flexed to prepare for the swing phase. This is called the "screw-home mechanism," indicating that the knee extension (in the last 30 degrees to full extension) is generally accompanied by external rotation of the tibia, and the knee flexion is accompanied by the internal rotation of the tibia relative to the femur (Moglo & Shirazi-Adl, 2005). In general, ankle dorsiflexion, eversion, and abduction work together to make the sole face laterally, ankle plantar flexion, inversion, and adduction co-occur to make the sole face medially (Nordin & Frankel, 2001). Thus, at the heel strike, the ankle displays slight adduction with ankle plantar flexion, and as the gait cycle progresses, a small increase in ankle abduction occurs when the ankle goes into a dorsiflexed position (Figure 2.7L). During the TST, ankle adduction shows a peak with maximal ankle plantar flexion. As the ankle is transitioned to dorsiflexion, ankle abduction is accompanied during the swing phase.

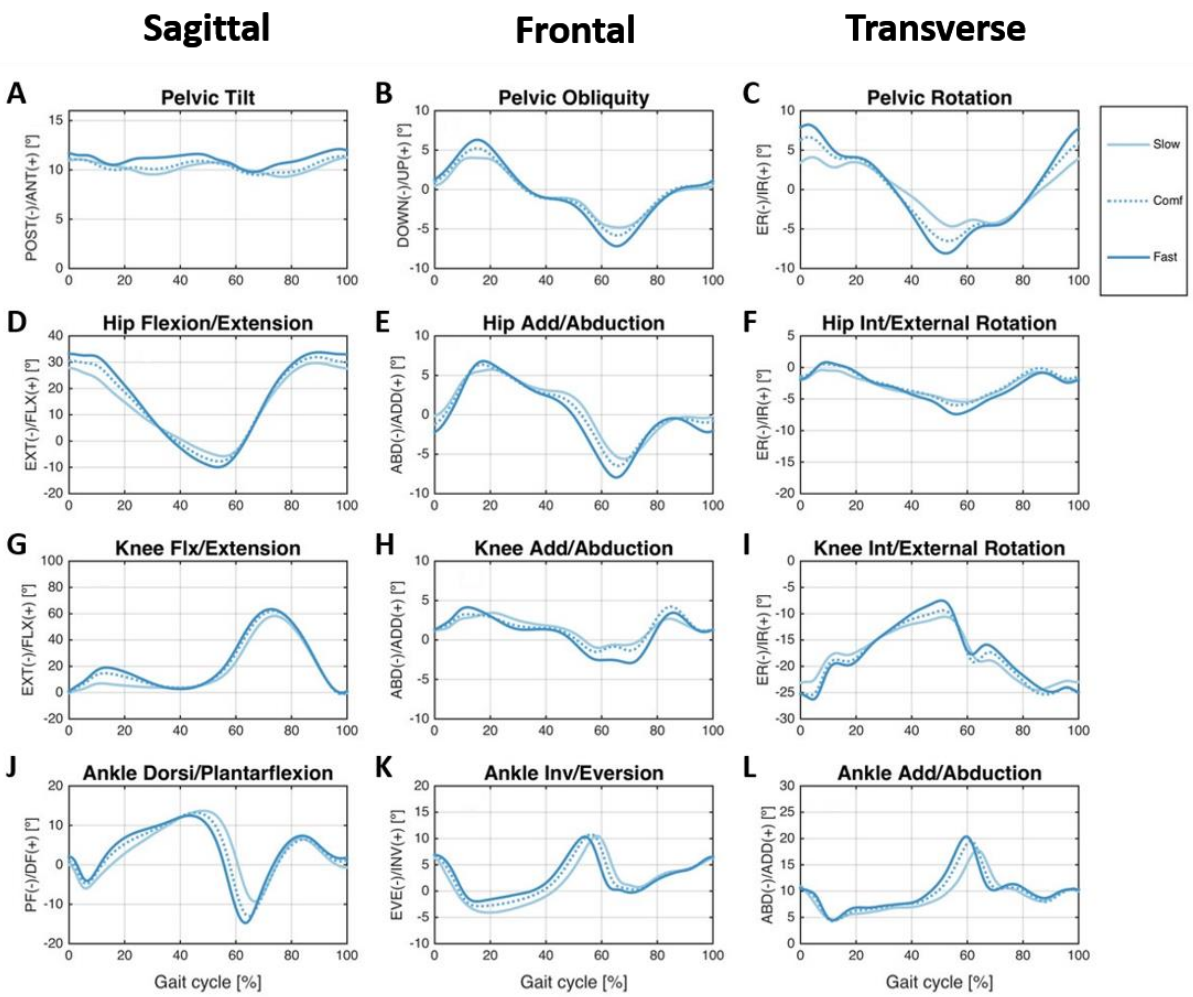

Figure 2.7. 3D angular displacement of pelvis, hip, knee, and ankle joints during over-ground walking. Each curve indicates a different walking speed from slower (lightest blue, 30 % slower than comfortable speed) to faster one (darkest blue, 30 % greater than comfortable speed). The preferred walking speed is represented as a dashed line (Fukuchi et al., 2018).

Lower limb muscle activations during walking

Figure 2.8 shows the typical activation of lower extremity muscles during natural walking, and Figure 2.9 shows the timing of the muscle activation throughout the gait cycle. The gluteus maximus and hamstrings (biceps femoris) are active during the late swing and following IC, decelerating the forward movement of the leg by eccentrically contracting at the end of swing (Winter & Yack, 1987), then contracting concentrically as the hip begins to extend contributing to the initiation of hip extension during early stance (Winter & Yack, 1987). The gluteus maximus

also contributes to accelerating knee extension by controlling the femur during early SLS (Arnold et al., 2005). The gluteus medius, which is a hip abductor, begins at the end of TSW and continues its activity through most of the stance until the weight loading begins on the contralateral side (Perry & Burnfield, 2010; Winter & Yack, 1987). The activity of the hip abductors stabilizes the pelvis in the frontal plane throughout the stance phase and provides support for hip and knee extension during mid to late stance (Anderson & Pandy, 2003; Arnold et al., 2005; Winter & Yack, 1987). During the gait cycle, the hip flexor does not show significant actions, but the primary pattern of the hip flexors begins in late stance and continue their activity into the early swing to slow hip extension down and initiate hip flexion for limb progression (Arnold et al., 2005; Gottschall & Kram, 2005). The adductor longus and brevis are responsible for hip flexion during the swing phase, showing its first activation around late TST and remains active until the ISW phase (Perry & Burnfield, 2010). For approximately the first 25% of the gait cycle during LR and early MST, both quadriceps and hamstrings are co-activated at the knee. In this period, the knee joint is flexed, and the activation of the knee extensor muscle decelerates knee flexion by eccentric control. During the late swing phase, the activation of the hamstring increases in order to decelerate hip flexion and control the knee extension eccentrically in preparation for the next IC. The ankle plantar flexor, gastrocnemius, progressively increases its activation from the beginning of the stance phase until the middle of TST with the greatest burst of activity from heel-off to toe-off as the body rotates over the plantarflexing foot, followed by the rapid decrease in activation until it ends around PSW phase. During the PSW, the plantar flexors act concentrically, producing a propulsive “push-off.” Four muscles anterior to the ankle joint, named the tibialis anterior (TA), extensor digitorum longus (EDL), extensor hallucis longus (EHL), and peroneus tertius (PT), are responsible for dorsiflexion of the joint, participating in the IC and LR phases of stance to

decelerate plantar flexion and to provide foot control during swing phase. Dorsiflexor muscles show a biphasic pattern with peak activity during the LR phase and ISW. TA shows its peak activation during IC while toe extensors are highly active at the end of ISW. During IC and the first half of the LR, the contraction of the dorsiflexor muscles are eccentric to control the lowering of the forefoot. During the ISW phase, these muscles show a second peak of activation to ensure foot clearance from the ground. The activations decrease during MSW but increase again to prepare the next IC.

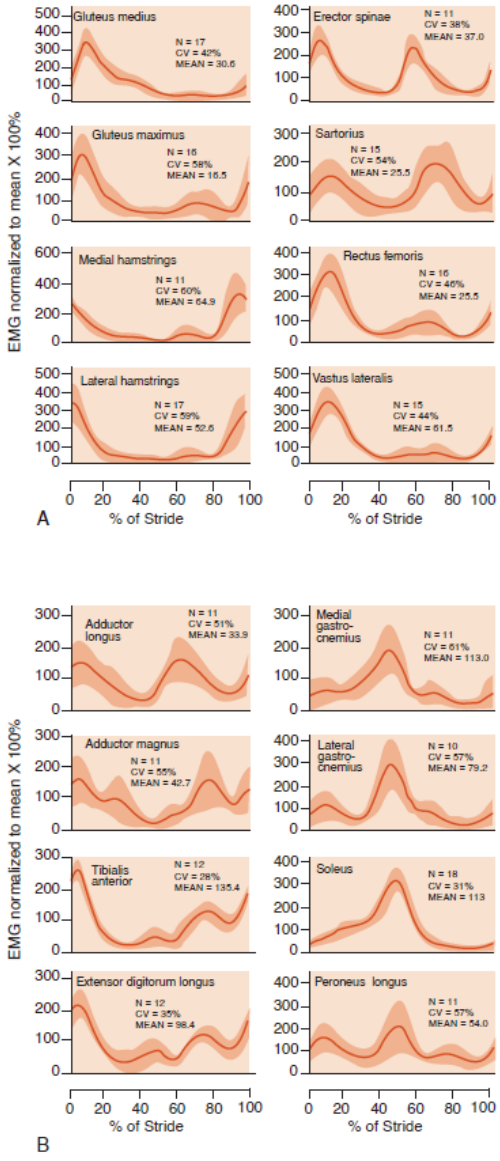

Figure 2.8. EMG activation of lower limb muscles during walking (Winter & Yack, 1987).

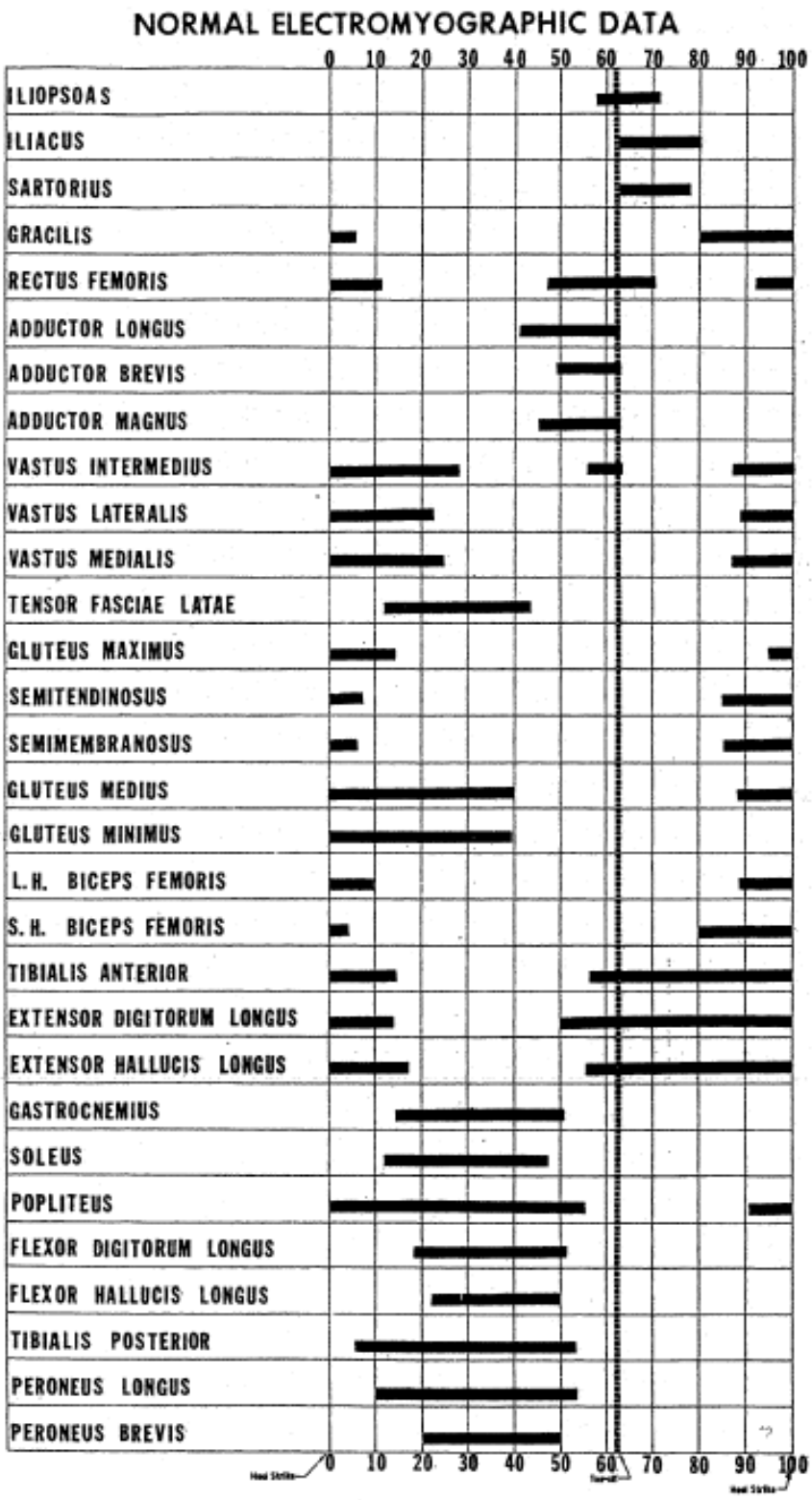

Figure 2.9. Adult muscle phasic activity chart – Shriners Hospital, San Francisco (Sutherland, 2001).

UPPER LIMB DURING WALKING

Kinematics of arm swing

The primarily sagittal motions of the upper limb during walking, also known as arm swing, are one of the distinctive characteristics of human walking (Jackson et al., 1983). When walking at a comfortable speed, the arm and the ipsilateral leg show 1:1 out-of-phase coordination: As the right upper limb goes backward due to shoulder extension, the right lower limb moves forward with hip flexion (Donker et al., 2001; Wagenaar & van Emmerik, 2000). The frequency of arm swing is synchronized with stride frequency at walking speeds higher than 0.8 m/s, while at speeds lower than 0.8 m/s, the frequency of arm movement is synchronized with the step frequency showing a 2:1 arm to leg swing ratio (Donker et al., 2001; Van Emmerik et al., 1998; Wagenaar & van Emmerik, 2000). Murray et al. investigated the shoulder and elbow joints' motion during walking at different walking speeds (Murray et al., 1967). The ipsilateral shoulder is in its fully extended position at the beginning of the gait cycle and begins forward flexion until it reaches its peak flexion around halfway of the gait cycle when the contralateral heel strikes the ground (Figure 2.10). For the latter half of the gait cycle, the shoulder joint returns to its maximal extended position as the ipsilateral lower limb moves forward during the swing phase. The range of motion of the shoulder during faster walking speeds is higher than during comfortable walking speed, mainly due to the increased shoulder extension (Murray et al., 1967). Similarly, the elbow joint shows a monophasic curve during the gait cycle, with peak flexion occurring around the contralateral heel strike (Figure 2.10). Again, the amplitude of the elbow motion is also higher during fast walking, but unlike the shoulder, it is mainly due to increased elbow flexion, not due to the increased elbow extension. While spatial characteristics of individual arm swing are variable between subjects, the temporal relationship between upper and lower limbs and the amplitude of shoulder and elbow

motion within the individual subject is highly reproducible (Murray et al., 1967). More recently, it has been reported that the amplitude of shoulder and elbow angle trajectories increases at higher walking speeds (Hejrati et al., 2016). Also, at slower walking speed, the shoulder joint reached the maximal flexion angle before the contralateral heel strike, and the opposite pattern occurred at faster walking speed, given that the maximal flexion of shoulder angle generally occurs with the contralateral heel strike at comfortable walking speed (Hejrati et al., 2016).

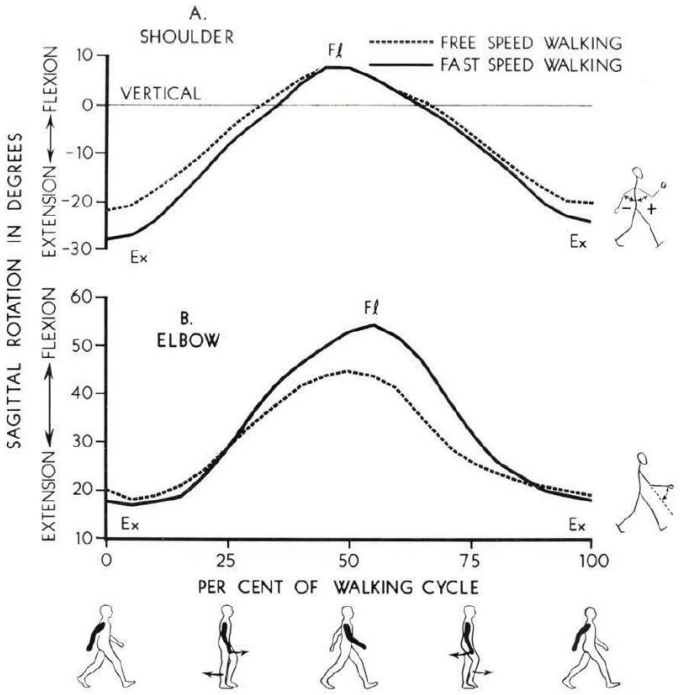

Figure 2.10. Angular displacement of shoulder and elbow joint in sagittal plane during a gait cycle with free and fast walking speeds averaged across thirty healthy subjects (Murray et al., 1967).

Upper limb's contribution to locomotion

The primary role of arm swing during walking and running appears to minimize the body's total angular momentum (Elftman, 1939b). Elftman observed that the angular momentum of the arms about the body's vertical axis nearly entirely cancels out the lower limb's angular momentum during the stance phase of the gait cycle (Figure 2.11), resulting in the total angular momentum of the whole body nearly around zero. More recent studies also support the angular momentum

hypothesis, showing that the GRF moment between the foot and the ground increased significantly without arm swing (Li et al., 2001; Witte et al., 1991). Lack of arm swing is also associated with an increase in energy expenditure because a more considerable moment is required to be generated by the lower limb muscles (Collins et al., 2009; Umberger, 2008). Similar evidence has been reported that the arm moments act to cancel the opposite moments of the lower limb so that the net angular momentum in all three axes is nearly zero during walking (Herr & Popovic, 2008) and running (Hinrichs, 1987, 1990a). According to previous studies where the effect of arm swing on energy expenditure was investigated, restricted arm swing reduces gait efficiency as indicated by increased oxygen consumption and metabolic rate. The decrease in efficiency likely occurs because the angular momentum generated by the lower limbs cannot be fully canceled out without the counteracting effect of the arm movement (Collins et al., 2009; Ortega et al., 2008; Umberger, 2008; Yizhar et al., 2009). Unilateral arm constraint during walking also affects inter-segmental

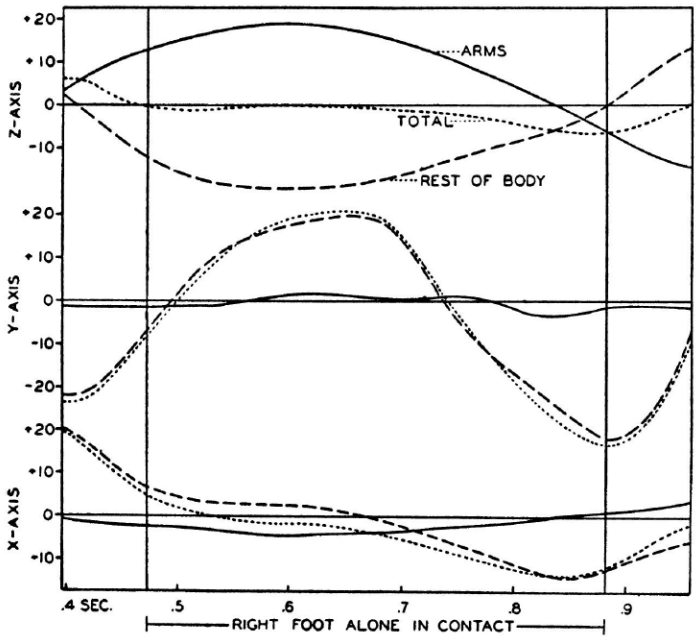

Figure 2.11. Angular momentum about the center of gravity (CoG) of the body for the arms, the rest of the body, and the body as a whole, in three principal axes. Z-axis: vertical, Y-axis: mediolateral (ML), X-axis: anteroposterior. Angular momentum in kg.cm.sec (Elftman, 1939b).

coordination showing altered frequency and phase relations between upper and lower limbs (Ford et al., 2007). Interestingly, this upper limb asymmetry induced by constraining one arm results in the increased arm swing amplitude in the contralateral limb. This is assumed as an adaptive strategy for maintaining coordination between upper and lower limbs and preventing further asymmetry as it counteracts the angular momentum generated by the increased hip motion when walking at a velocity greater than 1.1 m/s (Ford et al., 2007). The greater upper body torque contributes to offset the torque caused by the lower body (Elftman, 1939b; Stokes et al., 1989; Wagenaar & Beek, 1992).

Another possible function of the arm swing is to assist with the pelvis-trunk segments' anti-phase coordination, keeping the body and head more stable (Kubo et al., 2006). In this study, axial trunk stiffness during walking was measured using the angular displacement between the trunk and pelvic segments. Results showed that the torque generated by arm swing counteracted the torque from axial trunk stiffness, leading to suppression of axial thoracic rotation, which might be beneficial to maintain the head stability (Kubo et al., 2006). Additionally, previous studies supported the pelvis-trunk coordination hypothesis showing increased activities of trunk muscles, such as the external/internal obliques, thoracic/lumbar erector spinae, latissimus dorsi (LD), and multifidus when the arm swing was restricted during walking. This indicates that the arm swing is necessary to counteract the trunk rotation torque (Callaghan et al., 1999; Cappozzo, 1983).

One more potential role for arm swing is to decrease the vertical CoM oscillation, leading to decreased energy expenditure in walking, in that the observed vertical CoM displacement in the arms constrained condition was 4.9 ± 1.2 cm when compared to 4.1 ± 1.2 cm in arm swing condition (Yang et al., 2015). Although the CoM displacement of the human body during walking is influenced by many other determinants mentioned above (section 1.4), there have been several

studies supporting the argument that optimal vertical CoM trajectory is necessary for energy efficiency (Gordon et al., 2009; Hinrichs, 1990b; Murray et al., 1967; Yang et al., 2015). More specifically, this argument is supported by the inverse relationship between the vertical trajectory of the CoM of the entire body and the CoM of the upper limbs resulting in a cancellation effect, contributing to the decrease of total vertical displacement of CoM of the entire body and further decrease in energy expenditure (Hinrichs, 1990b; Murray et al., 1967). In a recent study where the effect of arm swing restriction on the vertical displacement of the body's CoM during treadmill walking was examined, a significant increase in vertical CoM displacement was observed when walking with the arms constrained compared to the walking with arm swing (Yang et al., 2015). Since the CoM of the arms is at the highest elevation when the CoM of the rest of the body is at the lowest elevation during double limb support (and vice versa during MST), the increase in the body's CoM vertical displacement without arm swing is likely due to the absence of this canceling effect between the arm and the rest of the body (Yang et al., 2015).

Upper limb muscle activations during walking

A recent study has reported the upper limb muscle activations during natural walking with free arm swing (Figure 2.12) (Kuhtz-Buschbeck & Jing, 2012). At IC, the ipsilateral posterior deltoid (PD), trapezius (TRAP), and latissimus dorsi (LD) show relatively weak activity. The electromyography (EMG) activation was at a minimal level, around 25% of the gait cycle, as the arm moves forward passing the trunk during MST. The activation of TRAP followed by PD, triceps brachii (TB), anterior deltoid (AD), and LD increase, reaching peaks during the TST. The eccentric contraction of PD, LD, and TB contribute to the lengthening of these muscles as the arm moves forward with the maximum activity right before the contralateral heel contact. During this time, concentric activation of the AD and biceps brachii (BB) also occurs but shows weak

activation compared to the extensor muscles. As the arm moves backward, all muscles show weak activation during the ISW phase. During mid- and TSW, the concentric activations of TB, PD, and LD contribute to the shoulder and elbow extension. In this period, BB and AD show eccentric activations. The eccentric muscle activations in both forward and backward arm swing are mainly to control and decelerate the opposite arm swing movement.

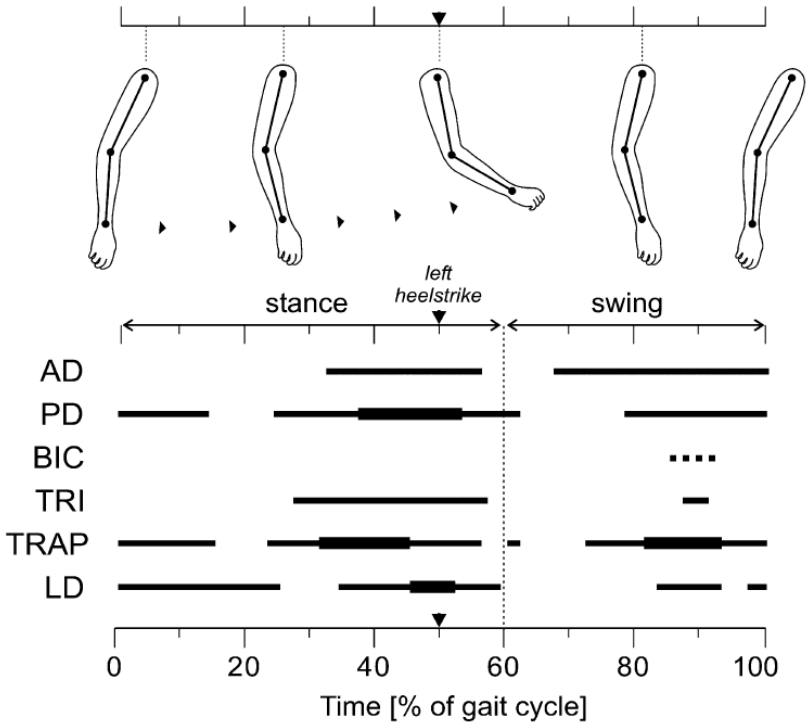

Figure 2.12. Corresponding forward and backward of arm swing and the timing of muscle activation during walking with natural arm swing (6 km/h). Thick black lines in anterior deltoid (AD), posterior deltoid (PD), and triceps (TRI) indicate the muscle activation greater than 5% maximal voluntary contraction (MVC). In trapezius (TRAP) and latissimus dorsi (LD), they indicate the muscle activation greater than 10 % MVC. For AD, PD, and TRI, thin black lines represent the EMG activity less than 1% MVC, and less than 3% MVC for TRAP and LD. Dotted line indicates mean biceps brachii (BIC) less than 1% MVC. (Kuhtz-Buschbeck & Jing, 2012).

NEURAL CONTROL OF HUMAN LOCOMOTION

Neural control of lower limb motions during locomotion

Complex hierarchical neurological control systems contribute to the generation of locomotion patterns (Kandel, Schwartz, Jessell, Siegelbaum, et al., 2000). Although there is no direct evidence for the existence of central pattern generator (CPG) in human, there have been theoretical approaches where neural activity associated with CPG have been found in invertebrate and vertebrate preparations (Duysens & Pearson, 1998; Duysens & Van de Crommert, 1998; Grillner, 1975; Grillner & Dubuc, 1988; Van de Crommert et al., 1998). According to their theory, at the lowest level, the CPG is a network of neurons in the spinal cord that produce rhythmic movement patterns due to the intrinsic inhibitory and excitatory connections within the network, without the external sensory feedback or descending command from the supraspinal centers (Duysens & Pearson, 1998; Rossignol, 2010; Stein, 1997). Brown (1911) demonstrated the existence of CPGs in the spinal cord for rhythmic locomotor activities in cats (Brown, 1911). These CPGs are responsible for rhythmic and sequential motoneuron/muscle groups' activation and are adjusted by local sensory feedback to respond to the unexpected perturbation (Grillner, 2011).

At higher levels of the CNS, the basal ganglia, which consist of nuclei located deep in the brain hemispheres, is important for the selection of motor programming as it receives inputs from the cortex and thalamus (Grillner et al., 2008; Nakazawa et al., 2012). The level of activity is determined by the brainstem locomotor regions, such as diencephalon (SLR: subthalamic locomotor region), mesopontine (MLR: mesencephalic locomotor region), regulating the activation level of the spinal GPGs through reticulospinal neurons (Grillner et al., 2008; Nakazawa et al., 2012). At rest, the output of these locomotor systems in the brainstem is inhibited, and only when these systems are disinhibited is locomotion initiated. This connection from locomotor

regions to the reticulospinal neurons and to the CPGs are the main direct command center for limb propulsion (Grillner et al., 2008; Nakazawa et al., 2012).

Results also supported the idea that the neural control of leg flexor (TA) and extensor (gastrocnemius, GM) muscles are interconnected differently as the responses of arm muscles (BB, TB, and deltoideus) after tibial nerve stimulation are nore associated with the compensatory TA responses (Dietz et al., 2001) when compared to the GM responses. Two critical feedback sources have been reported to modulate CPG function: loading and unloading of the limb and hip position (Duysens et al., 2000; Duysens & Pearson, 1980). During the stance phase, the loading signal increases the leg extensor activation and, at the same time, inhibits the initiation of the swing phase. At the end of the stance phase, the inhibition for the swing phase decreases as the loading signal decreases (Duysens, 2002; Duysens et al., 2000; Duysens & Pearson, 1980). Additionally, while the leg flexors are more sensitive to visual stimuli, the leg extensors are more sensitive to proprioceptive stimuli acting continuously as antigravity muscles (Beloozerova & Sirota, 1988; Dietz, 1992). Furthermore, stretch reflex from the hip flexor muscles induced by the hip extension at the end of the stance phase is considered as a second signal for CPG to initiate the swing phase (Hiebert et al., 1996).

Integration of neural control of upper and lower limb during locomotion

The coupling of the upper and lower limbs has also been observed during non-locomotor tasks as well as during locomotion (Baldissera & Cavallari, 2001; Jeka & Kelso, 1995; Serrien & Swinnen, 1998; Swinnen et al., 1995). For example, Kelso showed the same preference for in-phase and anti-phase movement between lower and upper limbs as between upper limbs only (Jeka et al., 1993; Kelso & Jeka, 1992; Kelso, 1995). Such behavioral preferences result from the neural coupling between the cervical and lumbar enlargements in the spinal cord, connected via long

propriospinal projections (Juvin et al., 2005, 2007; Meyns et al., 2013). The CPG also plays an essential role in generating rhythmic motion of the upper and lower limb (Dietz, 2002; Ferris et al., 2006; Gerasimenko et al., 2010; Gurfinkel et al., 1998; Solopova et al., 2014). More recently, experimental evidence has accumulated to suggest that rhythmic movements of the upper limb are also likely regulated via CPG circuitry (Zehr et al., 2004).

Previous studies have presented evidence for the neural coupling between upper and lower limbs by examining the modulation of interlimb reflex responses during rhythmic movements. Baldissera et al. found a cyclic H-reflex modulation in a wrist flexor during rhythmic movements of the ipsilateral foot (Baldissera et al., 1998). H-reflex refers to Hoffmann's reflex, which is a reflective reaction of the peripheral motor nerve after a low-intensity electrical stimulus, and it is used to activate only the primary muscle spindle afferents (Robertson et al., 2013). Tibial nerve stimulation-induced activity in proximal arm muscles (TB) only during walking, while there were no arm muscle responses during standing with arm swing and sitting (Delwaide & Crenna, 1984). Similar results were found in another study, where more robust muscular responses of the TB and deltoid were observed following tibial nerve stimulation during walking (Dietz et al., 2001). Such observations highlight the potential existence of 'residual function' related to evolution from quadrupedal locomotion in humans, quadrupedal locomotion, such that the functional and flexible coupling between cervical and thoracolumbar centers via neuronal pathways is reflected in the arm swing during walking (Dietz et al., 2001). Zehr and Haridas (2003) also found that during natural arm swing while treadmill walking, the cutaneous nerve stimulation applied to radial nerve innervating the hand muscles evoked the reflex responses in PD and TB (Zehr & Haridas, 2003). Similar reflex modulations during rhythmic upper limb movement and arm cycling and locomotion suggest that similar neural control mechanisms (CPGs) are used during cyclical movements of the

arms and legs to control the reflex output. This study provided evidence supporting Dietz (2001) in that the sensory transmission from the tibial nerve afferents to the lumbar spinal cord (Zehr & Haridas, 2003). All of these results indicate that the neuronal coupling of the upper and lower limb is task-dependent and facilitated by the CPG activity during walking (Dietz, 2002; Dietz et al., 2001; Dietz & Michel, 2009).

Such task-dependency of the neuronal coupling between upper and lower limbs can be adaptive for skillful hand movements. For example, the interlimb coupling in the cervical propriospinal neuronal system may be inhibited to allow for direct cortico-motoneuronal control of hand muscles to facilitate selective activation of individual muscles (Figure 2.13) (Dietz, 2002; Nicolas et al., 2001). This flexible coupling of upper and lower neural circuits enables humans to utilize the upper limb to generate motions from the very basic locomotor movement pattern to well-elaborated manipulation (e.g., manipulating a cell phone or carrying a cup of coffee).

Although the interspinal connection between the cervical and thoracolumbar CPGs is bidirectional, it has been reported that the caudo-rostral connections are stronger than their reverse counterparts, such that lower limb movements exert a more substantial influence on the upper limb than vice versa (Eke-Okoro, 1994; Meyns et al., 2013). In rats, hindlimb CPGs strongly activated the forelimb CPGs. Even without lumbar CPG activity, lumbar afferent stimulation can successfully evoke the cervical CPG rhythmicity, whereas cervical sensory input cannot produce the lumbar generator without cervical CPG activity (Juvin et al., 2005). Strong caudo-rostral projections also exist in humans such that the arm movement frequency is significantly affected by that of the leg, but the opposite is not the case during simultaneous arm and leg cycling movements (Sakamoto et al., 2007).

However, there is still evidence that the descending motor command from the upper limb motions can influence the lower limb muscle activation. Active arm swing facilitated the lower limb muscle recruitment during stepping in people with spinal cord injury (SCI) (Behrman & Harkema, 2000). Another study done with SCI subjects observed increases in EMG activity of the lower limb caused by the upper limb movement. Kawashima et al. (2008) investigated the effect of different types of upper limb movements (resting, passive, and active) on the lower limb motor output during locomotor-like movements (Kawashima et al., 2008). They found that passive and active arm movements induced greater muscular activations in the soleus muscle compared to resting arm condition in cervical incomplete SCI subjects whose neural connection between control center in the cervical and lumbar spinal cord is still intact, indicating that the movement

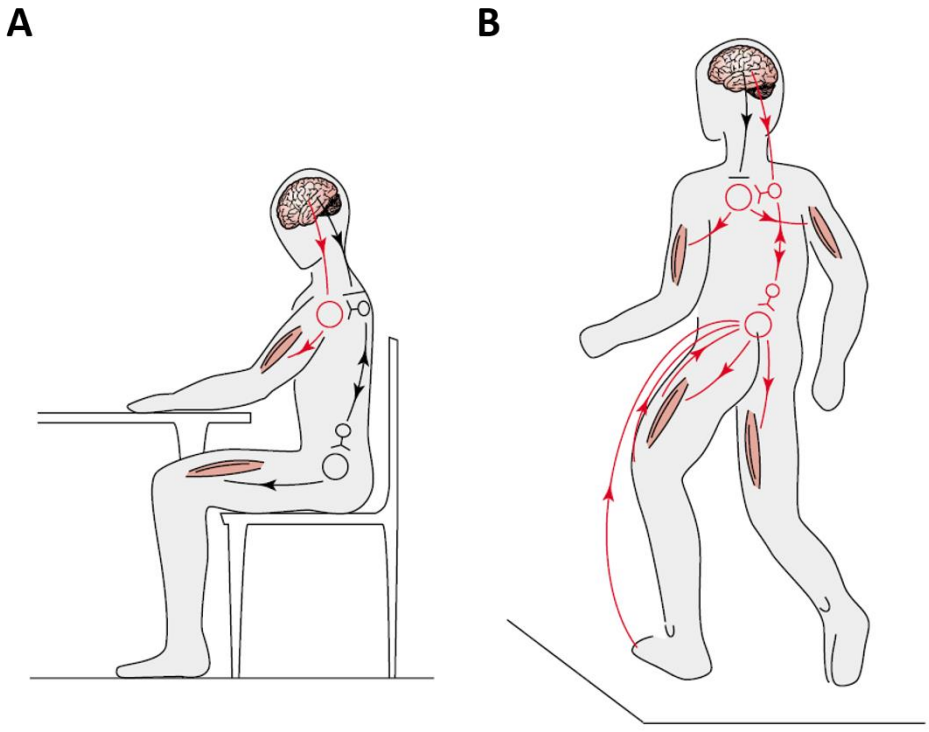

Figure 2.13. Task-dependent neuronal control of arm movement. A. Strong and direct brain command (red lines) is predominant over the certival propriospinal neuronal system allowing the skilled hand movements. B. Brain command is controlled by interneurons during locomotion. Propriospinal systems in cervical and thoraco-lumbar levels are coupled and coordinate upper and lower limb movements (Dietz, 2002).

control of upper and lower limbs is interdependent via interconnections resident within the spinal cord during locomotion-related movements. (Kawashima et al., 2008). The authors suggested that this result is likely due to the afferent sensory input induced by the upper limb movements that can influence the lower limb motor output via propriospinal neuronal connections, not the direct neural command to the lower limbs. These findings can draw an important suggestion that upper limb rhythmic movements can enhance and assist the lower limb's locomotor movement in SCI rehabilitation (Ferris et al., 2006; Meyns et al., 2013).

Eke-Okoro et al. investigated the effect of different types of arm movements (one arm strapped, both arms strapped, full excursion, ipsilateral arm and leg moving in the same direction, and both arms swinging in the same direction). They found that altering arm movements during walking caused a decrease in walking velocity (Eke-Okoro et al., 1997). Interestingly, they also found that when both arms were strapped, participants showed the steepest slope in the relationship between stride length and stride frequency, meaning that they tended to increase their walking velocity by increasing stride frequency rather than stride length.

The CPG might determine the relationship between these two factors in different modes of locomotion by using the various afferent sensory inputs from the periphery and the higher-order regulation areas, such as the brainstem and cortex (Eke-Okoro et al., 1997). Huang (2004) suggested that the lower limb muscle activation has a positive relationship with upper limb muscle recruitment during recumbent stepping activity in healthy individuals (Huang & Ferris, 2004), and Kao (2005) also demonstrated that fast upper limb movements could facilitate neuromuscular recruitment of lower limb muscles during recumbent stepping (Kao & Ferris, 2005). A more recent study also showed that the active arm movements induced the increase of leg muscle activations in both extensors (soleus, medial gastrocnemius, and biceps femoris) and flexors (TA) during

submaximal recumbent stepping task (Kam et al., 2013). Interestingly, it has been shown that the maximal voluntary effort of the upper limb movement facilitated the muscle recruitment of the lower limbs during passive rhythmic movement, but it was not true when the lower limbs were maximally activated (Huang & Ferris, 2009). Also, Sylos-Labini et al. (2014) observed that only AP hand-walking motions that were performed as participants lay on the right side of the body and moved the treadmill belt horizontally with their both arms elicited the locomotor-like movements of the lower limbs, whereas mediolateral (ML) arm movements did not (Sylos-Labini et al., 2014). This result indicates that the induced lower limb movements are not due to increased excitation in the neural circuit of the spinal cord caused by muscle contraction of the upper limbs and the mechanism of neural coupling of the upper and lower limbs is direction-specific (Sylos-Labini et al., 2014).

In summary, current literature suggests that both rhythmic arm and leg movements are regulated via CPG circuitries (Zehr et al., 2004; Zehr & Haridas, 2003). A flexible and task-dependent neural coupling of upper and lower limbs via linkage between the pattern generators in the cervical and thoracolumbar spinal cord allows humans to perform skillful and functional upper limb movements as well as basic locomotor activities. During normal gait, CPG is dominant for generating the rhythmic pattern for locomotion, but when more functional hand tasks are required, more elaborate regulation of interlimb coordination can be achieved via supraspinal involvement.

Mechanisms for arm swing generation: passive and active control

There is some debate about the origin of arm swing during walking: some authors have argued that arm swing is purely passive – such that the arms swing much like a physical pendulum due to the forces applied by the trunk (Li et al., 2001; Pontzer et al., 2009). Others have suggested that active muscle contractions generate arm swing (Ballesteros et al., 1965; Barthelemy & Nielsen,

2010; Goudriaan et al., 2014; Hosue, 1969; Jackson et al., 1978; Kuhtz-Buschbeck & Jing, 2012; Wannier et al., 2001). A more recent consensus is that it is primarily passive, with some active muscular contribution (Canton & MacLellan, 2018; Meyns et al., 2013).

In his pioneering study of the arm swing's role during locomotion, Elftman (1939) suggested that the active neural drive to the muscles contributes to the arm movement in walking (Elftman, 1939b). Using an inverse dynamics approach (Elftman, 1939a; Robertson et al., 2013), Elftman showed that the muscles connecting the arm and the trunk, such as the deltoids and TRAP, exert a considerable resultant torque during the stance phase (Figure 2.14), supporting his argument that active arm swing serves to counteract the rotation of the body induced by the advancing lower limb. The active arm swing then decreases the body's net angular momentum and, consequently, the total rotation in the vertical direction.

However, Pontzer et al. (2009) suggested the hypothesis that the muscle activity presented during arm swing is not necessarily associated with the active neural contribution but that the arms are more likely acting as passive mass dampers, which reduce the rotation of the body (Pontzer et

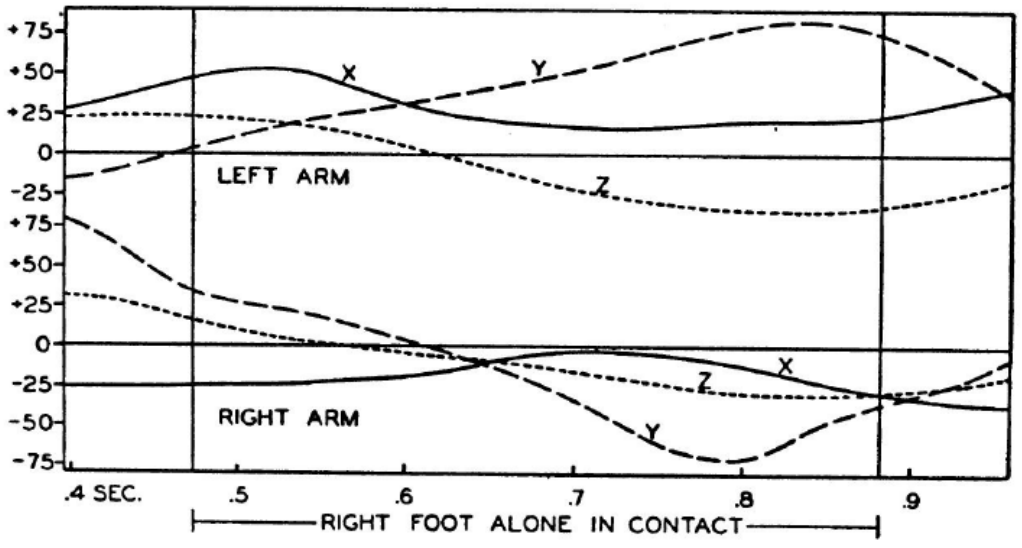

Figure 2.14. Resultant muscle torque on each arm, in three principal axes. Torque in kg.cm (Elftman, 1939b).

al., 2009). He also suggested that the net angular momentum suggested by Elftman as evidence for the active arm swing could also be generated by passive structures such as tendons and ligaments. This was partially inspired by the passive dynamic walker perspective (Collins et al., 2005). From this perspective, upper limb movement is generated by transferring forces from the lower limb movement and trunk to the shoulder (Pontzer et al., 2009), and active muscular contribution from the upper limb is minimal for swing movement during walking (Collins et al., 2009).

Despite Pontzer's perspective, consistent and reproducible rhythmic muscle activation during arm swing has been observed in several studies using surface and indwelling electrode EMG. Ballesteros et al. (1965) had observed rhythmic action potentials from the shoulder and upper arm muscles during both forward and backward arm swing while walking. EMG showed the activation in the LD, teres major, and PD during the backward swing, and the teres major and LD were activated during the forward swing (Ballesteros et al., 1965). Both backward and forward arm swing was also accompanied by the middle deltoid and TRAP activation to generate shoulder abduction to clear the trunk (Ballesteros et al., 1965; Ceccato et al., 2009; Hosue, 1969). Interestingly, Ballesteros et al. (1965) found that the shoulder muscles showed activations even when arm swing was constrained (Ballesteros et al., 1965), which can lead to the possible explanation that arm swing may be regulated via spinal CPG (Gray, 1956; Jackson et al., 1978). More recent studies have also provided evidence supporting active muscle contributions to arm swing (Barthelemy & Nielsen, 2010; Kuhtz-Buschbeck & Jing, 2012). As seen in Figure 2.12, natural walking generally involves the eccentric contraction of the PD showing activation peak around contralateral heel contact to limit the further forward flexion of the ipsilateral shoulder, and eccentric activation of TB around contralateral heel contact is likely responsible for limiting elbow flexion which is passively caused by walking task (Johann Peter Kuhtz-Buschbeck & Antonia

Frendel, 2015; Kuhtz-Buschbeck & Jing, 2012). It has also been found that the AD is responsible for active forward arm swing through concentric contraction during the ipsilateral stance phase and also for dampening the backward arm swing through eccentric contraction during the contralateral stance phase (Kuhtz-Buschbeck & Jing, 2012).

Another study was conducted to address the possibility of passive swing by using the computed arm kinematics of musculoskeletal modeling and dynamic simulation with and without active muscle contribution (Goudriaan et al., 2014). This study showed that only passive dynamics reduced the amplitude of swing and made the relative phase of arm movement more in-phase, indicating the active contribution is necessary to increase the swing amplitude and have an out-phase movement relative to the lower limbs (Goudriaan et al., 2014).

Other studies have also posed a challenge to the passive arm swing hypothesis. Jackson et al. examined the contribution of muscle torques in arm swing and concluded that arm swing would show a much higher amount of variation without muscular contribution (Jackson et al., 1978). Gutnik et al. suggested that muscular forces also contribute to the upper limb movement during walking rather than simple gravitational force acting alone (Gutnik et al., 2005). Barthelemy and Nielsen (2010) investigated the role of cortico-spinal drive in the control of arm swing during walking using transcranial magnetic stimulation (TMS) (Barthelemy & Nielsen, 2010). These results showed that the motor evoked potentials (MEPs) of the PD muscle were modulated during the gait cycle and that the short-latency intracortical inhibition (SICI) was also diminished during bursts of PD activity. Barthelemy and Nielsen concluded that the motor cortex makes an active contribution to the ongoing EMG activity in arm muscles during walking through the corticospinal tract by optimizing the backward and forward swing and phase-shifting between flexion and extension of the arm (Barthelemy & Nielsen, 2010).

Arm swing can also be interpreted in a combination of both passive dynamics and active neural control. A recent review suggested that a large part of arm swing is mechanically passive, but there is an active contribution from the muscles to initiate and terminate arm swing (Meyns et al., 2013). Although the relationships between the angular accelerations of the shoulders and trunk torsion and between arm acceleration and angular displacement of the shoulder which were interpreted as evidence of that arm swing occurs only due to the passive biomechanical linkage of body segments (Pontzer et al., 2009), it still cannot be concluded that those correlations are not related with the active contribution at all (Meyns et al., 2013). A combination of active control and passive dynamics has also been reported in other motor tasks such as ball bouncing (de Rugy et al., 2003), and the motor system may employ a similar principle for the regulation of arm swing during locomotion. For example, the arm segment can be modeled as a forced-driven harmonic oscillator with its preferred oscillation frequency (Holt et al., 1990; Turvey et al., 1988). In this scheme, the role of the muscle in regulating the arm movement is to either regulate the parameters of the oscillation or to generate forces at specific points for the movement cycle to maintain the kinetic energy of the swing. The former can be achieved by modulation of the limbs' apparent stiffness (Latash & Zatsiorsky, 1993). In a more recent study where passive dynamics versus active neural control was investigated by manipulation of pelvic motion introducing the change in the mechanical energy transfer from lower limbs during walking, the amplitude of arm swing was significantly decreased by the restriction of the pelvis, indicating the arm swing is affected by passive mechanics (Canton & MacLellan, 2018). However, the conservation of gait patterns and muscle activations indicates that there is also an active contribution (Canton & MacLellan, 2018).

INTEGRATION OF LOCOMOTOR AND MANUAL TASKS

Evolutionary considerations

Habitual bipedalism is a uniquely human characteristic compared to other animal species (Gebo, 1996; Schmitt, 2003). While there are several hypotheses about the evolution of this trait (more efficient energetics, increased field of view, reduction of body surface exposed to direct solar radiation), one prominent view is that bipedal locomotion allowed a more flexible means to transport objects and allowed object manipulation while walking (Hewes, 1961; Lovejoy, 1988). The use of the upper limb to transport food is also observed in other primates such as chimpanzees, baboons, and macaques (Kohler, 1959; Niemitz, 2010). Thus, it is reasonable to expect that the ability to walk on two feet developed to free both hands to do many other tasks such as carrying an infant or gathering and carrying food over long distances, or building and using tools for hunting while moving (Niemitz, 2010).

Reaching and grasping while walking

Activities of daily living often involve moving through the environment while simultaneously carrying and manipulating objects in hand. Everyday tasks, such as carrying a bag of groceries or a cell phone while moving from one place to another, require elaborate coordination between upper and lower limbs to generate smooth and efficient movements. These coordinated human movements can be obtained through appropriate sensory input and a proper amount of muscular force with precise timing. An increased interest in motor adaptations during combined tasks where both upper and lower limbs are involved has emerged over the last three decades. Cockell et al. found that participants tended to use the ipsilateral lower limb as the support limb when they were asked to pick the object up, regardless of the upper limb side (Cockell et al., 1995). A study carried out by Carnahan et al. (1996) revealed that picking up a small cylinder-shaped

object while walking caused an alteration in upper limb kinematics but did not induce the change in gait patterns, suggesting that maintaining lower limb stability was prioritized more than precise prehension during gait (Carnahan et al., 1996). In a similar study which transporting a cup filled with water from one place to another, Bertram et al. found a decrease in forwarding velocity of the trunk, indicating the different nature of the prehension task in terms of the level of difficulty of the task itself might induce the walking adjustments (Bertram et al., 1999). To obtain concise information on gait adjustments, Bertram extended this work by including locomotion analysis on lower limbs. The results supported his assumption in that the task with the higher level of difficulty (lifting and displacing the uncovered cup while walking) resulted in a greater duration of the stance phase (Bertram, 2002). In this study, the participants were asked to walk approximately 2 m and grasp a cup of water placed on a table, place the cup on the target, and continue walking for approximately 1.5 m at a comfortable walking velocity. To perform this task, the participants were asked to transport the cup to the target as quickly and as accurately as they could. It is interesting to note that even though there were some adjustments in both upper and lower limb movement patterns, the duration taken to complete the whole task was not significantly different between the covered and uncovered cup (only 170 ms longer with the uncovered cup). These results support the ideas of "motor abundance," indicating that the task's functional goal can be achieved with numerous movement strategies, and this is important for the motor system to deal with secondary tasks and/or unpredicted perturbations, allowing a variety of adaptive modulation patterns (Latash, 2012). Also, the upper and lower limbs can interact with each other to accomplish a task goal via individual and complementary adjustments that are task-specific synergies of upper and lower limb coordination (Bertram, 2002).

In a more recent study, the effects of different levels of difficulty of walking and prehension

tasks in healthy young individuals were investigated (Rinaldi & Moraes, 2015). First, they found that this prehension task during walking over the obstacle caused the increase in step duration and also an increase in the margin of dynamic stability in the AP direction during the approach phase and at object grasping, indicating that a more conservative walking pattern was preferred for dynamic stability while doing manual tasks simultaneously. In this study, the margin of dynamic stability was calculated as the difference between the position of the extrapolated CoM and the edge of the base of support (BOS) (Hof, 2008; Hof et al., 2005); where the extrapolated CoM considers the velocity and the position of the CoM in space, allowing to identify if the system is dynamically stable or not. Moreover, the walking task changed the characteristics of prehension as it reduced the time for reaching, maximal wrist velocity, and peak grip aperture velocity. In addition, grip aperture was affected by the presence of obstacles while walking, indicating that the walking task can influence not only the reaching movement but also the grasping behavior. In a later study, Rinaldi et al. (2017) found that older adults, especially those with previous fall experience, tended to decouple the walking and prehension tasks by adopting a more anti-phase pattern between the right shoulder and hip in the frontal plane when compared to the older adults without fall history. Also, they prioritized the movement of the right shoulder by increasing and decreasing the movement phase for the right and left shoulder, respectively. These results indicate that interlimb coordination patterns and motor control can be affected by aging and the history of falls, which might cause impaired locomotor control (Springer et al., 2006). Decreased functionality of neural activation has been observed in older adults (Beurskens et al., 2014; Bishop et al., 2010), and especially elderly adults with a history of falls might have difficulties to divide and switch attention in performing dual tasks (Springer et al., 2006). One theoretical interpretation of these findings is that relative overloading on supraspinal structures due to the reduction in neural

activity might cause disrupted rhythmic activity of the purported spinal CPGs and further decoupling of movements in the older adults (Beurskens et al., 2014; Rinaldi et al., 2017).

Coordinative adaptations of object transport while locomotion

During object transport while walking, the GRF generated from the foot's interaction with the ground acts as an external perturbation force that produces a sinusoidal trajectory of the trunk, upper limb, and of the transported object in the sagittal plane. Previous research suggested that the dampening of the transport path is a motor strategy to decrease IFs acting on the object, which is obtained by decoupling motion of the trunk and upper limb through the separate adjustment of the shoulder, elbow, and wrist joints, rather than holding the object with a rigid upper limb (Gysin et al., 2003a; Gysin et al., 2009). It has been suggested that during multi-joint movements, central motor commands to muscles are adjusted in a predictive manner in order to compensate for the interaction moments at certain joints caused by the motion in other joints (Gribble & Ostry, 1999).

Previous research has also shown that holding a cup of water in one hand during stepping down decreased participant's walking velocity as well as decreased CoM displacement in the medial-lateral direction, indicating the alteration of upper limb dynamics can also induce lower limb adaptations during a functional locomotor task such as stepping down a stair (Madehkhaksar & Egges, 2016). Another study involving a similar experimental task, i.e., transporting a cup filled with water while walking, also found that a flexible and coordinated control strategy through coordinated multi-joint motions is used to maintain the constant cup angle and to reduce the hand jerk as a dampening strategy (Togo et al., 2012).

A study investigating the effect of asymmetric load (hand-held bag) carrying during walking found the changes in hip abduction torque in both lower limbs and the magnitude of contralateral shoulder abduction in older women (Matsuo et al., 2008). A more recent study has

investigated the effect of asymmetrical load-carrying while stepping down a curb on interlimb coordination of the upper limbs and walking parameters in young adults (Silva et al., 2019). This study showed that carrying a bag in either the dominant and non-dominant hand altered the upper limb coordination pattern by restricting the movement of the carrying limb and reducing the anti-phase coordination pattern. In this study, however, there were no changes in the spatial-temporal gait parameters such as stride length, duration, and speed, indicating that young individuals might be able to deal with the perturbance without gait adaptations.

Placing additional weight on the upper limb during walking decreases the amplitude of arm swing with increased shoulder muscle activity (Donker et al., 2005; Donker et al., 2002; MacLellan & Ellis, 2019). This asymmetrical mass perturbation on one side of the upper limb also affected the contralateral upper limb, showing that interlimb neural coupling also exists between the left and right upper limbs. When adding a load of 1.8 kg on one side of the wrist, arm swing amplitude on the unweighted side increased while that of the weighted arm decreased (Donker et al., 2002). Interestingly, a significant increase in EMG activation in the deltoid muscles on the contralateral side was observed as well in the weighted arm without any changes in movement frequency of the limbs. The authors suggested that this increased EMG activity might be due to the interlimb neural coupling for both arms, where the motor command is sent to both arms resulting in a more significant movement of the unloaded arm (Donker et al., 2002). The authors also suggested that the observed adaptations in the arm movements were made primarily to conserve the fixed temporal relationship between arm and leg movements as a more efficient control strategy for balance under the peripheral disturbances, and one of the most basic aims of the motor system is to preserve the constant motor output with no changes in the phasic relationship between limbs (Donker et al., 2002).

GRIP FORCE REGULATION DURING OBJECT TRANSPORT

When carrying an object, an appropriate GF level needs to be generated by the fingers to prevent the object's slippage. Studies have shown that to complete this task, predictive control of grip is required to counterbalance the gait-induced IFs throughout the gait cycle — termed " GF-IF coupling" (Diermayr et al., 2008; Gysin et al., 2003a; Gysin et al., 2008), characterized by reduced hand jerk and maintaining a constant object angle (Togo et al., 2012). Here, the IF is a fictitious force that appears to be present when there is an acceleration caused by the locomotor activity, referred to as the resultant net force calculated from the vertical load force (LF) and AP horizontal force (HF) (Figure 2.15) (Diermayr et al., 2008; Gysin et al., 2003a).

In addition to maintaining a secure grasp through the anticipatory adjustment of GF on the transported object, synchronized vertical displacement of the trunk and transported object is

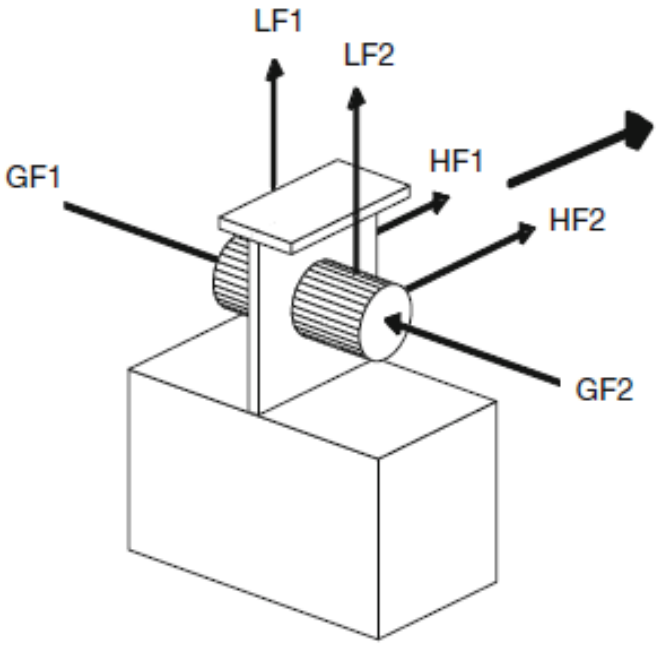

Figure 2.15. Two force transducers are inserted in grip instrument (seen from the back). The largest arrow indicates the walking direction, and the smaller arrows represent the direction of force. GF, grip force; LF. Load force; HF, horizontal force (in AP direction) (Diermayr et al., 2008).

achieved by coordinated movement of the upper limb to maintain the carried object's stability. When an external force is applied to the system, such as gait-induced IFs, the control process occurs to counteract the limb inertia produced by the perturbation, leading to maintenance of postural stability by a decrease of mechanical and physical oscillations of the body after perturbation (Lin & Rymer, 2000, 2001). Gysin et al. (2003) found evidence for anticipatory grip modulation during the object transport while walking because the GF and LF were nearly synchronized throughout the gait cycle (Figure 2.16A) (Gysin et al., 2003a).

Moreover, this study also found that the GF measured by a force transducer attached to the object and walking-induced IFs acting on the object are highly coupled, regardless of task constraints (Figure 2.16B) (Gysin et al., 2003a). Gysin et al. (2009) have proposed that the control of GF while walking is achieved not only by moment-to-moment predictions of IFs exerted on the object throughout the predictable variation in the gait cycle but also by the internal representations of the interactions between body segments where the inertia is transmitted to the object-digit interface providing the basis for the predictive GF control (Gysin et al., 2009). In addition, the authors suggested that this continuous GF modulation throughout the gait cycle and tight correlation between grip and IFs maximize the task efficiency by reducing the muscular energy consumption (Flanagan & Wing, 1993; Gysin et al., 2003a; Kinoshita et al., 1996).

Grasp control has also been investigated in individuals with neurological pathologies. Individuals with Parkinson's disease demonstrated a decreased ability to dampen the hand-held object's motion while walking (Albert et al., 2010). This group was not able to maintain the anticipatory coupling between grip and IFs during unperturbed walking. However, the change in GF relative to the IF was delayed when they had to step over an obstacle (Diermayr et al., 2011), resulting in difficulty during complex object transport and manipulation tasks.

To examine whether this GF-LF coupling comes from the instantaneous prediction by the

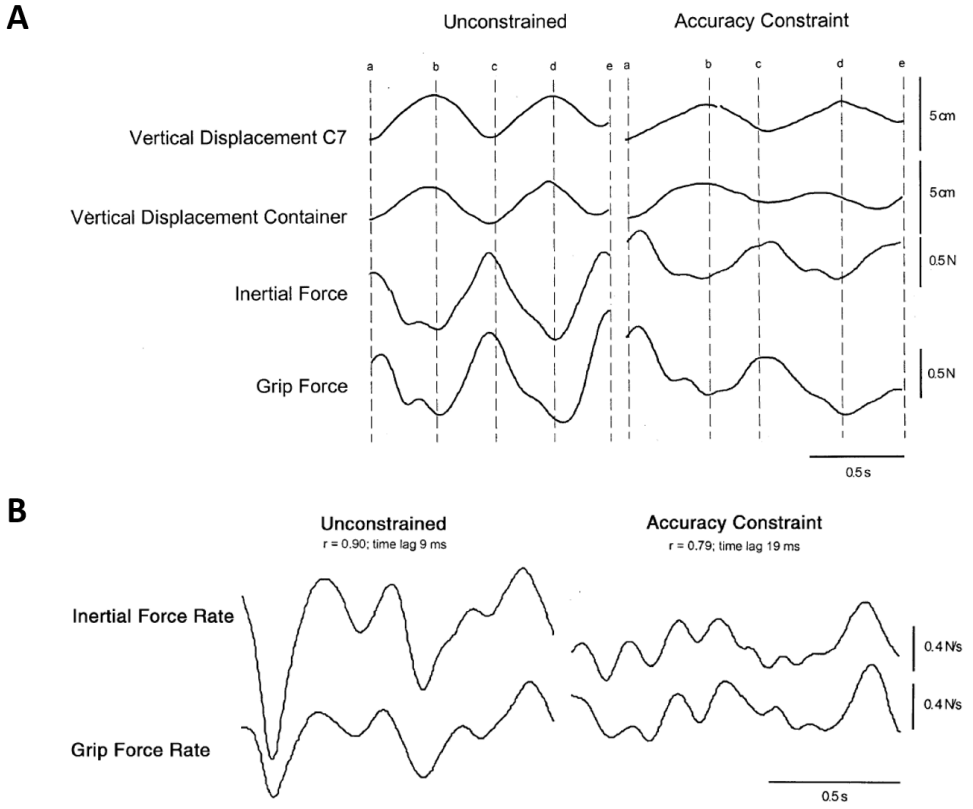

Figure 2.16. A. Vertical displacement of the trunk (C7) and hand-held container. Inertial and grip force are also presented. The vertical dashed lines represent heel contact (lines a, c, e) and MST (lines b, d). B. Spatio-temporal synchronicity between grip force rate (dGF/dt) and inertial force rate (dIF/dt) (Gysin et al., 2003).

CNS regarding the upcoming inertial changes or generalized time estimation for the normal walking, Gysin et al. incorporated five different walking variations into the experiment, including changes in step length (shorter or longer), stepping on and stepping over a stable or unstable obstacle (Gysin et al., 2008). Similarly, continuous and anticipatory grip adjustment, as well as a tight temporal coupling between GFs and IFs were present in all gait variations except the stepping on the unstable obstacle, suggesting that the CNS uses the feedforward system to predict the upcoming changes of IFs and to adjust the grasping forces instantaneously to maintain the object stability during the predictable gaits (Gysin et al., 2008). Feedforward internal model-based control, providing the relevant sensorimotor features regarding consequences of upcoming motion, have been reported as a basis for the anticipatory coupling between GF and LF (Blakemore et al., 1998; Flanagan et al., 2001; Flanagan & Lolley, 2001; Flanagan et al., 2003; Flanagan & Wing, 1997; Salimi et al., 2000; White et al., 2005; Alan M Wing & Susan J Lederman, 1998). However, a recent study also suggested the idea that GF-LF coupling during manipulation of a complex object may not arise from the explicit feedforward internal model-based control as it should be impossible to predict the object's changing LFs (Grover et al., 2021). The locomotor control network might contribute to this anticipatory control process during the various walking contexts (Choi & Bastian, 2007), and propriospinal connections linking the movement of upper and lower limbs might be involved in the force coupling during object transport during locomotion (Gysin et al., 2008).

Role of task constraint during object transport while walking

As described above, previous studies on object transport while walking have found that the tight coupling of GF-LF in relation to the gait events as well as synchronized movement trajectories of the trunk and carried object contribute to stabilizing the object (Diermayr et al., 2008; Gysin et al., 2003a). However, most of the studies on object transport during locomotion

have involved the objects with relatively predictable dynamics (Diermayr et al., 2008; Diermayr et al., 2011; Daniela Ebner-Karestinos et al., 2016), which allows the CNS to estimate the proper timing and magnitude of GF before the external perturbation. In this case, the carried object is relatively free to move in the AP direction and ML direction. In other words, the constraint on object transport is minimal in both object orientation and translation. The only significant constraint required to avoid slippage of the object is that the amount of GF matches or exceeds the LF (combination of weight and IF, when accelerations are present). Gysin et al. (2009) have found that the magnitude of GF fluctuation in the ML direction was less than 5% of maximum GF with a path of single sinusoid for each gait cycle when compared to two sinusoids in the vertical direction. In addition, during locomotion with a forward-oriented object, the GFs applied to the thumb and index finger were in-phase with a difference of less than 4% of maximum GF, indicating these forces increase and decrease simultaneously with a very small difference which is similar to during quiet standing. These results indicate that the GFs generated in the ML direction from lateral shifts of the body or out-of-plane motions have a minimal effect on the coupling between GF and IF (Gysin et al., 2003a; Gysin et al., 2009).

Gysin et al. (2003) investigated the effect of accuracy constraint during the object transport task while walking overground by having participants carry an uncovered water-filled container. The results of the study showed that the coupling of GF-LF was consistently controlled in an anticipatory manner, but the vertical displacements of the trunk, carried container, GF, and IF were significantly decreased during the task with accuracy constraint. Gysin et al. (2003) also found that participants showed slower walking velocity during the accuracy constraint condition, which is supported by a recent study (Mayer & Krechetnikov, 2012). Mayer and Krechetnikov have reported that coffee spills while walking are affected by the amount of liquid, the speed of walking,

and the cup's size, with spills occurring when the natural frequency of liquid oscillations and the frequency of human walking become the same. As individuals increase the number of steps and the rate of steps (velocity of walking), the increase in coffee sloshing is due to the resonant excitation, which indicates that one of the effective ways to avoid coffee spilling is to reduce the walking speed.

In his recent dissertation, Amado (2019) has attempted to broaden perspectives on this issue by incorporating a transported object with a higher precision demand. He used a ball-cup system as an object that increases the unpredictability of the task while increasing task constraints. When individuals carry this type of object or an uncovered cup filled with water, it can be easily expected that they would minimize the translation of the object (with respect to the trunk) not only in both AP and ML directions but also in the vertical direction to avoid the dropping the ball from the surface of the cup or spilling of the content inside of the cup under the continuous perturbation from the gait-induced IFs. Amado (2019) found the decrease in arm range of motion accompanied by changes in interlimb coordination between the pelvis-thorax as well as arm-leg segments during walking when holding the object of the cup-ball system when compared to normal walking and cup-alone conditions (Amado, 2019). Alterations in GF and coordination patterns provide one window into the neural control strategies, but how such constraints affect upper limb muscle coordination patterns remains unknown. Further investigation of muscular contributions to upper limb stabilization would help better understand how humans adapt to this task with higher task constraints.

Sensory information influences object transport while walking

Maintaining dynamic stability requires precise motor control using sensory integration from proprioception, visual, and vestibular inputs, informing about the state of the body with

respect to the environment. During object transport while walking, sensory information from visual and proprioceptive systems is critical to complete this task. Proprioception provides information about the body's position, movement velocity of the limbs, the loaded weight by the object. The sensory structures involved in proprioception include muscle spindles, Golgi tendon organs (GTOs), tactile and joint sensory receptors, such as Ruffini endings, Pacinian corpuscles, and free nerve endings (Kandel, Schwartz, Jessell, Biochemistry, et al., 2000). The perception of the object's mass and moment of inertia properties obtained from joints and muscles are also essential to gauge the proper level of GF to counteract the IFs. In addition, visual information about the carried object's location relative to the trunk and the upper limb enables the CNS to determine the movement trajectory of the upper limbs and the object's orientation. The CNS integrates the sensory information from these proprioceptive and visual systems to generate a more accurate motor command to accomplish this particular goal of the task (Sarlegna & Sainburg, 2009; van Beers et al., 1999).

Although the effect of alteration in sensory integration has not been thoroughly investigated in the literature focusing on object transport during walking, it has been suggested that the altered movement patterns are associated with the impaired sensory integration (Gordon et al., 2000; Quinn et al., 2001; Schwarz et al., 1992). Variability in the movement trajectories and forces have been observed during upper limb movement in people with Huntington's disease who are thought to have impairments in processing sensory information and using it to modulate motor output (Gordon et al., 2000; Schwarz et al., 1992). Quinn et al. reported that impairment in integrating sensory information might affect intersegmental dynamics during object transport tasks when participants lift and transport the object, generating more curvilinear movement trajectories during the early stage of the task (Quinn et al., 2001). Johansson and Flanagan also suggested that

sensory integration, especially tactile input, is critical for the proper estimation of GF to IFs or LFs during the grasping while walking task (Johansson & Flanagan, 2009). It has also been reported that people with impaired sensorimotor processing due to basal ganglia dysfunction, lacking tactile and proprioceptive sensory feedback, or cerebellar pathology showed an abnormal increase in GF during manual tasks such as drawer-pulling task or grasping an object (Nowak & Hermsdorfer, 2006; Wiesendanger & Serrien, 2001). The results of the studies above underline the importance of sensorimotor integration in terms of proper force control throughout the movements, indicating that the altered sensory integration might affect the motor output as the alternative motor control strategies are used to accomplish the movement goal to adapt to the alteration in sensory integration.

The body of literature on object transport has allowed using visual information regarding the carried object (Chiovetto & Giese, 2013; Gysin et al., 2003a). Therefore, it is reasonable to expect that from those studies, both central visions regarding the position of the object relative to the hand in space and proprioceptive information were available for participants to achieve the object transport task and to maintain the stability of the object. In reality, however, individuals transporting an object while walking sometimes need to shift their visual attention to other sources outside of the object leading to only peripheral vision available about the transported object, for example, looking at an attractive person passing by while holding a cup of coffee on the way to campus, making them rely on proprioception and peripheral vision to stabilize the hand-held object as well as the entire body.

Mayer and Krechetnikov reported that the completion of the task of carrying a cup of coffee while walking is considerably more affected by the sensory feedback, i.e., visual information, rather than the changes in basic parameters, such as small alterations in step length or frequency

in coffee spilling phenomena. Through the sensory feedback, not only human can identify the resonant sloshing frequency and then performs a targeted suppression of the resonant mode by kinematic and kinetic changes in the wrist, elbow, and shoulder joints. Studies involving the effect of visual information on the carried object would provide further insight into the neuromuscular strategies adopted by CNS for the successful completion of this task. (Mayer & Krechetnikov, 2012).

CHAPTER 3. INTER-LIMB COORDINATION OF SHOULDER MOVEMENT DURING OBJECT TRANSPORT: STUDY 1

INTRODUCTION

In the majority of previous studies on arm swing coordination during steady-state gait, researchers have utilized “passive” manipulations of limb asymmetry such as added mass (Donker et al., 2002; Haddad et al., 2006; Serrien & Swinnen, 1998) or physical arm restraints (Ford et al., 2007; Umberger, 2008). However, what would happen if constraints on the arm motion are more goal-oriented and functional as opposed to physically passive and artificial restraint? Such constraints are typical of functional carrying movements such as walking and looking at a cell phone screen in one hand – the cell phone constrains the motion of one arm to stabilize the screen to reduce retinal slip (de Brouwer et al., 2001). Does the decreased contribution to the angular momentum of the upper body from that constrained arm then lead to alterations of the contralateral arm movement as expected from the conservation of angular momentum strategy? In addition, a thorough understanding of the changes in the kinematics of the arm movements is fundamental to the interpretation of muscle activation patterns in the subsequent studies reported in the dissertation.

The term “coordination” is defined as "the organization of the different elements of a complex body or activity to enable them to work together," according to the Oxford dictionary (Stevenson, 2010). Coordinated movements are multidimensional: spanning multiple subsystems (Shirota et al., 2016), such as eye-hand coordination (Johansson et al., 2001), intersegmental coordination (Borghese et al., 1996), intralimb coordination (Cirstea et al., 2003), interlimb coordination (Ivry et al., 2003). The term interlimb coordination refers to the spatio-temporal relationships between kinematics, kinetics, and physiological variables of two or more limbs performing a task to achieve a common movement goal (Shirota et al., 2016). This interlimb coordination can be applied to tasks where two homologous limbs (for example, bilateral arms or

legs) are involved, where two non-homologous limbs (ipsilateral arm and leg) are involved, or where three or more limbs (arms and legs) are involved.

Researchers have studied interlimb coordination during motor tasks to understand how the CNS controls numerous degrees of freedom (DOF, motor redundancy), and therefore, how it produces effective and efficient movement strategies (Courtine & Schieppati, 2004; Dietz et al., 1994; Reisman et al., 2005; Shirota et al., 2016; Swinnen et al., 1995). They have reported that well-coordinated human movements indicate a sophisticated neural control system regulating motion at multiple joints and generating proper movement relationships between body segments. In addition, the ability to coordinate motions across various systems is critical for dealing with varying environmental circumstances with different terrain, velocity, and trajectories (Reisman et al., 2005).

Human walking involves a continuous modification of interlimb coordination of the upper and lower limbs regulating joint kinematics, as well as numerous muscle activations generating the proper amount of force with appropriate timing to maintain dynamic stability and to produce optimal motor patterns for the environment. The maintenance of reciprocal and out-of-phase motions of the limbs through interlimb coordination is essential during bipedal walking (Reisman et al., 2005). As reviewed in Chapter 2, the anti-phase temporal coordination of the upper limbs also plays a critical role in minimizing the body's total angular momentum (Elftman, 1939b; Herr & Popovic, 2008) and minimizing energy expenditure of gait (Collins et al., 2009; Ortega et al., 2008; Umberger, 2008; Yizhar et al., 2009).

The pattern of spatio-temporal coordination between the arms during gait is adaptive depending on the constraints imposed on the system (Haddad et al., 2006). In previous studies, asymmetrical constraints on the upper limbs have been introduced to understand the extent of

adaptability or plasticity of interlimb coordination dynamics (Donker et al., 2005; MacLellan & Ellis, 2019; Matsuo et al., 2008). Carrying a fixed 1.8 kg load attached to one of the wrists did not induce a change in temporal coordination between limbs, but different walking speeds affected the frequency coordination between arm and leg movements (Donker et al., 2005). Asymmetrical unilateral arm weighting fixed on participants' forearm reduced the arm swing excursion, but temporal coordination between limbs remained unaffected (MacLellan & Ellis, 2019). Matsuo et al. (2008) reported that carrying a 3- or 8-kilogram load in one hand while walking caused increased hip abduction torque on the ipsilateral lower limb and increased shoulder abduction on the contralateral side.

However, the characteristics of constraints imposed on the arm also influence limb coordination patterns during walking. For example, instead of adding a mass fixed on the wrist, Ford et al. (2007) restrained the arm swing by asking participants to place their arm in a sling anchored to the trunk using a Velcro strap. This study showed that the arm swing on the contralateral side increased compared to natural walking, especially when walking at higher speeds. More importantly, they found that constraining the arm in a sling resulted in altered frequency and phase relationships between the upper and lower limbs on the restrained side. More recently, Silva et al. (2019) investigated the effect of asymmetrical load carrying on interlimb coordination of the upper limbs during downward stair-stepping using a new type of task constraint where participants were required to hold a middle portion of the strap similar to the strap of a plastic bag, which makes the task less predictable due to the movement of the strap when compared to holding and carrying the bag in their hands without the strap holding a piece of wood fixed to the border of the bag (Silva et al., 2019). They found that this asymmetrical load-carrying decreased the frequency of the anti-phase shoulder coordination and reduced movements of the upper limb with the load.

Several researchers have examined adaptations of interlimb coordination during combined tasks whereby both the upper and lower limbs are involved, such as reaching and grasping during walking. Performing the upper limb task of placing an object on a surface while walking changed the arm-leg coordination pattern from anti-phase towards in-phase as the reaching movement of the arm and stepping forward of the ipsilateral lower limb occurred simultaneously (Rinaldi & Moraes, 2015) and affected the upper limb coordination (Rinaldi et al., 2017). However, the level of precision required on the placement task did not affect interlimb coordination between shoulders (Rinaldi et al., 2017). Another study reported no evidence for preferred interlimb coordination patterns during the prehension while walking and these two tasks are planned and controlled independently using separate motor control mechanisms (Bellinger et al., 2019). Since reaching to grasp is a relatively transient event while walking, the results of the study can vary depending on the biomechanical constraints, such as the height of the table where the object is placed, the horizontal distance between the walking trajectory and the table, speed of walking, and the properties of the object.

While most of these previous studies have focused on limb coordination with passive manipulations of constraint to induce limb asymmetry, a recent study incorporated object transport with different precision demands (Amado, 2019). Amado (2019) investigated the effect of carrying a cup of water on a human's intrinsic dynamics during walking. To model the behavior of the actual task of carrying a glass of water, he used the conceptual task where the lid with a target circle was placed on top of the glass and a small ball was placed on the top of the target surface to represent the fluid in the cup. He found that this asymmetrical upper limb task affected the pelvis-thorax coordination pattern by shifting to a more in-phase pattern compared to natural walking. Arm-leg coordination was also affected by the task, showing the frequency of 2:1 in the constrained side

while the unconstrained side maintained a 1:1 frequency relationship.

The purpose of this study was to examine the changes in the kinematic pattern of interlimb coordination of the upper limbs while carrying an object in one hand during walking. Since carrying an object in one hand would break the natural coordination of the arm swing between the two arm movements, it is reasonable to expect that carrying an object in hand would constrain not only the upper limb used for carrying but also should affect the motion of the contralateral limb. And this change might cause altered coordination patterns between upper limbs to maintain overall gait stability and to adapt to this ecological constraint. The task involved grasping a cylindrical object while holding the elbow flexed at approximately 90 degrees, representing typical object transport cases in daily activities such as carrying a cup of coffee or cell phone while walking. In this study, upper limb coordination was examined, specifically between the shoulder joints, the angular displacement of bilateral shoulder and elbow joints using kinematics analysis, and upper limb muscle activations. A vector coding technique (Chang et al., 2008) was used to quantify the interlimb coordination changes between both shoulder joints during the task with the dominant and non-dominant hand when compared to natural walking. The vector coding method has been used in previous studies to provide a more direct measure of interlimb coordination utilizing the analysis of the angle-angle plot of two separate segments of joints motion (Hamill et al., 1999; Van Emmerik et al., 2014). In addition, muscular activations of major upper limb muscles were recorded in order to investigate whether observed kinematic alterations are mainly due to the changes in muscle activations or not.

Hypotheses

It was hypothesized that transporting an object would result in a decreased movement amplitude of the shoulder and elbow joints accompanied by a concurrent increase in the amplitude

of the contralateral shoulder and elbow joints as reported earlier (Ford et al., 2007; Matsuo et al., 2008). The alteration of arm movement would then also lead to a change in interlimb coordination between shoulders. Lastly, the muscle activation patterns would differ between dominant and non-dominant arms based on the observed differences in controlling inter-segmental dynamics of dominant and non-dominant limbs (Sainburg, 2002)

METHODS

Participants

Eight healthy right-handed adults free of orthopedic, cardiovascular, and neuromuscular deficits participated in this study (four females, 23±3.30 years, 172.11±9.81 cm, 67.13±8.75 kg). Edinburgh Handedness Inventory score was + 86.08 on average ranged between 70 and 100. The Edinburgh Handedness Inventory was performed to identify each participant's dominant hand. If a participant scored greater than +40, the participant was determined as right-handed, if a participant scored between -40 and +40, then the participant was classified as ambidextrous, and if a participant scored less than -40, then the participant was determined as a left-handed. All participants signed a written informed consent document approved by the Institutional Review Board at Louisiana State University.

Experimental protocol

The experimental protocol consisted of participants walking on a treadmill in five conditions: 1) holding an object in the dominant arm (D-OBJ), 2) holding an object in the non-dominant arm (ND-OBJ), 3) dominant arm-positioning without an object (D-NOBJ), 4) non-dominant arm-positioning without an object (ND-NOBJ), and 5) treadmill walking without any object or instructed arm-positioning (TW). The transported object was a 15 oz. cylindrical aluminum can (height: 11.2 cm, diameter: 15 cm, mass: 425 g). During the object transport

conditions (D-OBJ and ND-OBJ), participants were instructed to walk on the treadmill at their preferred over-ground walking speed (see below) while holding the object in their dominant or non-dominant hand. They were asked to keep their elbow at approximately 90° of flexion and maintain a vertical orientation of the object while walking. Since it has been reported that GF modulates the activation pattern of shoulder muscles (Hodder & Keir, 2012; Sigholm et al., 1984; Smets et al., 2009; Sporrong et al., 1995), the no-object condition was also included in order to identify the effect of GF generated by the muscle activation of fingers. In the no-object conditions (D-NOBJ and ND-NOBJ), participants were asked to hold their arm similarly to the D-OBJ/ND-OBJ conditions, but they had no physical object and were told to keep the arm as if they are carrying an imaginary object. Five experimental conditions were presented in randomized blocks consisting of two trials, each with at least 25 strides.

Self-selected over-ground walking speed was determined by asking participants to walk on a 3.6-meter walkway at a comfortable pace (i.e., they were instructed to walk as naturally as possible at their comfortable walking speed along the walkway before attaching any equipment). This procedure was repeated three times, and the average speed was applied when they walk on the treadmill.

Data collection and analysis

Whole-body 3D kinematics were acquired using a 4-sensor Codamotion CX1 optoelectronic system (Codamotion, Rothley, UK). An infrared marker was placed at the spine of the C7 vertebrae, and 24 markers were placed bilaterally on the acromion process (shoulder), lateral epicondyle of the humerus (elbow), ulna- and radius-styloid processes (medial and lateral wrists, respectively), metacarpophalangeal (MCP) joint of a middle finger, distal phalanx (DP) of a middle finger, greater trochanter (hip), lateral epicondyle of the femur (knee), lateral malleolus

of the tibia (ankle), posterior surface of the calcaneus (heel), head of fifth metatarsus (fifth toe), and head of first metatarsus (hallux). All markers were placed on the skin, except for the heel, fifth toe, and hallux, which were placed on the participants' shoes. Missing data segments of less than 100 ms were interpolated using a cubic spline algorithm (spline.m in Matlab 2020b). All kinematic data were sampled at 100 Hz and were low-pass filtered using dual-pass, second-order, Butterworth filter with a cut-off frequency of 7 Hz.

A gait cycle was defined based on heel strikes. Heel contact was determined using a vertical velocity threshold of 120 mm/frame. All gait cycles of each marker's data were then time-normalized to 100 data points, with each data point representing 1% of the gait cycle. The first three and the last two gait cycles of each trial were excluded from the analysis to ensure walking speed and stride length consistency. Kinematics and EMG of the body's dominant and non-dominant sides were analyzed based on the ipsilateral gait cycle.

Angular displacement of shoulder and elbow joints

The shoulder angle in the sagittal plane (θ_{ss}) during each gait cycle was computed using the inverse tangent function to calculate the angle generated by the vertical line parallel to the trunk and the line connecting the shoulder and elbow markers (Figure 3.1A). The angle was calculated for both shoulders, and the angular displacement was quantified using the peak-to-peak amplitude difference within each gait cycle. The angular shoulder movement in the transverse plane was calculated, representing the upper torso's movement pattern during walking. The angle between the vector connecting the acromion markers and the walking direction vector (θ_{sw}) was computed using the dot product (Figure 3.1B). The walking direction vector was estimated from the first component vector from the principal component analysis (PCA) on heel markers (left and right) in the X-Z plane (Figure 3.1C). Identification of the precise walking direction on a treadmill was

needed because the global coordinate system X-axis was slightly not parallel to the treadmill belt direction. The elbow joint angle (θ_E) was estimated using the dot product of the 3D- kinematic data of the shoulder, elbow, and medial wrist markers (Figure 3.1D).

For these three angular displacements (shoulder in sagittal and transverse planes and 3D-elbow angle), the angular displacement over the time-normalized gait cycle was averaged over all trials for each experimental condition for each participant. This mean angular displacement was

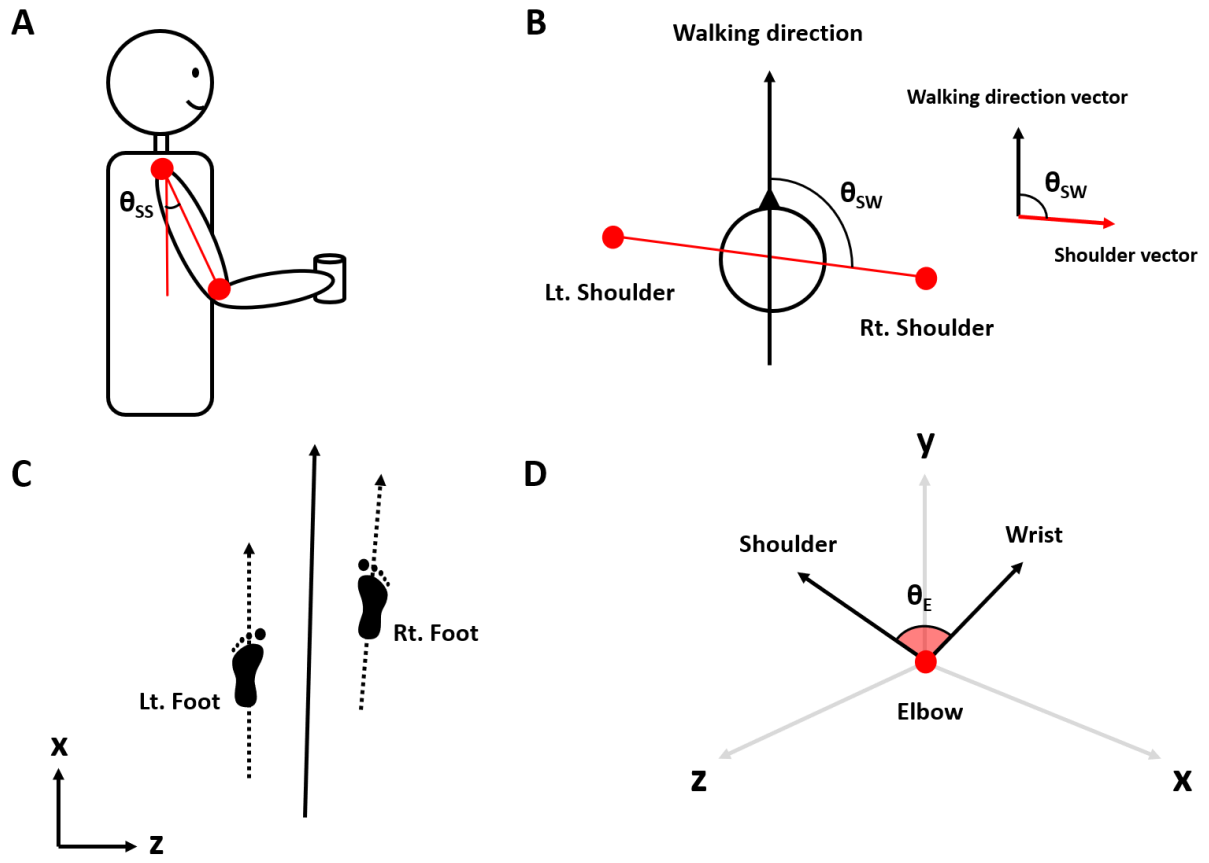

Figure 3.1. A. Shoulder angle in sagittal plane (θ_{SS}) calculated by shoulder and elbow markers. B. Shoulder angle in transverse plane estimated using the dot product between two vectors: walking direction vector and transverse left-right shoulder vector. Shoulder angular displacement in transverse plane is computed by subtracting 90° from the angle between shoulder and walking direction vectors ($\theta_{ST} = \theta_{SW} - 90°$). C. Calculation of walking direction vector. D. Elbow angle computed by the dot product of two vectors: elbow-shoulder vector and elbow-wrist vector.

then normalized with respect to the angular displacement during natural walking (0%).

Interlimb coordination of the upper limbs

To investigate the coordination pattern between the angular displacement time series of left and right arm movements during walking while carrying an object, a vector coding method was used (Chang et al., 2008). First, an angle-angle plot was created: the angular displacement time series of right shoulder joint in the sagittal plane in each time point was plotted on the horizontal axis (x-axis), and the angular displacement of the left shoulder joint in the sagittal plane in each time point was plotted on the vertical axis (y-axis). In order to verify the relative contribution of two shoulder joints, and the coupling angle (CA, γ) was calculated by two consecutive pairs of shoulder angles on the angle-angle plot as the angle subtended from a vector adjoining two successive data points relative to right horizontal (Chang et al., 2008; Van Emmerik et al., 2014):

$$\gamma_i = \tan^{-1}\left(\frac{y_{i+1}-y_i}{x_{i+1}-x_i}\right) \qquad x_{i+1} - x_i > 0, \tag{1}$$

$$\gamma_i = \tan^{-1}\left(\frac{y_{i+1}-y_i}{x_{i+1}-x_i}\right) + 360 \qquad x_{i+1} - x_i > 0,\ y_{i+1} - y_i < 0, \tag{2}$$

$$\gamma_i = \tan^{-1}\left(\frac{y_{i+1}-y_i}{x_{i+1}-x_i}\right) + 180 \qquad x_{i+1} - x_i < 0, \tag{3}$$

$$\gamma_i = \begin{cases} \gamma_i = 90 & x_{i+1} - x_i = 0,\ y_{i+1} - y_i > 0 \\ \gamma_i = -90 & x_{i+1} - x_i = 0,\ y_{i+1} - y_i < 0 \\ \gamma_i = -180 & x_{i+1} - x_i < 0,\ y_{i+1} - y_i = 0 \\ \gamma_i = Undefined & x_{i+1} - x_i = 0,\ y_{i+1} - y_i = 0, \end{cases} \tag{4}$$

where $0° \leq \gamma \leq 360°$ and x and y indicate the coordinates of the angle-angle plot. i represents the consecutive data points in a cycle. The CA for each participant and condition was obtained from the angle-angle plot based on the angular displacements of bilateral shoulders from the individual gait cycle (Figure 3.2A). The computed CAs represent the spatial relationship from which four unique coordination patterns and the identification of four coordination patterns using 22.5° of bins is based on the vertical, horizontal, and diagonal (positive and negative) line segments (Chang

et al., 2008). The four coordination patterns included (1) Anti-Phase (rotating in the opposite direction, 112.5º<γ<157.5º & 292.5º<γ<337.5º), (2) In-Phase (rotating in the same direction, 22.5º<γ<67.5º & 202.5º<γ<247.5º), (3) right shoulder dominancy (RSh-Phase, 0º<γ<22.5º, 157.5º<γ<202.5º, 337.5º<γ<360º), and (4) left shoulder dominancy (LSh-Phase, 67.5º<γ<112.5º, 247.5º<γ<292.5º) (Figure 3.2B). The anti- and in-phase coordination patterns indicate the motions in both shoulder joints move in the opposite and the same directions, respectively. The CAs of 0°, 90°, 180°, and 270° indicate the movement is performed mainly by one of the shoulder joints, termed R-Shoulder Phase (RSh-Phase) if the right shoulder moves primarily while the left does not and L-Shoulder Phase (LSh-Phase) if the left shoulder primarily moves while the right does not.

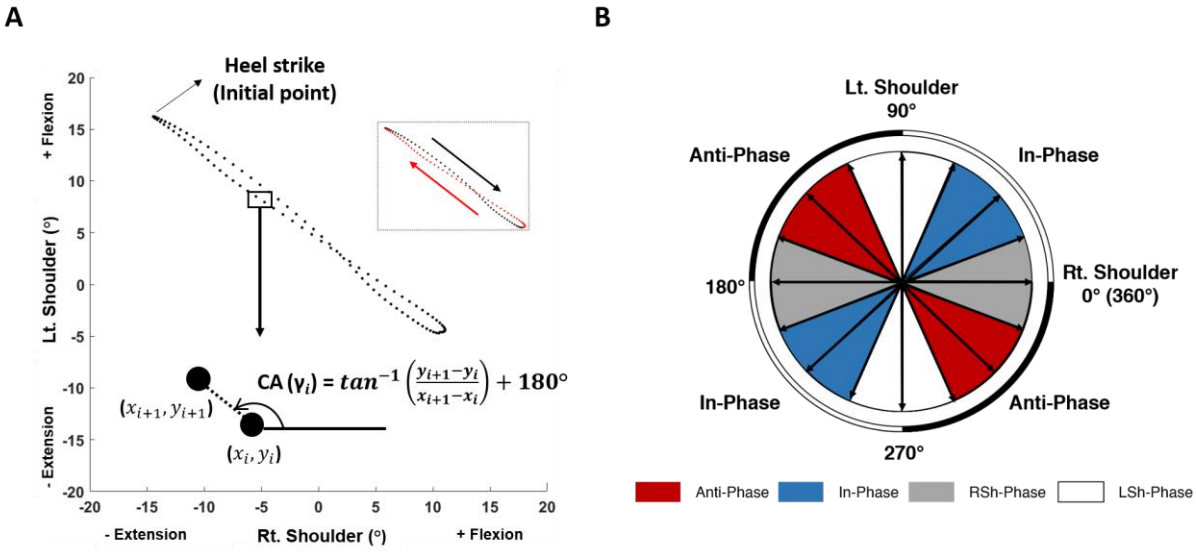

Figure 3.2. A. Calculation of coupling angle (CA) on angle-angle plot during object carrying with dominant limb (right side). Red arrow indicates the first half of gait cycle. Since $x_{i+1} - x_i < 0$, in this case, 180° should be added for the CA. B. A polar plot shows the coordination pattern classification of in-phase and anti-phase.

Surface electromyography (EMG)

Bilateral activations of six upper limb muscles were recorded at 2000 Hz using two 16-channel MA-300 surface EMG systems (Motion Lab Systems Inc., Baton Rouge, LA, USA). Each

participant's skin was cleaned with alcohol wipes at the recording sites. The locations for the electrode placements were determined according to the surface EMG for the non-invasive assessment of muscles (SENIAM) guidelines (Hermens et al., 2000) or by palpation. Electrodes were secured by adhesive tape to reduce motion artifact. Self-adhesive elastic sports bandages were used to provide additional security of holding these electrodes onto the skin during data collection. Upper limb muscles that are mainly responsible for the prehension and the stabilization of shoulder and elbow joints were recorded, including the trapezius (TRAP), anterior deltoid (AD), posterior deltoid (PD), biceps brachii (BB), triceps brachii (TB), and brachioradialis (BR), bilaterally. EMG signals were monitored in real-time during the experiment to ensure quality recordings and to detect any detachments of the electrodes. The raw signals were high-pass filtered using a dual-pass, second-order, Butterworth filter with a cut-off frequency of 30 Hz, full-wave rectified, and then low-pass filtered using dual-pass, second-order, Butterworth filter with a cut-off frequency of 10 Hz. For time normalization, processed EMG data were interpolated to 100-time points representing a gait cycle determined by the ipsilateral heel contacts. For amplitude normalization of EMG profiles, the activation of individual muscles was normalized by the highest amplitude across all three (treadmill walking, no-object, and object) conditions within each participant. Therefore, a value of 1 represents the maximum activation of the muscle across all conditions for a single subject. The mean muscle activation from time- and amplitude-normalized EMG during each gait cycle will be calculated across participants.

Statistical analysis

First, the angular displacement of the shoulder and elbow joints during each condition was referenced to the baseline which is the angular displacement during natural treadmill walking for each subject as a percent increase or decrease in the arm motion compared to treadmill walking

condition (TW). For example, a +25% increase in shoulder amplitude in the OBJ condition means that the amplitude of shoulder motion increased by that amount compared to free-swinging arm movement during treadmill walking (TW).

Then, the relative angular displacement during the NOBJ and OBJ conditions were examined using a two-way within-subjects ANOVA with Hand (carrying vs. non-carrying side) and Object (NOBJ vs. OBJ) as factors to identify statistically significant changes in the angular displacement of the shoulder in sagittal plane and elbow joint compared to the TW. To directly test the hypothesis about the change in the movement amplitude of the non-carrying arm, a one-sample repeated-measures *t*-test was used to determine whether the relative angular displacement was significantly different from 0% on the non-carrying side.

In addition, a two-way within-subjects analysis of variance (ANOVA) with Side (dominant vs. non-dominant) and Object (NOBJ vs. OBJ) was performed to determine the statistical differences in angular displacement of the shoulder in both sagittal and transverse planes and 3D angular displacement of elbow joint. And a two-way within-subjects ANOVA with Side (dominant vs. non-dominant) and Object (TW vs. NOBJ vs. OBJ) was performed to determine the statistical differences in mean EMG activation levels on the non-carrying side.

For each participant and experimental condition, the computed CAs from the mean angle-angle plot from all strides were classified according to Chang et al. (2008) as 1) Anti-phase, 2) In-phase, 3) Left Shoulder Phase, 4) Right Shoulder Phase. The percentage of occurrence of these coordination patterns was evaluated within each time-normalized stride cycle and averaged across all strides within a condition (TW, NOBJ, OBJ). The percent occurrence of these coordination patterns was compared using a one-way repeated measures ANOVA to investigate whether there was a significant difference between the TW, NOBJ, and OBJ for each condition on the dominant

(right) and non-dominant (left) sides. Tukey's HSD tests were used for post-hoc testing. All statistical analyses were performed using SAS (version 9.4, SAS Institute Inc., Cary, NC, USA), and statistically significant differences were determined at a p-value<0.05.

RESULTS

Across all participants, the mean walking speed was 1.1±0.08 m/s ranged between 1.02 and 1.23 m/s. The mean preferred walking stride time was 1.16±0.03 s ranged between 1.05 and 1.24 s, with the mean timing of contralateral heel contact occurring at 49.7±2.8% of the gait cycle across all participants. Ipsilateral toe-off occurred at 66.3±3.3% of the gait cycle. Mean stride time and timing of gait cycles did not significantly differ across participants (p>0.05).

Angular displacement of the shoulder joint in sagittal plane

Sample angular displacement trajectories for both dominant and non-dominant shoulder joints for each condition are plotted in Figure 3.3.

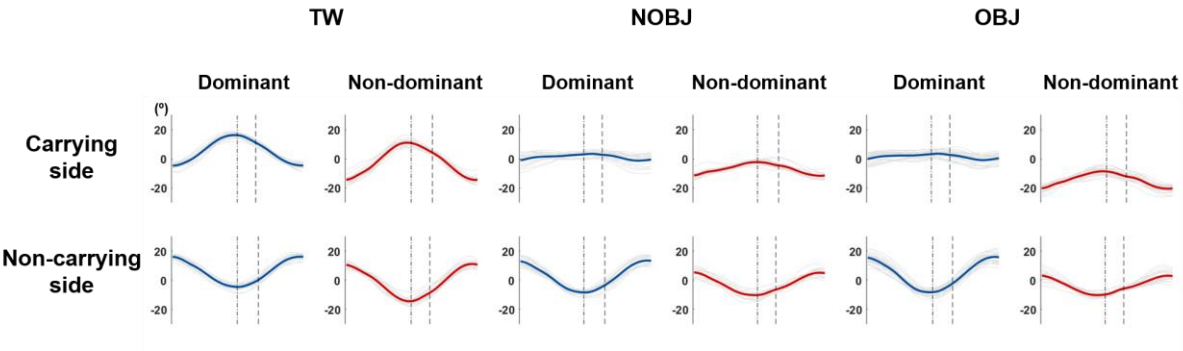

Figure 3.3. Trajectory of angular displacement of shoulder joint in sagittal plane from one representative participant. The thin gray lines represent the angular displacement from individual strides and the thick blue and red lines represent the mean across individual walking strides. On each graph, the first vertical lines (-.) indicates the time when the contralateral heel contacted with the ground. The second vertical lines (--) indicates ipsilateral toe-off, dividing the gait cycle into stance and swing phases.

There was a main effect of Hand (carrying vs. non-carrying side) for both dominant ($F_{(1,20)}$=19.42, p=0.0003) and non-dominant ($F_{(1,16)}$=83.61, p<0.0001) NOBJ and OBJ conditions

(Figure 3.4). For the dominant side (right), there was a significant difference in shoulder angular displacement between the carrying (right) and non-carrying side (left) during NOBJ condition (p=0.0027) and OBJ condition (p=0.019). The right shoulder (carrying side) showed a reduction of angular displacement of -56.3±8.4% and -70±2.9% during NOBJ and OBJ conditions compared to TW. The left shoulder (non-carrying side) showed the relative angular displacement of -14.0±6.7% and -19.9±17.9% during the NOBJ and OBJ conditions, respectively. Similarly, for both NOBJ and OBJ conditions, the one-sample repeated-measures t-tests showed that the angular displacement of the shoulder in the carrying side was significantly different from the angular displacement during TW (p=0.001 and p<0.0001, respectively).

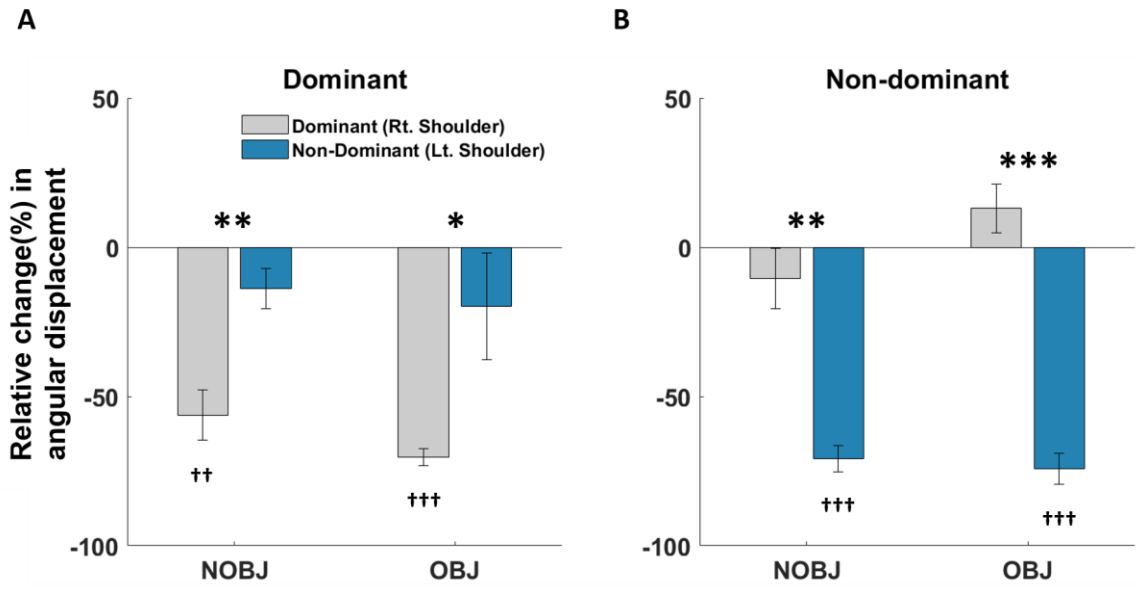

Figure 3.4. Group averaged angular displacement of shoulder in sagittal plane with standard error when a right shoulder was involved in NOBJ and OBJ conditions (A) and when a left shoulder was involved in NOBJ and OBJ conditions (B). The angular displacements during NOBJ and OBJ conditions were normalized by the angular displacement during TW (0%). Statistical difference in angular displacement compared to the contra-lateral side is displayed with asterisk (*p<0.05, **p<0.01, ***p<0.001). Statistical difference with respect to 0% is displayed with cross (†p <0.05, ††p<0.01, †††p<0.001**).**

For the non-dominant side, there was a significant difference in shoulder angular displacement between carrying (left) and non-carrying side (right) during NOBJ condition

(p=0.001) and OBJ condition (p<0.0001). The left shoulder (carrying side) showed the relative angular displacement of –70.9±4.5% and -74.1±5.2% during NOBJ and OBJ conditions, respectively. The right shoulder (non-carrying side) showed the relative angular displacement of -10.5±10.2% and 13.0±8.1% during NOBJ and OBJ conditions, respectively. For both NOBJ and OBJ conditions, the angular displacement of the shoulder in the carrying side was significantly different from the angular displacement during TW (p=0.0001 and p=0.0001, respectively).

There was no significant main effect of Side (dominant vs. non-dominant) ($F_{(1,18)}$=2.41, p=0.1382) and Object (NOBJ vs. OBJ) ($F_{(1,18)}$=2.09, p=0.1653) for both carrying and non-carrying sides.

Angular displacement of shoulder joint in transverse plane

Figure 3.5 shows the angular displacement trajectory in the transverse plane of both dominant and non-dominant shoulder joints for each condition from one representative participant. Figure 3.6 shows the group averaged relative angular displacement of shoulder joint for both dominant and non-dominant NOBJ and OBJ conditions. In this plane, there was no significant

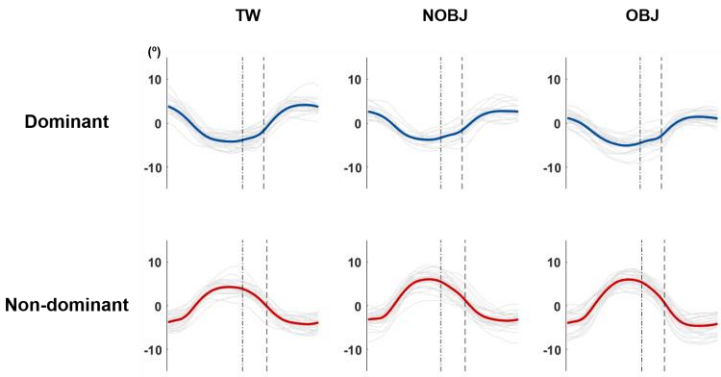

Figure 3.5. Trajectory of angular displacement of shoulder joint in transverse plane from one representative participant. The thin gray lines represent the angular displacement from individual strides and the thick blue and red lines represent the mean across individual walking strides. On each graph, the first vertical lines (-.) indicates the time when the contralateral heel contacted with the ground. The second vertical lines (--) indicates ipsilateral toe-off, dividing the gait cycle into stance and swing phases.

main effect of Side (dominant vs. non-dominant) and Object (NOBJ vs. OBJ). In addition, the relative angular displacement of the shoulder joint in this plane was not significantly different from the angular displacement during TW (0%).

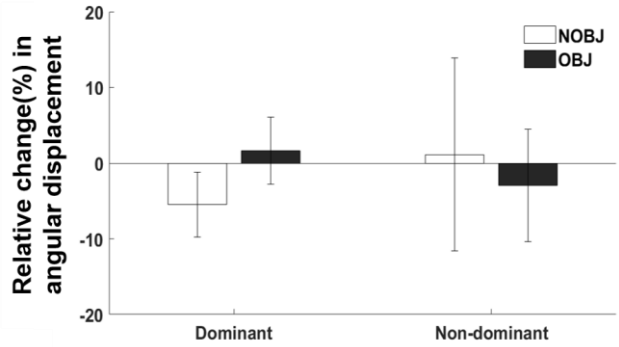

Figure 3.6. Group averaged angular displacement of shoulder in transverse plane with standard error. The angular displacements during NOBJ and OBJ conditions were normalized by the angular displacement during TW (0%).

3D angular displacement of elbow joint

Figure 3.7 shows the angular displacement trajectory of the elbow joint for each condition from one representative participant. There was a main effect of Hand (carrying vs. non-carrying) for both dominant ($F_{(1,20)}$=44.36, p<0.0001) and non-dominant ($F_{(1,16)}$=209.04, p<0.0001) NOBJ and OBJ conditions (Figure 3.8). For the dominant side, there was a significant difference between carrying (right) and non-carrying side (left) during NOBJ (p=0.007) and OBJ condition (p<0.0001). The right elbow joint (carrying side) showed the relative angular displacement of -55.7±12.2% and -76.6±6.2% during NOBJ and OBJ conditions, respectively. The left elbow joint (non-carrying side) showed the relative angular displacement of -8.9±6.8% and -10.2±7.3% during NOBJ and OBJ conditions, respectively. For both NOBJ and OBJ conditions, the angular displacement of the elbow joint in the carrying side was significantly different from the angular displacement during TW (p=0.006 and p<0.0001, respectively).

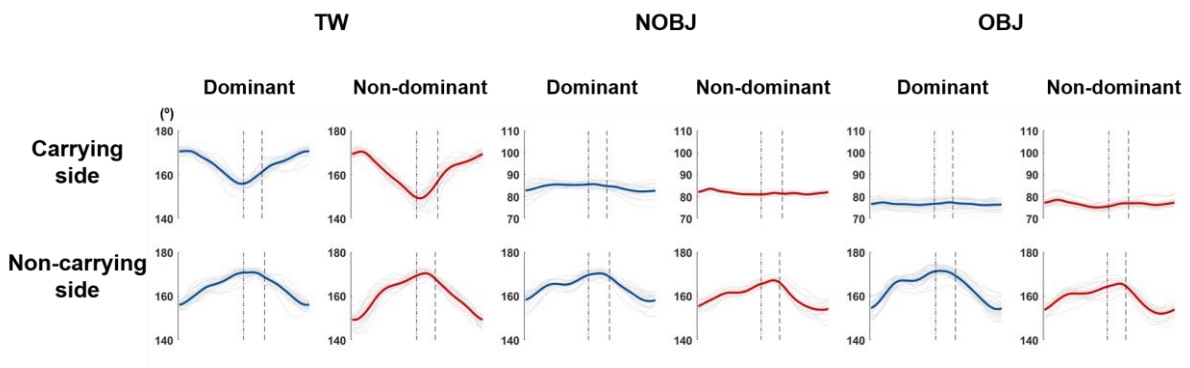

Figure 3.7. 3D angular trajectory of elbow joint from one representative participant. The thin gray lines represent the angular displacement from individual strides and the thick blue and red lines represent the mean across individual walking strides. On each graph, the first vertical lines (-.) indicates the time when the contralateral heel contacted with the ground. The second vertical lines (--) indicates ipsilateral toe-off, dividing the gait cycle into stance and swing phases.

Similarly, for the non-dominant side, there was a significant difference in elbow angular displacement between carrying (left) and non-carrying side (right) during NOBJ condition and OBJ conditions (p<0.0001). The left elbow (carrying side) showed the relative angular displacement of –88.2±1.3% and -87.8±1.4% during NOBJ and OBJ conditions, respectively. Right elbow (non-carrying side) showed the relative angular displacement of -3.3±8.4% and -1.7±6.4% during NOBJ and OBJ conditions, respectively. For both NOBJ and OBJ conditions, the angular displacement of the elbow in the carrying side was significantly different from the angular displacement during TW (p<0.0001). In addition, there was a significant main effect of Side (dominant vs. non-dominant) in carrying arm during NOBJ condition ($F_{(1,18)}$=8.09, p=0.01).

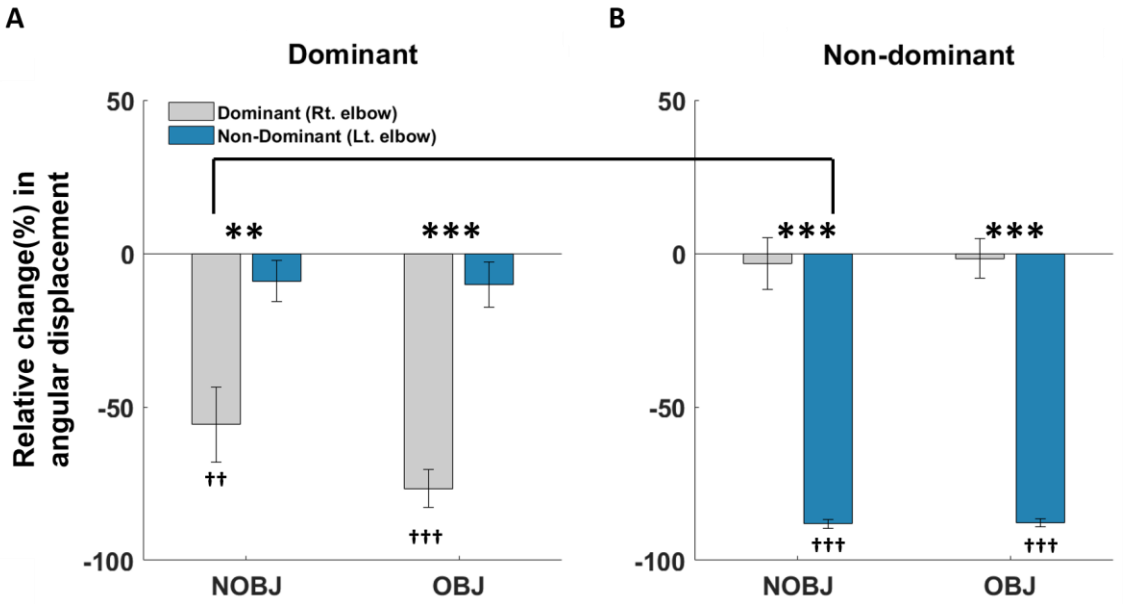

Figure 3.8. Group averaged angular displacement of elbow joint with standard error when a right elbow was involved in NOBJ and OBJ conditions (A) and when a left elbow was involved in NOBJ and OBJ conditions (B). The angular displacements during NOBJ and OBJ conditions were normalized by the angular displacement during TW (0%). Statistical difference in angular displacement compared to the contra-lateral side is displayed with asterisk (*p<0.05, **p<0.01, ***p<0.001). Statistical difference with respect to 0% is displayed with cross (†p <0.05, ††p<0.01, †††p<0.001**).** Statistical difference between carrying sides is displayed with a bar.

Interlimb coordination of shoulder joints

Figure 3.9 illustrates the angle-angle diagrams in each condition from one representative participant. As seen in this figure, during NOBJ and OBJ conditions, the shoulder showed relatively vertical orientation when compared to the diagonal pattern during natural treadmill walking due to the decrease in angular displacement in the corresponding side.

As expected, the anti-phase pattern was most prevalent during TW, but as participants placed their elbow in a flexed position (NOBJ) or held the object in their hand (OBJ), there was a decrease in the frequency of the Anti-Phase pattern with a concomitant increase in the frequency of opposite shoulder pattern (LSh-Phase or RSh-Phase) in both dominant and non-dominant experimental conditions.

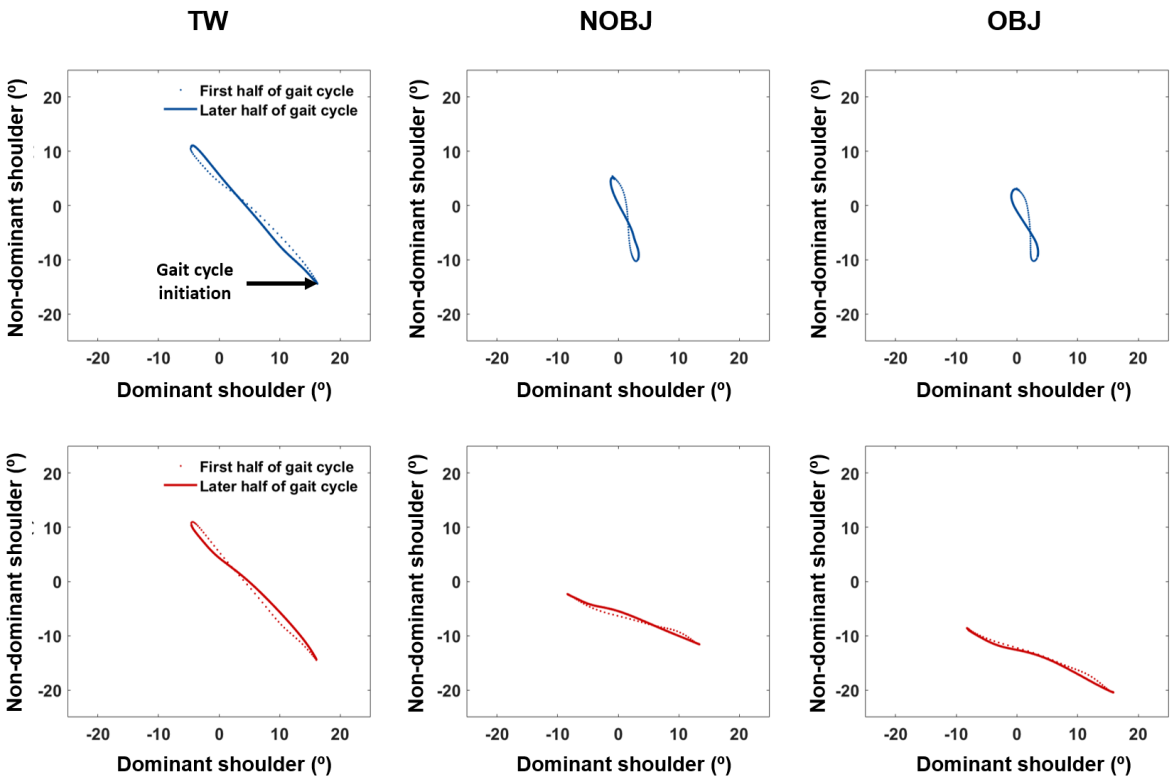

Figure 3.9. The angle-angle plot for each condition. Angular displacement of dominant shoulder plotted in x-axis and that of non-dominant shoulder was plotted in y-axis. The three angle-angle plots in the first row indicate the relative angular displacement of bilateral shoulders during natural walking, arm placement with dominant limb, and object transport with dominant limb, in order. Three plots in second row the relative angular displacement of bilateral shoulders during natural walking, arm placement with non-dominant limb, and object transport with non-dominant limb, in order. On each graph, the dotted line represents the first half of gait cycle, and the solid line represents the latter half of gait cycle. The coupling angle (CA) in each data time point of this angle-angle plot was computed and classified into one of the four coordination patterns.

Figure 3.10 shows the relative frequency of coordination patterns for each condition and arm. For the dominant side, one-way repeated measures ANOVA showed that the anti-phase pattern significantly decreased during the NOBJ and OBJ condition compared to TW (p=0.0006 and p=0.0003, respectively). In addition, there was a significant increase in the in-phase coordination pattern during OBJ condition compared to TW (p=0.02). Also, there was a significant increase in LSh-phase during NOBJ and OBJ conditions compared to TW (p=0.005 and p=0.003, respectively).

For the non-dominant side, the anti-phase pattern during NOBJ condition significantly decreased compared to TW (p=0.03), and LSh-phase during OBJ condition significantly decreased when compared to TW (p=0.04). There was a significant increase in RSh-phase coordination during NOBJ and OBJ conditions when compared to TW (p=0.004 and p=0.002, respectively).

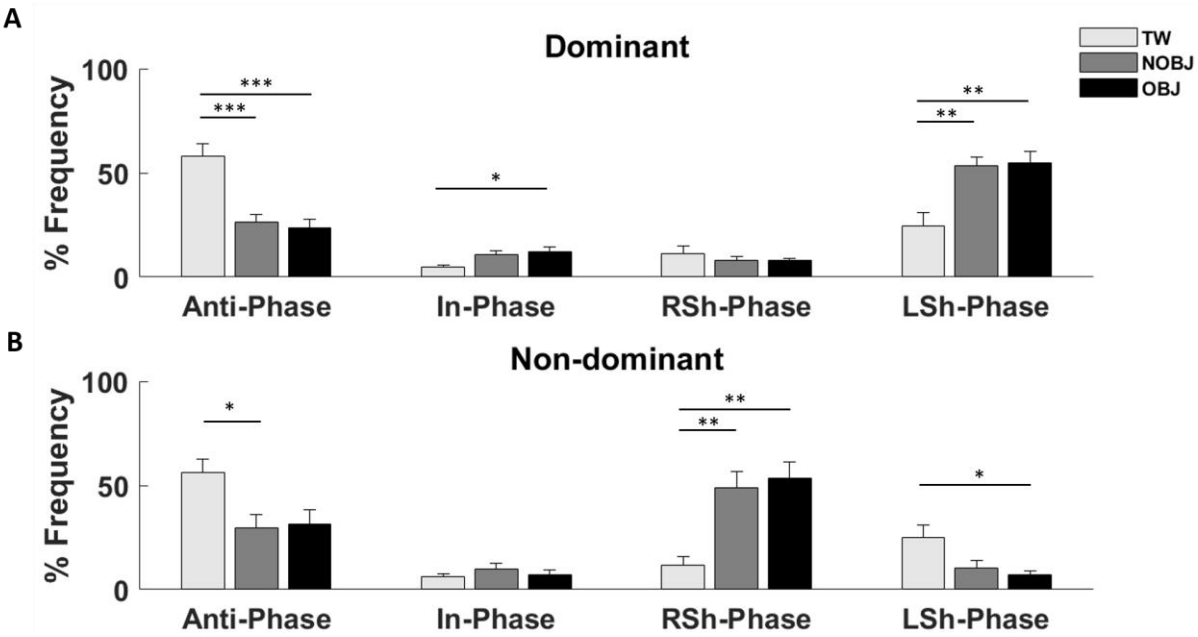

Figure 3.10. Group averaged relative frequency of occurrence of four coordination patterns with standard error for each condition for dominant (A) and non-dominant (B) limbs. Statistical difference between coordination patterns is displayed with asterisk (*p<0.05, **p<0.01, ***p<0.001).

Surface electromyography (EMG)

The group averaged mean EMG levels showed a main effect of object conditions in most of the muscles when compared to TW, except for TB (Figure 3.11). Mean amplitude of TRAP and AD during object transport was higher when compared to TW (TRAP: F(2,41)=6.48, p=0.0025, AD: F(2,41)=3.76, p=0.03). A main effect of object condition was also present in BB (F(2,41)=53.78, p<0.0001) and BR (F(2,41)=23.59, p<0.0001). The mean amplitude of BB during the object transport task was higher than in NOBJ and TW (p<0.0001). The mean amplitude of BR during the object transport task was higher than in NOBJ (p<0.0004) and TW (p<0.0001). The

mean EMG level of BR during NOBJ was higher than in TW ($p=0.03$). While most of the muscles showed an increase in mean EMG level during NOBJ and OBJ conditions, PD was the only muscle that showed a decrease in mean EMG activation during OBJ condition when compared to TW ($F(2,41)=3.45$, $p=0.04$). There was no significant side difference in mean EMG level on the contralateral side.

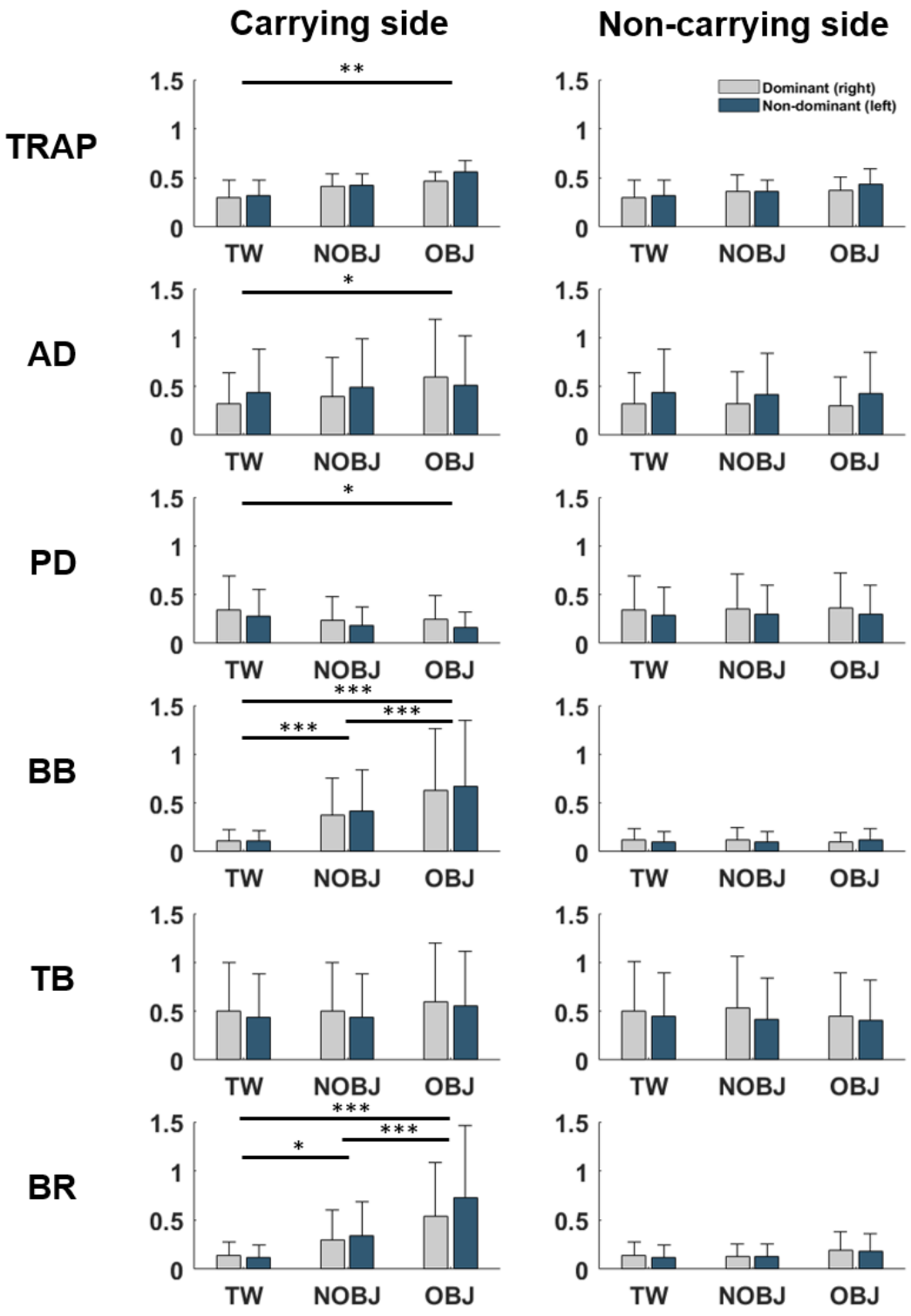

Figure 3.11. Mean EMG with standard deviation (+SD) for carrying and non-carrying limbs. Group averaged (n = 8) and normalized mean EMG magnitude of individual muscle throughout the gait cycle for each condition. Statistical difference between conditions is displayed with asterisk (*p < 0.05, **p < 0.01, and ***p < 0.001).

DISCUSSION

The aim of this study was to examine changes in the kinematic patterns of interlimb coordination in young healthy individuals while transporting an object in either a dominant or non-dominant hand. In addition to the change in the upper limb used for carrying the object, the alteration in contra-lateral upper limb was also investigated on how this functional upper limb task affected the overall reciprocal arm swing pattern. As expected, the relative angular displacement of flexion-extension of shoulder joint used for arm placement and object transport task (NOBJ and OBJ) significantly decreased compared to natural treadmill walking. However, the results of this study did not support our hypothesis that there would be an increase in angular displacement of the shoulder joint in the non-constrained side such that the movement amplitude of the contralateral limb did not show the expected increases in amplitude as predicted from the conservation of total angular momentum framework. In fact, although it was not statistically significant, there was a tendency to decrease the angular displacement in both shoulder and elbow joints in the non-constrained side during NOBJ and OBJ conditions, except for non-dominant OBJ condition.

The reduced amplitude of arm swing has been observed in previous studies when the arms were constrained passively by using a sling (Donker et al., 2002; Ford et al., 2007) or by adding additional weight (MacLellan & Ellis, 2019). Previous studies have reported that an increase in swing amplitude of the contralateral arm when the ipsilateral arm is constrained is one of the CNS's strategies to counteract the angular momentum caused by the stepping motion of the contralateral lower limb in order to maintain the upper and lower coordination (Elftman, 1939b; Ford et al., 2007; Stokes et al., 1989; Wagenaar & Beek, 1992). However, this seems affected by different walking conditions, such as walking velocity. In the study by Ford et al. (2007) where the effect

of different walking velocity on inter-segmental coordination was investigated, he and his colleagues found that this increased arm swing amplitude in the non-constrained side was observed as walking velocity increased, especially at a velocity equal or greater than 1.10 m/s, regardless of constrained side (whether it is the right or left hand). This kinematic change was primarily to cope with the increased angular momentum by increased contralateral hip excursion and lower limb torque due to the faster walking velocity (Ford et al., 2007). These inconsistent results might be due to the several differences in experimental characteristics. First, the average comfortable walking velocity in the current study was 1.1±0.08 m/s which was very similar velocity from where Ford et al. (2007) began observing the increase in angular displacement in the non-constrained side, but because Ford et al. (2007) didn't report the comfortable walking velocity of their participants, it would be hard to compare the results of these two studies directly (1.1 m/s could be the faster or slower velocity for these participants and we don't know). Second, the nature of the task was different in that the task in this study required greater stabilization to maintain the object by minimizing the motion of the upper limbs while Ford et al. (2007) passively restrict the motion of one side of the arm. This could be the CNS's priority leading to the overall reduction in angular displacement in both constrained and non-constrained sides to secure the stability of the hand-held object as it prevents further asymmetry of the body that might perturb the stability of the object while walking. Moreover, this strategy might be used regardless of handedness as no significant difference was observed between dominant and non-dominant sides. Therefore, these inconsistent results between studies might result from the different task constraints, and the CNS adopts a proper strategy for the specific condition whether it stabilizes the body by minimizing the overall motions or increasing the motion in opposite side to balance the trunk angular momentum.

Unlike the previous studies where researchers have suggested that the decreased ability of

the constrained arm to counteract the angular momentum from the lower trunk necessarily gave rise to the decrease in pelvis-trunk counter-rotation (Ford et al., 2007; LaFiandra et al., 2003; Stokes et al., 1989), there was no significant difference in angular displacement of shoulder joint in transverse plane when compared to the angular displacement during natural treadmill walking. It might be possible that the restriction of shoulder movement on the constrained and the non-constrained sides could have been sufficient to balance the trunk angular momentum, leading to less necessity of decreasing angular motion in the trunk to counteract the angular momentum about the longitudinal axis.

As hypothesized, transporting an object in one hand caused the change in the upper limb coordination patterns. During natural treadmill walking, an anti-phase pattern was predominant (over 50% of the gait cycle), similar to previous studies (Rinaldi et al., 2017; Silva et al., 2019). There was a decrease in the relative frequency of the anti-phase pattern with NOBJ and OBJ conditions. Although this anti-phase pattern has been reported to contribute to balance the trunk angular momentum (Bruijn et al., 2008; Elftman, 1939b), Silva et al. suggested that the reduction of upper limb movement with load carrying as well as the mass of the object itself might be sufficient enough to balance the trunk angular momentum and to dampen the perturbation caused by the asymmetrical load carriage (Silva et al., 2019). As expected, this asymmetrical upper limb constraint increased the phase of contralateral shoulder pattern for both dominant and non-dominant object conditions (LSh-Phase pattern during dominant object carrying and RSh-Phase pattern during non-dominant object carrying) while the phase of the ipsilateral shoulder remained constant or decreased. This indicates that the shoulder involved in NOBJ and OBJ conditions did not move much while walking compared to the free contra-lateral arm.

Due to the nature of the task, the relative movement of the elbow joint was significantly

reduced when the elbow was in a flexed position without the object (NOBJ) and with the object (OBJ) and adding a mass (OBJ) did not significantly affect the magnitude of angular displacement in the elbow joint. It would be possible that CNS can modulate the apparent stiffness or damping behavior of the upper limb via the different levels of muscular activation. In fact, the EMG results of this study supported this idea in that the mean activations of BR and BB that are main elbow flexors are significantly greater during OBJ condition compared to NOBJ condition. Interestingly, the results of this study also showed the side difference in that the elbow joint on the non-dominant side presented significantly greater displacement amplitude compared to the dominant side during NOBJ condition. This result was supported by the previous study in that the non-dominant left side would stabilize a system without much movement modification (fluctuation) (Sainburg, 2002). Although there was a difference between the nature of the experimental task, in the research by Sainburg where limb dominancy was investigated during discrete upper limb movement, he suggested that non-dominant arm is less efficient in movement control accompanied with larger muscle torque and small joint interaction torque when compared to dominant arm (L. B. Bagesteiro & R. L. Sainburg, 2002; Bagesteiro & Sainburg, 2003; Sainburg, 2005). Moreover, similar to the shoulder joint in the sagittal plane, the unconstrained elbow joint showed a decrease in movement amplitude during both NOBJ and OBJ conditions regardless of the side, supporting the idea mentioned above in that CNS would decrease the overall range of motion in the elbow joint as well.

The mean activation of upper limb muscles did not significantly differ between sides. As it was expected, EMG analysis showed greater amplitude in activation in most of the arm muscles during NOBJ and OBJ conditions when compared to the activation during natural walking, except for PD and TB, and these results were partially matched with the previous findings (Johann Peter

Kuhtz-Buschbeck & Antonia Frendel, 2015). In this previous study, the author found the increase in muscle activity in TRAP, AD, PD, BB, and TB when the load was carried with the hand ipsilateral to muscles studied, but they also found that there was a decrease in muscle activations in AD, PD, and TB when the arm swing was immobilized. The differences between our study and this previous study are probably originated from the different nature of the task in that the object transport task in the current study involved load carriage in one hand but did not completely immobilize the upper arm, generating the mixed results. It would be possible that the decrease in PD activation was due to the characteristic of the object transport task reducing eccentric contraction while forward movement due to the decrease in arm swing motion, but the increase in AD activation was primarily due to the mass of the object maintaining the flexed position during the task. For the muscle activations in the non-carrying side, there was no significant difference between sides or between object conditions, indicating that the kinematic changes in shoulder and elbow joints were not mainly due to the changes in muscular contributions.

In summary, this asymmetrical and functional upper limb task did not show the predicted significant side difference regarding its kinematic changes, except for the elbow flexion angle during NOBJ condition. In addition, there was no significant side difference in shoulder coordination patterns and EMG activations. However, these results may be affected by the walking velocity used in this study; participants walked at their comfortable speed, while faster than comfortable speeds may unmask the asymmetry in upper limb coordination (Ford et al., 2007). Future studies involving the alterations in gait parameters and temporal coordination patterns would provide more comprehensive information to understand the basic underlying mechanism of the effect of limb dominance on this task.

CHAPTER 4. MUSCLE SYNERGY FOR UPPER LIMB DAMPING BEHAVIOR DURING OBJECT TRANSPORT WHILE WALKING: STUDY 2

INTRODUCTION

Walking while transporting a grasped object is one of the most common dexterous tasks individuals perform every day, such as when carrying a cup of coffee, a cell phone, or a bag of groceries. A significant challenge for the CNS in this task is to preserve the stability of the grasped object when it is perturbed by inter-segmental interaction torques and the reaction forces arising from the interaction of the foot and the ground. One may question how the CNS organizes the multi-segmental joint and muscle coordination patterns to deal with such gait-induced perturbations?

One well-documented strategy is the predictive and continuous control of GF throughout the gait cycle based on an internal model of the carried object (Diermayr et al., 2008; Gysin et al., 2003b; Gysin et al., 2008; Togo et al., 2012). These studies showed that the GF is typically very closely modulated with the inertial LF of the object during locomotion, with peak LF occurring less than 30 ms following heel contact, indicative of feedforward GF modulation (Flanagan & Wing, 1995; Gysin et al., 2003b). A similar coupling between GF and LF was observed during voluntary movement of the upper limb alone (Flanagan et al., 1993; Flanagan & Tresilian, 1994; Flanagan & Wing, 1995; Johansson & Westling, 1984; A. M. Wing & S. J. Lederman, 1998; Zatsiorsky et al., 2005). However, one recent study highlighted that the degree of GF-LF coupling might not be as temporally consistent as previously reported (Grover et al., 2018). These researchers observed periods of high GF-LF coupling are followed by periods of looser coupling

This chapter was previously published as Song, A., Kuznetsov, Nikita A., Winges, Sara A., MacLellan, Michael J., "Muscle synergy for upper limb damping behavior during object transport while walking in healthy young individuals," *Experimental Brain Research* 238 (2020): 1203-1218. Reprinted by permission of Springer Nature.

(Grover et al., 2018; Grover et al., 2019), which were interpreted as an intermittent, not continuous control policy for object stabilization. Modulation of GF has also been explained by the equilibrium point hypothesis as emerging from shifts in the referent aperture of the fingers to be smaller than the size of the object (Pilon et al., 2007).

In addition to explicit co-variation of GF with LF, participants also utilize a GF safety margin when carrying an object such that GF is higher than what is minimally necessary to avoid object slipping (Cole & Johansson, 1993). A safety margin has been hypothesized to be related to the predictability of the LFs experienced by the object, such that less predictable dynamics lead to higher safety margins (Hadjiosif & Smith, 2015).

Another strategy available to the CNS is to increase the dynamic stability of the upper limb by modifying its apparent stiffness and damping via altered muscle activation patterns (Lacquaniti et al., 1982; Milner & Cloutier, 1998; Zhang & Rymer, 1997). Viscoelastic properties of the muscle contribute to providing postural stability and compliant responses to external forces (Bizzi et al., 1976; Lacquaniti et al., 1982; Milner & Cloutier, 1993; Partridge, 1966; Rack, 1966) through a reflex control (Lin & Rymer, 2000, 2001; Milner & Cloutier, 1998). As such, fluctuations of LF may not be explicitly predicted based on an internal model but dampened out as a result of increasing apparent stiffness of the endpoint kinematic chain (Ambike et al., 2015). Vertical dampening of the object position is also evident at the kinematic level through a decoupling of the trunk and upper limb by separate adjustments of the shoulder, elbow, and wrist joints, rather than holding the object with a rigid upper limb (Gysin et al., 2003b).

In previous studies, it has been found that these object stabilizing strategies during gait can be altered by several factors, such as age, neurological pathology, and different modes of walking (Diermayr et al., 2011; D. Ebner-Karestinos et al., 2016; McIsaac et al., 2012). In these previous

studies, researchers have focused on the kinematic aspects of object transport and with a particular emphasis on GF. However, the organization of upper limb muscle coordination patterns in object-transport tasks that contributes significantly to the observed kinematics and kinetics has not been extensively examined. Since the object transport task while walking involves a significant number of upper limb muscles to be coordinated, the perspective that multi-muscle control is governed by a small collection of motor modules might provide a better understanding of object stabilization during this task. The use of muscle synergies to simplify control of a large number of DOF in the musculoskeletal system is one hypothesis for neuromotor control (Lacquaniti et al., 2012; Saito et al., 2018; Ting & McKay, 2007). Although this hypothesis remains controversial (Kutch & Valero-Cuevas, 2011; Ranganathan & Krishnan, 2012; Tresch & Jarc, 2009), the muscle synergy concept could be a useful method to characterize the neuromuscular control strategies in human movement (Ivanenko et al., 2006; Lacquaniti et al., 2012; Neptune et al., 2009; Ting & McKay, 2007; Yokoyama et al., 2016).

Accordingly, the goal of this study was to identify the neuromuscular control strategies used by the CNS for controlling the upper limb during object transport while walking. The task involved gripping a cylindrical object while holding the elbow flexed at approximately 90 degrees, which is representative of typical cases of object transport in daily activities such as carrying a cup of coffee while walking. In this study, the upper limb damping behavior was investigated using kinematic analysis, muscle activation. Non-negative matrix factorization (NNMF) approach (Lee & Seung, 1999) was used to examine the muscle synergy patterns underlying the upper limb damping behavior and GF modulation during the task.

Methodological background: non-negative matrix factorization (NNMF)

The question "how does CNS control movements?" has been discussed for many years in

neuroscience and motor control/behavior areas. During the coordinated movement, similarity across kinematic, kinetic, electromyographic, and neural signals can be found (Bernstein, 1966). Movement control by CNS requires not only a physiological process but also incorporating complex interactions between segments and system and the environment. Bernstein defined the coordinated movement as “the process of mastering redundant DOF of the moving organ, in other words, its conversion to a controllable system” (Bernstein, 1966).

The computational methods, such as NNMF and PCA, have been used to analyze large sets of data for providing insight into motor control (Ting & Chvatal, 2010). This is based on the possible explanation that CNS coordinates movements as a combination of small groups of motor modules (muscle synergies) in order to reduce the dimensionality of the movement and simplify the control of a large number of DOF in the musculoskeletal system; thus, CNS uses a smaller number of synergies, rather than controlling individual muscles and joints (Ebied et al., 2018).

NNMF is a matrix factorization method where the matrices consist of nonnegative values. It is a group of decomposition algorithms in multivariate analysis and linear algebra where a matrix V is factorized into two matrices, W (weighting coefficient) and H (activation patterns), which is applied in the processing of audio or photographic spectrums or muscular activity.

In behavioral studies, researchers have used this computational technique to extract the underlying synergies from the EMG signals during a specific task or natural behavior. Ivanenko et al. (2005) found consistent five basic locomotor patterns from sixteen muscles from lower limbs and trunk, accounting for most of the variability in EMG signals (Ivanenko et al., 2005). Other studies have also shown the combination of few muscle synergies in upper limb reaching movements (d'Avella et al., 2006), obstacle clearance (MacLellan, 2017), cycling movements (Hug et al., 2011; Wakeling & Horn, 2009), and postural control (Ting & McKay, 2007).

Hypotheses

It was hypothesized that transporting an object would result in increased kinematic damping behavior compared to natural walking and arm-positioning condition without an object, accompanied by greater upper limb muscle activation in order to maintain the flexed elbow and hand position to stabilize the hand-held object. It was also hypothesized that transporting an object would lead to the emergence of new stabilizing synergies on top of the basic activation patterns identified during treadmill walking without object transport. As reported earlier (Ivanenko et al., 2005; Ivanenko et al., 2006), additional muscle synergies have been identified as voluntary motor tasks were added upon an original motor task, such as obstacle clearance while walking. Also, time-ordered proximal-to-distal sequencing of activation patterns in anticipation of gait-related reaction forces and reactive control based on proprioceptive feedback about object displacement was also expected as possible control strategies for the object transport task (Frédéric Danion & Mark L. Latash, 2011; Diermayr et al., 2008; Flanagan & Tresilian, 1994; Gysin et al., 2008; Hirashima et al., 2002; Murphy et al., 1985). These possible control strategies would be evident in the NNMF synergy loadings and their temporal evolution over the gait cycle. Lastly, damping behavior for an object transport task during locomotion was hypothesized to differ between the dominant and non-dominant arms considering the observed differences in controlling inter-segmental dynamics of dominant and non-dominant limbs (Leia B. Bagesteiro & Robert L. Sainburg, 2002; Sainburg, 2002).

METHODS

Participants

Eight healthy right-handed adults free of orthopedic, cardiovascular, and neuromuscular deficits participated in this study (four females, 23±3.30 years, 172.11±9.81 cm, 67.13±8.75 kg).

Edinburgh Handedness Inventory score was +86.08 on average ranged between 70 and 100. The Edinburgh Handedness Inventory was performed to identify each participant's dominant hand. If a participant scored greater than +40, the participant was determined as right-handed, if a participant scored between -40 and +40, then the participant was classified as ambidextrous, and if a participant scored less than -40, then the participant was determined as a left-handed. All participants signed a written informed consent document approved by the Institutional Review Board at Louisiana State University.

Experimental protocol

The experimental protocol was the same as the protocol described in study 1.

Data collection and analysis

Kinematic data collection and data analysis were the same as study 1.

Damping ratio (DR)

The damping behavior of the upper limb within the gait cycle was quantified using a Damping ratio (DR) calculated as the amplitude difference in peak-to-peak vertical displacement of the marker at C7 vertebrae and the MCP joint of the object-carrying hand (or the hand involved in arm-placement without an object) using the following equation (Albert et al., 2010):

$$DR = \frac{(\text{Max.}-\text{Min.})\ of\ MCP}{(\text{Max.}-\text{Min.})\ of\ C7}, \quad (5)$$

, where the marker at C7 represents the trunk (or body) motion, and the marker at MCP represents the displacement of the object (for transporting conditions) and that of the hand (for arm-placement conditions). DR < 1 signifies that the range of vertical motion of the hand is lower than the vertical range of motion of the trunk – indicating the presence of arm stabilization against gait-induced perturbations. DR > 1 signifies a relatively greater range of motion in the hand than in the trunk, indicating a lack of arm stabilization. DRs from each gait cycle were used to calculate the averaged

values for individual participants in conditions where participants hold their elbow joint in a flexed position (D-NOBJ, D-OBJ, ND-NOBJ, and ND-OBJ).

Relative elbow flexion angle

To examine whether the flexed elbow position is consistently maintained or not, the elbow flexion angle during each gait cycle was estimated using the dot product of the 3D kinematic data of the shoulder, elbow, and medial wrist markers. The mean flexion angle was calculated over the time-normalized gait cycle. Mean angle was normalized such that an angle of 0° represents mean elbow angle (typically around 90° flexion), positive values indicate greater elbow extension, and negative values mean greater flexion with respect to the mean angle.

Surface electromyography (EMG)

Data collection and analysis had the same process as study 1, but four additional muscles were recorded, flexor carpi radialis (FCR), extensor carpi ulnaris (ECU), flexor digitorum superficialis (FDS), and extensor digitorum communis (EDC). Since the anticipatory muscular activity was expected with the maximum activation before or around heel contacts as reported earlier in previous studies (Gysin et al., 2003b; Johann P. Kuhtz-Buschbeck & Antoniz Frendel, 2015; Kuhtz-Buschbeck & Jing, 2012), the timing of the activation peak of each individual muscle was determined as the time when the peak amplitude of the linear envelope curve occurred (Akashi et al., 2008) in two different sub-regions of a gait cycle (region 1: 26-75%, region 2: 76-100%) which are related to contra- and ipsilateral heel contacts, respectively.

Muscle synergy analysis

NNMF was applied to extract underlying muscle synergies in the processed (i.e., filtered, rectified, time-, and amplitude-normalized) EMG recordings. To eliminate any possibility of distortion from tonic muscle activity and to focus on the phasic muscle activation patterns on

muscle synergies, the minimum of the averaged processed EMG was subtracted. For each participant and condition, the measured EMG (E) was decomposed into underlying upper limb muscle synergies using the following low-rank approximation ($\hat{E}$):

$$\hat{E} = W \times H + e, \quad (6)$$

where $\hat{E}$ ($m \times t$ matrix, where m is the number of muscles and t is the number of data points, t = 100) is the estimate of muscle activity, E, based on a linear combination of weighting coefficient W ($m \times n$ matrix, where n is the number of synergies extracted from EMG data of ten upper limb muscles) and activation patterns H ($n \times t$ matrix). W and H were estimated by minimizing the root mean square residual error (e) between the original EMG matrix (E) and $\hat{E}$ (nnmf.m in Matlab 2019a). The variance of the muscle activation accounted for (VAF, r^2) by the extracted synergies was calculated using the following equation:

$$r^2 = 1 - SSE/SST, \quad (7)$$

where SSE is the sum of squared errors, and SST is the total sum of squares. The number of muscle synergies to retain for the analysis was determined as the smallest number of synergies that is sufficient to explain more than 90% of the variance of the EMG data (>90% VAF). The best linear fit method was also used as a secondary tool to confirm the VAF method (d'Avella et al., 2006) to compare the number of synergies extracted between methods. The best linear fit method was based on linear regression with the assumption that beyond the ideal number of synergies (N^i), the additional synergies only explain noise or minimal additional data variation, as showing a change in slope at the point of N^i and the straight slope after N^i on the r^2 vs. number of synergy curve (d'Avella et al., 2006). From this, the smallest number of synergies was determined as a correct number of synergies (N^i) when the residual mean square error (RMSE) of the linear fit from that number of synergies to the seventh (set as a maximum number in this study) synergy is less than

10^{-4}. If there was a difference in the number of synergies between the methods due to the presence of atypical pattern, the number of synergies was then determined based on inspection of the relation between the measured EMG of each muscle and its NNMF reconstruction – the minimal number of synergies that captures more than 90% in each muscle was selected in this study (L. H. Ting & S. A. Chvatal, 2010).

In order to compare the similarity between the synergies identified through NNMF in each participant, a factor clustering technique was performed as the synergies are grouped across participants, and the best matching scalar product of the weighting coefficients normalized to the Euclidean norm was used to calculate the similarity between extracted synergies (Cheung et al., 2005). An initial set of weighting coefficients was obtained from the muscle activation during treadmill walking, and the side-averaged muscle activations of dominant (Rt.) and non-dominant (Lt.) arms were used to avoid any side bias. These group-averaged weighting coefficients were used as an initial set to compare vectors in each individual for all conditions using the best matching scalar product. The initial set of weighting coefficients was iteratively updated with each subsequent participant and condition by applying a weighted average method for each identified pattern to have an equal contribution on the set used for comparison (Martino et al., 2015). Every possible combination was compared between each participant's synergy set and the synergy set from group-averaged muscle activations. Specifically, each synergy in the template was iteratively updated with only one synergy from the individual participant that maximized the scalar product. If two synergies from the participant were matched with one synergy in the template with the scalar product greater than 0.6, then the synergy with the higher scalar product was selected, and the other synergy then became an option for the rest of the synergies in the template. If a scalar product between the mean set and a synergy identified within an individual participant was less than 0.6,

then that synergy was determined to be a new synergy in the comparative set. All analyses were conducted in Matlab 2019a (Mathworks, Natick, MA, USA).

Statistical analysis

A one-way within-subject ANOVA was used to examine differences in walking speed and stride time across transport conditions. One sample *t*-test was used to determine whether the DR was significantly different from 1.0 for each condition. A two-way within-subjects ANOVA with Hand (dominant vs. non-dominant) and Object (treadmill walking vs. no-object with arm-placement vs. object transport) was performed to identify statistically significant differences in vertical displacement of C7 and MCP, DR, relative elbow flexion angle, the timing of activation peak of individual muscles, and mean EMG activation level. If the main effect of an object or Hand × Object interaction was determined to be statistically significant, a Tukey's HSD post-hoc test was performed to determine differences between conditions. All statistical analyses were performed using SAS (version 9.4, SAS Institute Inc., Cary, NC, USA), and statistically significant differences were determined at a p-value<0.05.

RESULTS

Across all participants, the mean walking speed was 1.1±0.08 m/s ranged between 1.02 and 1.23 m/s. The mean preferred walking stride time was 1.16±0.03 s ranged between 1.05 and 1.24 s, with the mean timing of contralateral heel contact occurring at 49.7±2.8% of the gait cycle across all participants. Ipsilateral toe-off occurred at 66.3±3.3% of the gait cycle. Mean stride time and timing of gait cycles did not significantly differ across participants (p>0.05).

Damping ratio (DR)

Figure 4.1A shows a representative vertical displacement of the C7 and MCP joint markers during the gait cycle. As expected, these markers displayed a sinusoidal pattern with the highest

peaks corresponding to the ipsilateral and contralateral single support phase, and the lowest peaks were present immediately following ipsilateral and contralateral heel contacts. The sinusoidal pattern was similar across all participants and conditions. While the mean vertical displacement of C7 did not show the main effect of hand or object across participants (p>0.05, D-NOBJ: 0.037±0.005 m, D-OBJ: 0.036±0.006 m, ND-NOBJ: 0.036±0.005 m, ND-OBJ: 0.035±0.006 m), the mean vertical displacement of MCP was significantly greater in the non-dominant hand (main effect of hand: $F_{(1,20)}$=5.21, p=0.034, D-NOBJ: 0.051±0.003 m, D-OBJ: 0.045±0.008 m, ND-NOBJ: 0.058±0.009 m, ND-OBJ: 0.054±0.08 m). Overall, the DRs from individual gait cycles from each participant were above 1.0 during all four conditions (p<0.001, see Figure 4.1B), indicating greater vertical displacement in the hand relative to the trunk. Regardless of the presence of the object, the dominant arm showed greater damping behavior than the non-dominant arm with a lower DR (main effect of hand: $F_{(1,27)}$=4.52, p=0.043). Though there was no main effect of the object, the DRs were slightly smaller during OBJ condition than the NOBJ condition in both dominant and non-dominant arms. There was no interaction effect of hand and object on damping behavior.

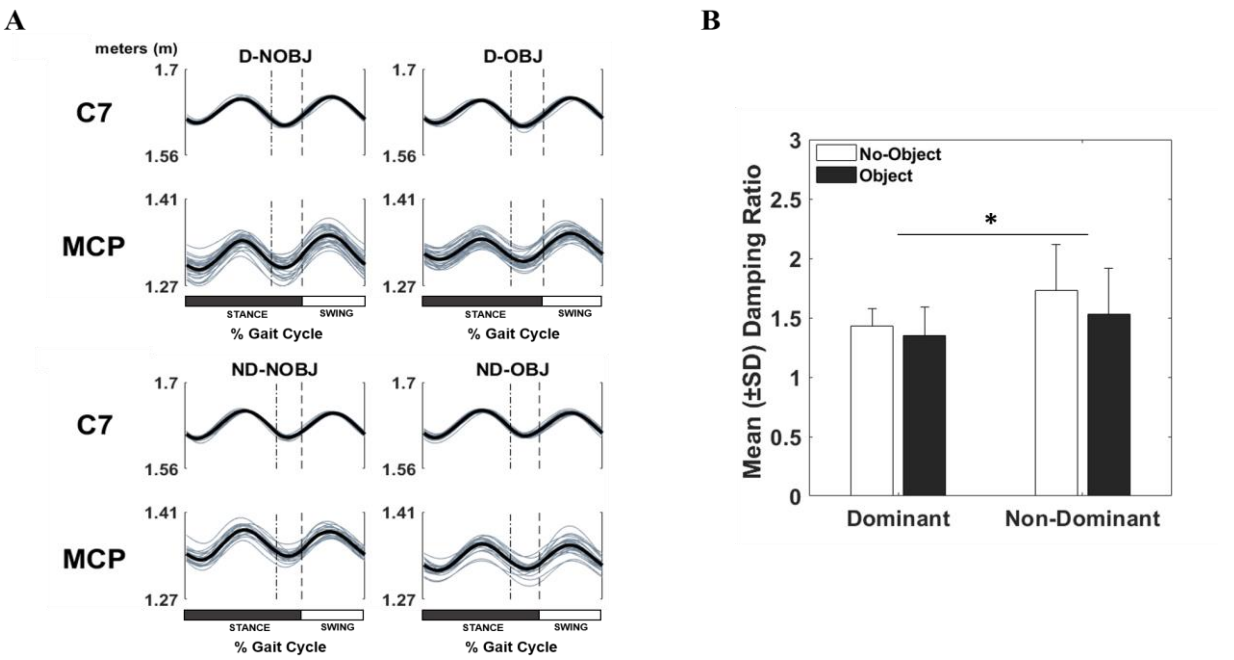

Figure 4.1. A. Vertical trajectories of C7 and MCP markers in four different conditions from a representative participant. Grey lines represent the vertical displacement from individual strides, and the black (thick) lines represent the mean across individual walking strides. The first vertical line (-.) located around 50% of the gait cycle indicates the time when the contralateral heel contacted with the ground. The second vertical line (--) around 60-70% of the gait cycle indicates ipsilateral toe-off, dividing the gait cycle into stance and swing phases. B. Mean damping ratio (DR). Error bars depict standard deviation (+SD) across participants. The main effect of hand (p = 0.043) is presented with an asterisk (*). C7, 7th cervical spine; MCP, metacarpophalangeal joint. Reprinted by permission from Springer Nature: Springer Nature, *Experimental Brain Research* (Song et al., 2020), Muscle synergy for upper limb damping behavior during object transport while walking in healthy young individuals, Song, A., Kuznetsov, Nikita A., Winges, Sara A., MacLellan, Michael J, Copyright (2020).

Relative elbow flexion angle

Figure 4.2A shows the elbow flexion angle and relative elbow flexion angle from a representative participant, and Figure 4.2B shows the mean (±SD) range of relative elbow flexion angles across participants. Relative elbow flexion angle reached peak flexion slightly before both ipsi- and contra-lateral heel contacts and gradually increased right after heel contacts toward elbow extension. No significant main or interaction effects for the mean range of elbow flexion angle were evident (p>0.05).

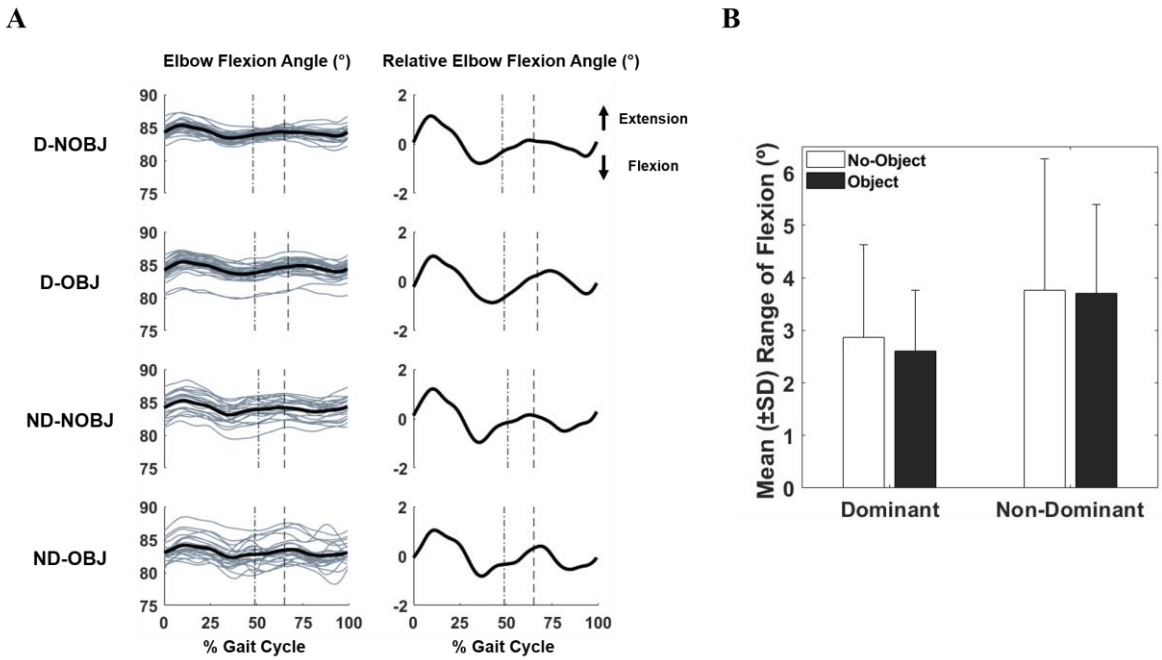

Figure 4.2. A. Elbow flexion angle and relative elbow flexion angle from a representative participant. In the left panel, gray lines represent the elbow flexion angle from individual strides and thick black lines in both left and right panels represent the mean elbow flexion angle and mean relative elbow flexion angle across individual walking strides, respectively. B. Mean (±SD) range of relative elbow flexion angle across participants for each condition. No statistically significant difference was observed in both transporting arm and object/no-object conditions. Reprinted by permission from Springer Nature: Springer Nature, *Experimental Brain Research* (Song et al., 2020), Muscle synergy for upper limb damping behavior during object transport while walking in healthy young individuals, Song, A., Kuznetsov, Nikita A., Winges, Sara A., MacLellan, Michael J, Copyright (2020).

Surface electromyography (EMG)

The group averaged (N=8) amplitude- and time-normalized EMG profiles during walking with different arm conditions are shown in Figure 4.3, and the estimated timings of muscle activation peaks in two regions of the gait cycle are shown in Table 4.1. Most of the muscles in the OBJ and NOBJ conditions presented a clear biphasic pattern with the maximum amplitudes around or immediately preceding the heel contact of each limb. The magnitudes of activation were lowest during regular treadmill walking compared to OBJ and NOBJ transport conditions with the exception of PD. Also, the number of muscles displaying distinct activation patterns and their

mean activation level increased as the experimental conditions progressed from treadmill walking to object transport.

In treadmill walking, the primarily activated muscles were TRAP, AD, PD, and TB. TRAP reached its peak first, followed by AD reaching its peak before contralateral heel contact, and PD, BB, and TB reached their peaks at the contralateral heel contact almost simultaneously. These muscles showed relatively similar timings reaching their peaks at nearly the same time before ipsilateral heel contact. During the no-object condition, the timing of the maximum burst of TRAP and AD was switched such that AD and BB reached their peaks first, followed by TRAP and BR prior to both contra- and ipsilateral heel contacts. In the object condition, similar to the no-object condition, AD and BB reached their peaks first, followed by TRAP, TB, and FCR before contralateral heel contact. However, this activation order was not consistent with regard to ipsilateral heel contact. The latest peaks occurred for BR and wrist/finger flexor and extensor muscles (FCR, ECU, FDS, and EDC), with peaks around or slightly before both contralateral and ipsilateral heel contacts. There was no significant main effect of hand for all ten muscles ($p>0.05$), but the main effect of object condition was observed in AD having earlier timings of peak activation during no-object and object conditions when compared to treadmill walking before both contra- and ipsilateral heel contacts. Similarly, BB and BR showed a main effect of object condition reaching its peaks earlier during no-object and object conditions than during treadmill walking, but it was only observed in region 1 (prior to contralateral heel contact). Since the wrist and finger muscles were generally not activated in treadmill walking, only no-object and object conditions were included in statistical analysis, and FCR showed relatively delayed timing of activation peak when participants carried the object in their hands before contralateral heel contact when compared to no-object condition ($p<0.05$).

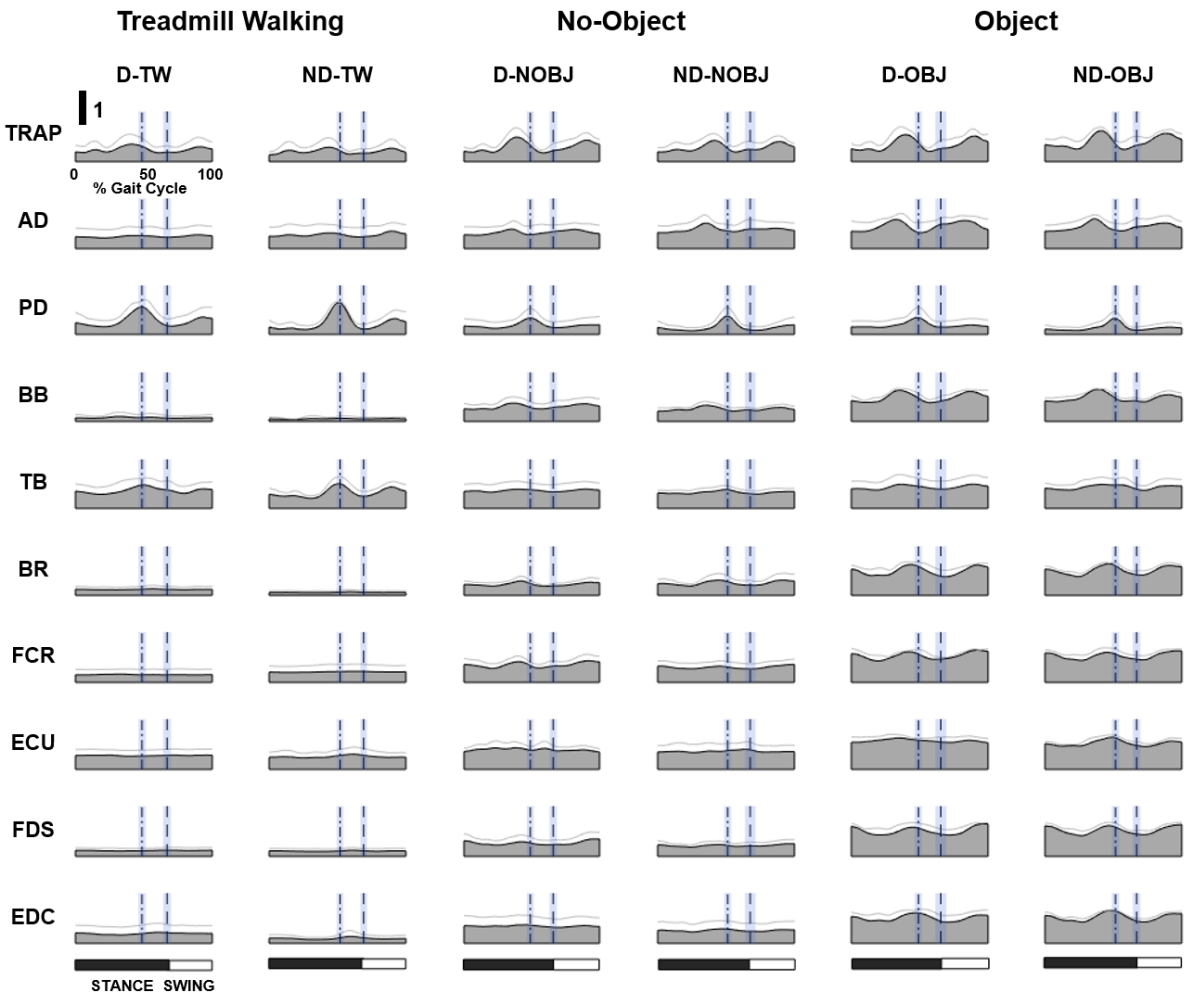

Figure 4.3. Group averaged (n=8) amplitude- and time-normalized EMG (see method) during walking with different arm conditions. A gray area with black edge represents the mean EMG across participants, and a light gray line in each plot represents standard deviation (+SD). The first vertical line in each graph represents the group mean timing of contra-lateral heel contacts, and the second vertical line represents that of ipsilateral toe-off. SD for both timings was displayed with a blue area. Muscles recorded: trapezius (TRAP), anterior deltoid (AD), posterior deltoid (PD), biceps brachii (BB), triceps brachii (TB), brachioradialis (BR), flexor carpi radialis (FCR), extensor carpi ulnaris (ECU), flexor digitorum superficialis (FDS), and extensor digitorum communis (EDC). D, dominant; ND, non-dominant; TW, treadmill walking; NOBJ, no-object transport; OBJ, object transport. Reprinted by permission from Springer Nature: Springer Nature, *Experimental Brain Research* (Song et al., 2020), Muscle synergy for upper limb damping behavior during object transport while walking in healthy young individuals, Song, A., Kuznetsov, Nikita A., Winges, Sara A., MacLellan, Michael J, Copyright (2020).

Table 4.1. Group mean timings of activation peak (±SD, % gait cycle) of individual muscles for both regions 1 and 2 across all conditions and *p* values for main effects of hand. D, dominant; ND, non-dominant; TW, treadmill walking; NOBJ, no-object transport; OBJ, object transport.

Muscle	Region 1 (26-75% of Gait Cycle)							
	Treadmill Walking		No-Object		Object		*p* value	
	D-TW	ND-TW	D-NOBJ	ND-NOBJ	D-OBJ	ND-OBJ	Hand	Object
TRAP	41.9 (4.9)	42.8 (2.6)	40.3 (4.2)	40.7 (3.4)	39.6 (4.2)	40.8 (2.3)	NS	NS
AD	45.7 (7.0)	43.8 (7.2)	38.2 (3.8)	35.8 (5.6)	35.2 (2.1)	36.8 (3.0)	NS	0.0019
PD	49.8 (1.2)	49.4 (1.0)	50.1 (3.3)	50.1 (1.4)	50.0 (1.1)	50.0 (1.7)	NS	NS
BB	49.4 (14.4)	49.1 (10.0)	37.9 (3.4)	37.3 (3.6)	37.3 (3.8)	39.6 (2.6)	NS	0.0002
TB	47.0 (5.3)	50.6 (3.2)	44.3 (7.6)	48.4 (6.2)	43.4 (7.2)	44.9 (10.4)	NS	NS
BR	54.9 (14.4)	58.3 (14.6)	41.4 (2.2)	43.3 (5.4)	45.5 (5.0)	47.3 (2.8)	NS	0.0042
FCR			41.2 (1.3)	41.2 (5.6)	43.6 (3.3)	45.8 (3.7)	NS	0.0485
ECU			49.5 (9.9)	49.8 (11.5)	46.3 (12.4)	49.2 (2.4)	NS	NS
FDS			46.0 (5.5)	43.1 (3.8)	45.7 (5.0)	47.3 (2.7)	NS	NS
EDC			46.3 (6.0)	45.7 (6.3)	48.0 (4.5)	48.1 (1.6)	NS	NS
	Region 2 (76-100% of Gait Cycle)							
	Treadmill Walking		No-Object		Object		*p* value	
	D-TW	ND-TW	D-NOBJ	ND-NOBJ	D-OBJ	ND-OBJ	Hand	Object
TRAP	92.3 (5.4)	90.7 (5.1)	91.0 (5.5)	88.9 (3.6)	90.1 (6.0)	89.0 (3.4)	NS	NS
AD	90.8 (7.0)	90.1 (2.6)	84.9 (4.4)	83.6 (6.1)	85.4 (4.8)	86.1 (4.5)	NS	0.0054
PD	90.1 (7.1)	92.3 (4.9)	93.1 (7.1)	93.7 (4.9)	89.8 (4.1)	92.3 (5.9)	NS	NS
BB	89.8 (10.0)	88.6 (7.3)	87.3 (4.8)	87.7 (4.2)	88.1 (5.4)	90.1 (2.0)	NS	NS
TB	88.6 (9.0)	89.9 (3.9)	88.5 (7.5)	91.4 (7.8)	89.1 (6.4)	94.6 (6.5)	NS	NS
BR	89.7 (8.8)	90.9 (10.6)	92.3 (6.5)	89.1 (4.5)	91.3 (4.7)	93.6 (4.2)	NS	NS
FCR			94.2 (4.5)	94.5 (7.7)	94.6 (5.1)	95.2 (5.0)	NS	NS
ECU			86.2 (6.0)	84.7 (8.1)	87.2 (4.7)	93.0 (4.3)	NS	NS
FDS			95.4 (4.0)	95.1 (5.7)	96.0 (4.5)	98.1 (3.1)	NS	NS
EDC			88.9 (4.3)	92.6 (8.0)	93.3 (4.3)	95.0 (4.6)	NS	NS

The mean EMG level increased in most muscles in the OBJ and NOBJ conditions compared to treadmill walking, except for PD and TB (Figure 4.4). The mean EMG amplitude showed a main effect of arm condition in TRAP ($F_{(2,36)}$=7.19, p=0.002) and AD ($F_{(2,39)}$=6.14, p=0.005), specifically the mean amplitude during object transport was higher when compared to treadmill walking (TRAP: p=0.002, AD: p=0.003). A main effect of arm condition was also present in BB ($F_{(2,39)}$=162.67, p<0.0001) and BR ($F_{(2,36)}$=75.85, p<0.0001). These two elbow flexors showed higher activation when participants held their elbow in a flexed position (NOBJ and OBJ) than in treadmill walking (p<0.001), and when compared to the no-object condition, the mean amplitude was significantly higher when participants carried the object (p<0.001). As expected, a main effect of arm condition for the mean amplitude was shown in the wrist and finger muscles, including FCR ($F_{(2,27)}$=37.82, p<0.0001), ECU ($F_{(2,27)}$=21.89, p<0.0001), FDS ($F_{(2,36)}$=123.88, p<0.0001), and EDC ($F_{(2,36)}$=29.50, p<0.0001). Post-hoc tests showed that mean amplitudes of these four muscles were significantly different in all three arm conditions, presenting the highest activation during object transport, followed by arm positioning without the object, and lowest during treadmill walking (p<0.05). The mean amplitude of PD showed a main effect of arm condition ($F_{(2,39)}$=4.10, p=0.02). Interestingly, PD displayed the highest activation during treadmill walking and decreased when participants held their arms in an elbow flexion position without the object (p=0.05) and showed the lowest activation when they carried the object (p=0.04).

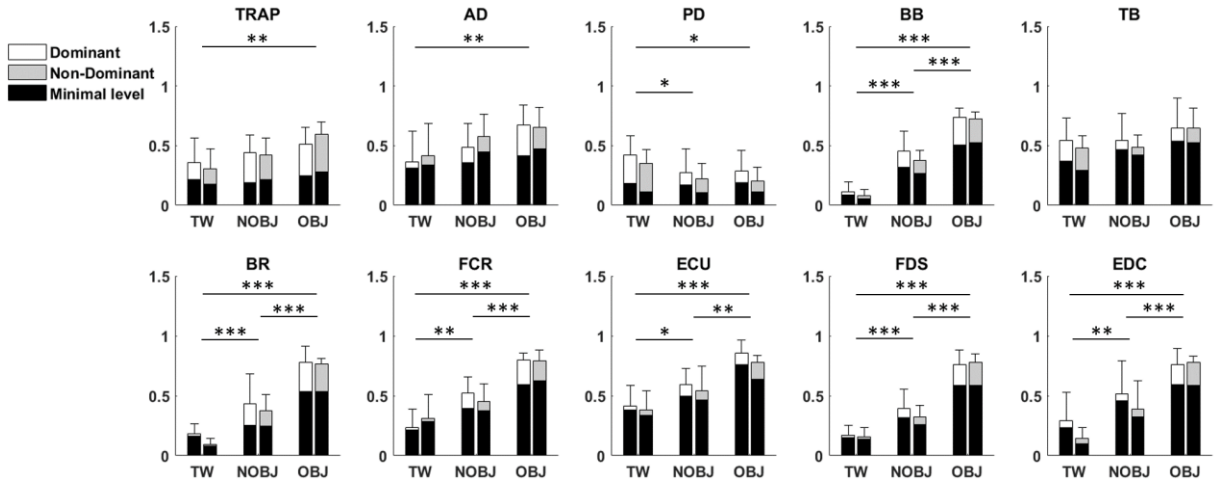

Figure 4.4. Group averaged (N=8) mean EMG magnitude of individual muscle throughout the gait cycle for each condition. Statistical difference between conditions is displayed with asterisk (p<0.05: *, p<0.01: **, and p<0.001: ***). In addition, the group averaged minimal level of muscle activation across participants is presented (black bar). Reprinted by permission from Springer Nature: Springer Nature, *Experimental Brain Research* (Song et al., 2020), Muscle synergy for upper limb damping behavior during object transport while walking in healthy young individuals, Song, A., Kuznetsov, Nikita A., Winges, Sara A., MacLellan, Michael J, Copyright (2020).

Muscle synergy analysis

The number of extracted synergies across participants and conditions ranged between one and five. The mean VAF (±SD) that met the criterion of 90% across participants for the dominant side during treadmill walking (D-TW) was 94% (±2.63%), 95% (±2.22%) for non-dominant treadmill walking (ND-TW), 94% (±1.74%) for dominant no-object (D-NOBJ), 93% (±1.93%) for non-dominant no-object (ND-NOBJ), 94% (±2.16%) for the dominant object (D-OBJ), and 93% (±1.45%) for the non-dominant object (ND-OBJ). The mean number of synergies (±SD) identified for dominant treadmill walking (D-TW) was 2.75 (±1.19), 2.71 (±0.45) for non-dominant treadmill walking (ND-TW), 3.63 (±0.86) for dominant no-object (D-NOBJ), 3.14 (±0.64) for non-dominant no-object (ND-NOBJ), 3.38 (±0.69) for the dominant object (D-OBJ), and 3 (±0.53) for the non-dominant object (ND-OBJ).

The group-averaged weighting coefficients from the extracted muscle synergies are shown

in Figure 4.5. The clustering analysis (described in the method) identified seven synergy patterns (SYN1-SYN7 in Figure 4.5) that were evident in the majority of participants (>50% in each condition). The mean scalar product of the weighting coefficient vectors between individual participants and the group mean was 0.87 (range 0.77 to 0.92), indicating a relatively high degree of similarity between these synergies identified through NNMF in each participant for all conditions. For the treadmill walking condition, two synergies (SYN2 and SYN4) were identified for the dominant arm and one synergy (SYN2) for the non-dominant arm. Both of these synergies were mainly related to the activation of shoulder and elbow extensor muscles (PD and TB). The second synergy (SYN2) was observed in both arms during treadmill walking and remained when participants positioned their arm in elbow flexion without the object (NOBJ) but disappeared during object transport condition (OBJ). During the no-object condition, two additional synergies (SYN1 and SYN6) accompanied SYN2. SYN1 primarily consists of the activity of shoulder flexor (AD). SYN6 mainly consists of the activities of TRAP and BB. During the object transport condition, these two synergies (SYN1 and SYN6) were also observed consistently, but SYN2 was no longer present. Besides, a new synergy (SYN7), consisting of wrist and finger joint muscle activations (FCR, FDS, and EDC) as well as elbow flexor (BR), was identified in both arms. Object transport was also associated with two additional unilateral synergies: SYN5 for the dominant arm and SYN3 for the non-dominant arm.

Figure 4.6 shows the temporal pattern of change in the weighting coefficients for SYN1-SYN7 over the gait cycle. The group averaged activation peaks of temporal muscle activation patterns from identified synergies are presented in Table 4.2. Most of the activation patterns have one or two peaks either before or around the heel contacts. Similar to the activation peaks of PD and TB from EMG profiles, SYN 2 and SYN4 showed their peaks around contra-lateral heel

contact and slightly before ipsilateral heel contact during treadmill walking and no-object conditions. SYN1 and SYN6 mainly consisted of the activity of AD and TRAP during no-object, and object conditions showed their peaks 10-15% before both sides of heel contacts. SYN3, SYN5, and SYN6, which are responsible for wrist and finger muscles, showed their peaks right before both heel contacts.

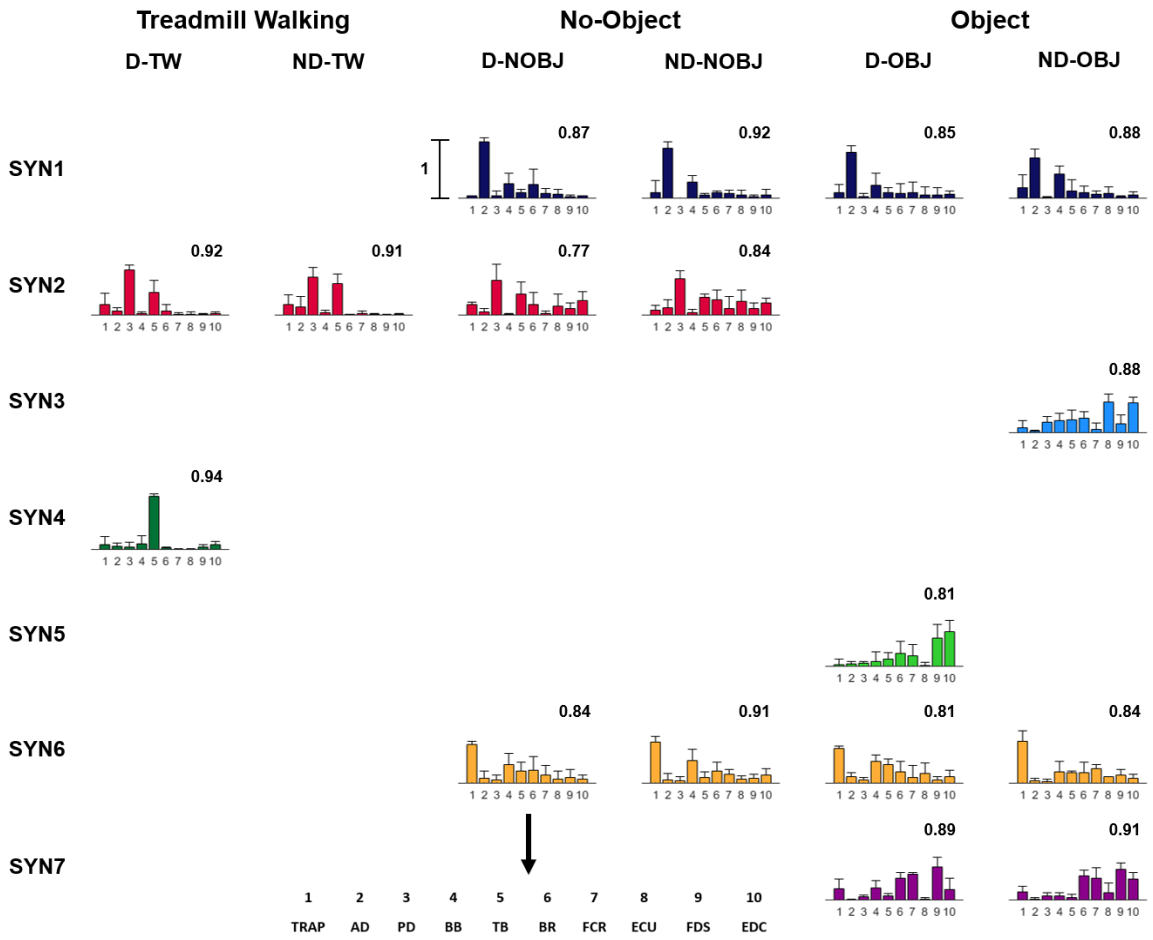

Figure 4.5. Group averaged weighting coefficients (W) and standard deviation (+SD) of extracted muscle synergies for the dominant and non-dominant arms in the three transport conditions. The mean scalar product between individual participants and the group averaged weighting coefficients are presented on each graph. Synergies depicted in the same color between conditions indicate the same synergies with the mean scalar product greater than 0.6. SYN, synergy. Reprinted by permission from Springer Nature: Springer Nature, *Experimental Brain Research* (Song et al., 2020), Muscle synergy for upper limb damping behavior during object transport while walking in healthy young individuals, Song, A., Kuznetsov, Nikita A., Winges, Sara A., MacLellan, Michael J, Copyright (2020).

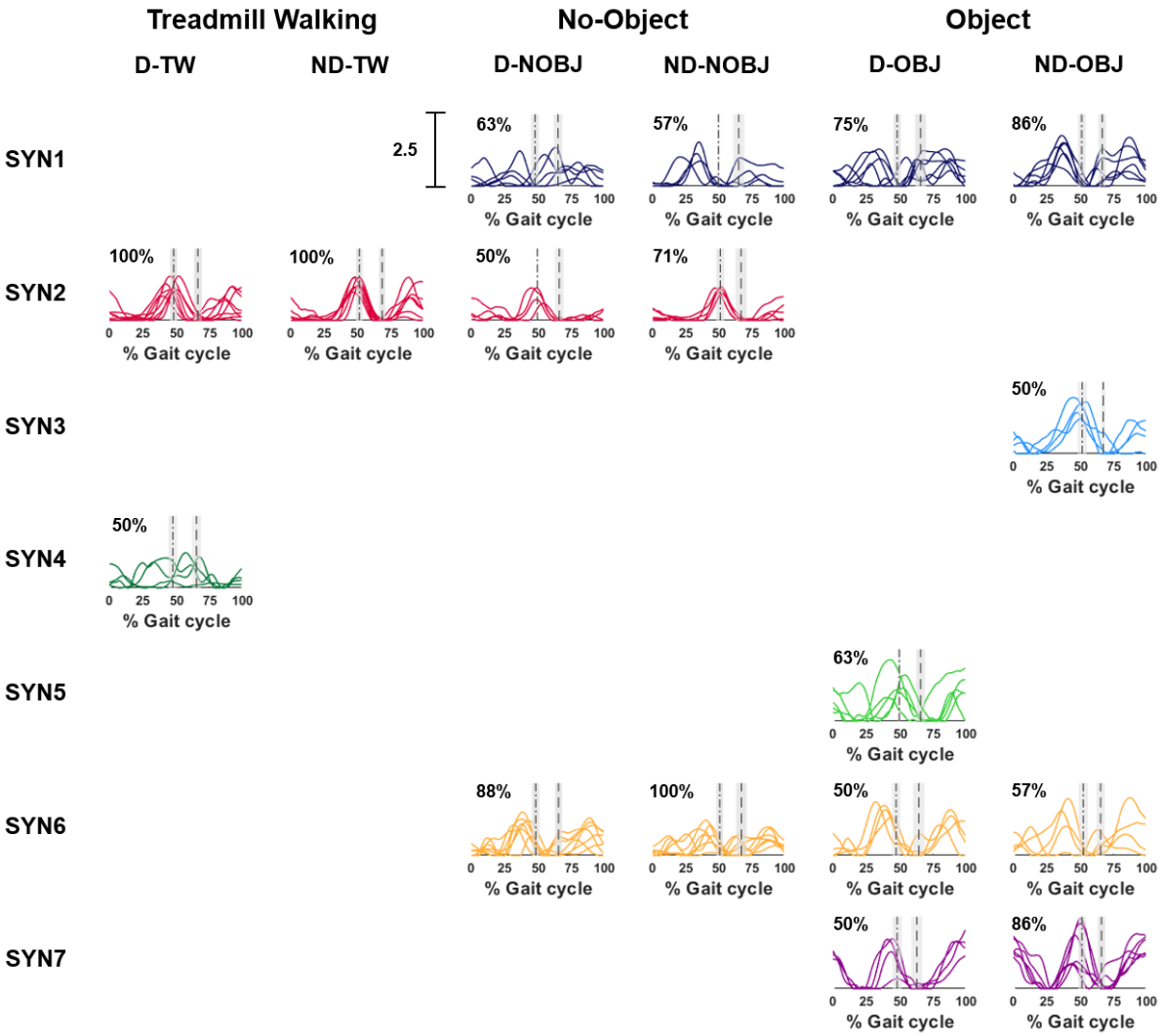

Figure 4.6. Temporal activation pattern (H) of extracted muscle synergies. Each line indicates the activation pattern from the individual participant who showed the muscle synergy. The number on each graph indicates the % of participants showed the specific muscle synergy pattern. The first vertical line (-.) indicates the mean timing of contralateral heel contact and the second vertical line (--) indicates the mean timing of toe-off across participants who presented each pattern. SDs for both timings were presented in light gray areas, calculated from those participants who presented that specific muscle synergy pattern. SYN, synergy. Reprinted by permission from Springer Nature: Springer Nature, *Experimental Brain Research* (Song et al., 2020), Muscle synergy for upper limb damping behavior during object transport while walking in healthy young individuals, Song, A., Kuznetsov, Nikita A., Winges, Sara A., MacLellan, Michael J, Copyright (2020).

Table 4.2**.** Group mean timings of activation peak (±SD, % gait cycle) of identified synergies for both regions 1 and 2 across all conditions. Each group mean and SD were calculated from the participants who displayed that specific muscle synergy pattern. D, dominant; ND, non-dominant; TW, treadmill walking; NOBJ, no-object transport; OBJ, object transport. Reprinted by permission from Springer Nature: Springer Nature, *Experimental Brain Research* (Song et al., 2020), Muscle synergy for upper limb damping behavior during object transport while walking in healthy young individuals, Song, A., Kuznetsov, Nikita A., Winges, Sara A., MacLellan, Michael J, Copyright (2020).

Synergy	Region 1 (26-75% of Gait Cycle)					
	Treadmill Walking		No-Object		Object	
	D-TW	ND-TW	D-NOBJ	ND-NOBJ	D-OBJ	ND-OBJ
SYN1			60.8 (13.6)	34.0 (5.1)	39.5 (6.7)	36.0 (4.0)
SYN2	47.6 (3.8)	49.7 (1.8)	49.8 (2.5)	51.4 (1.9)		
SYN3						50.0 (3.4)
SYN4	53.8 (10.0)					
SYN5					48.2 (5.6)	
SYN6			39.7 (3.7)	41.9 (5.2)	39.0 (4.0)	39.7 (2.1)
SYN7					45.0 (2.6)	48.4 (2.3)
	Region 2 (76-100% of Gait Cycle)					
	Treadmill Walking		No-Object		Object	
	D-TW	ND-TW	D-NOBJ	ND-NOBJ	D-OBJ	ND-OBJ
SYN1			82.4 (4.5)	79.3 (3.4)	87.0 (4.6)	86.3 (4.6)
SYN2	92.9 (4.8)	90.7 (3.5)	94.0 (6.4)	94.0 (5.0)		
SYN3						94.0 (4.9)
SYN4	82.8 (10.0)					
SYN5					96.4 (4.1)	
SYN6			90.9 (6.6)	88.3 (3.5)	89.5 (6.0)	89.0 (3.7)
SYN7					96.5 (3.6)	96.8 (4.9)

DISCUSSION

This study investigated the neuromuscular strategy used by the CNS for controlling the upper limb while transporting an object in hand during locomotion. Changes in identified muscle synergies involved in this task and the timing of their activation were examined by analyzing patterns of surface EMG using the NNMF technique (Lee & Seung, 1999) for the dominant and non-dominant limbs. Higher damping was observed in the dominant compared to the non-dominant arm without a clear difference between the no-object and object transport conditions. All muscles showed higher mean levels of activation during object transport except for PD, with activation peaks occurring around or slightly prior to heel contact. The NNMF results indicated that the stabilization of the shoulder and elbow joints by several muscle synergies also plays a significant role in maintaining object stability in addition to modulation of finger GFs during locomotion.

Two of the identified upper limb synergies (SYN1 and SYN6) were related to shoulder and elbow flexion and were active during both object and no-object conditions. The main synergy observed during treadmill walking condition primarily involved activations of PD and TB (SYN2), which is consistent with previous studies that found that natural walking involving eccentric contractions of PD while the arm moves forward with the peak activations around contralateral heel contact (Johann P. Kuhtz-Buschbeck & Antoniz Frendel, 2015; Kuhtz-Buschbeck & Jing, 2012; MacLellan & Ellis, 2018). An additional muscle synergy (SYN7) associated with wrist and finger muscles became active only during the object transport condition. Temporal activation patterns of a majority of the proximal muscles were consistent with previous studies that investigated upper limb muscle activations during locomotion resulting from quadrupedal arm-leg coordination (Johann P. Kuhtz-Buschbeck & Antoniz Frendel, 2015; Kuhtz-Buschbeck & Jing,

2012; Sylos-Labini et al., 2018). Interestingly, the temporal pattern of activation of these muscle synergies seemed to follow the proximal-to-distal pattern in anticipation of heel contacts. The SYN1 and SYN6 associated with shoulder and elbow muscles peaked in activity approximately 10% of the gait cycle prior to heel strike and were followed by the activation of the wrist and finger muscles (SYN7), which occurred nearly in synchrony with heel strikes (see Table 2 for the timing of peaks of these synergies). It is well-documented that a critical aspect of the CNS control strategy for object transport during locomotion is the modulation of GF in anticipation of changes in the inertial LFs (Diermayr et al., 2008; Gysin et al., 2003b; Gysin et al., 2008), but the results of this study also suggest that the CNS additionally stabilizes the shoulder and elbow joints as part of the strategy to resist the disturbance caused by heel contacts with the ground. This anticipatory upper limb muscle activation supports the idea of proximal-distal sequencing control of CNS reported earlier (Aruin & Latash, 1995; Cordo & Nashner, 1982; Dounskaia, 2010; Dounskaia et al., 1998; Friedli et al., 1984; Hirashima et al., 2007; Massion, 1992; Shiratori & Latash, 2000), indicating that proximal muscles mainly generate stabilization for the dynamic motion of entire limb and this is beneficial for stable and accurate distal joint actions when responding to external perturbations.

The mean levels of activation of elbow flexors and wrist/hand muscles (BB, BR, FCR, ECU, FDS, and EDC) were significantly higher during the object transport task suggesting that the increase in the phasic activation detected by the NNMF was also supplemented by increased apparent stiffness due to higher muscle co-contraction levels. Increased tonic (minimal) level of activations of all muscles except for PD during object transport likely contributes to the stability of the upper limb and the object, supporting conclusions in previous studies (Lametti et al., 2007; Osu et al., 2002; Selen et al., 2006; Zakotnik et al., 2006). Moreover, the wrist joint that is more distal to shoulder and elbow joints seems to use a co-contraction strategy, suggesting these muscles

contribute to the grasp stability by increasing wrist and finger joints apparent stiffness through the simultaneous contraction of agonist and antagonist. This idea can be supported by earlier work that found increased activation of both wrist flexor and extensor muscles to increase wrist joint stiffness to damp the oscillations during the task where participants were asked to perform targeted wrist movements against unpredictable loads (Milner & Cloutier, 1993; Milner; & Cloutier, 1995).

The average DRs for each participant were greater than one, indicating the greater vertical displacement of the object than that of the trunk during transport. Previous studies have reported DRs lower than one during self-paced and fast over-ground walking in healthy young adults (Albert et al., 2010; Gysin et al., 2003b). Our object transport task placed relatively low precision demands on the control of object orientation (participants were instructed to "hold the elbow at 90 degrees," and the object was an aluminum can), while these previous studies utilized a gripping instrument filled with or without water, which places higher task constraint on control moments of force acting on the object (Gysin et al., 2003b). Another potential reason for the difference could be the different walking conditions (treadmill vs. overground walking). One previous study suggested that the magnitude of the vertical GRF during MST was greater during treadmill walking compared to overground walking (White et al., 1998), which could lead to greater reaction force acting on the object. Moreover, walking on the treadmill could be perceived as a task itself requiring corrections of stride time and length to maintain the central position on the treadmill belt (Roerdink et al., 2019), leading to a less amount of attention for the object in hand, resulting in greater vertical displacement.

Although only right-handed individuals participated in this study, the results suggested that upper limb damping behavior during object transport could be influenced by hand dominance. The dynamic dominance hypothesis (Sainburg, 2002) suggests that the dominant limb system is

specialized for controlling trajectory using feed-forward mechanisms for predictable task dynamics (Yadav & Sainburg, 2014), whereas the non-dominant limb is specialized for controlling limb position using sensory feedback-based error correction mechanism. Previous studies showed that the dominant arm is superior in controlling inertial interactions of limb segments, such that the dominant arm adopts a more torque-efficient movement pattern than the non-dominant arm, while the non-dominant arm showed less efficient movement control caused by larger muscle torque and small joint interaction torque to generate similar movement speeds and accuracy to dominant arm (Leia B. Bagesteiro & Robert L. Sainburg, 2002; Bagesteiro & Sainburg, 2003; Przybyla et al., 2012; Sainburg, 2002, 2005). Other researchers found that time delay of GF relative to LF was present only in the non-dominant arm during a bimanual coordination task (Jin et al., 2011). It has been reported that the object transport task is performed by mainly anticipatory motor control with shorter time lag than the minimal time required for feedback control involving coordinated adjustment of GF based on predicted postural changes when walking (Diermayr et al., 2008; Gysin et al., 2003b; Gysin et al., 2008). However, those previous studies used only the dominant arm for the task, the limited information on temporal coordination between grip and LF in non-dominant arm leaves an unsolved question on whether or not the difference in DR between arms results from different control mechanisms between dominant and non-dominant arms. Nonetheless, since the dominant arm is more often associated with daily tasks requiring precise anticipatory control, higher damping behavior in the dominant arm may result from a more advanced control capability of the CNS accumulated through the life experience. A few studies that investigated the effect of handedness on muscle synergies have shown that identified synergy sets were similar between dominant and non-dominant limbs during hands-and-knees crawling (Xiang et al., 2017) and during upper limb target-matching task (Roh et al., 2013) in healthy

individuals. However, Duthilleul et al. (Duthilleul et al., 2015) reported that the dominant arm showed a higher number of extracted muscle synergies and the variability of muscle synergies between dominant and non-dominant arms was dependent on the task with different levels of difficulty.

There was an apparent oscillatory pattern of the elbow flexion angle over the gait cycle such that participants tended to increase flexion slightly before ipsilateral and contra-lateral heel contacts. On the one hand, these adjustments may be indicative of feedforward control to maintain a constant orientation of the object while walking. From a different perspective, the observed oscillation could be induced by a time-varying inertial forcing in the presence of constant centrally specified reference position command (Feldman & Levin, 1995). Similar amplitude of elbow fluctuation even with the additional mass of the object during object transport suggests that the CNS may have modulated the apparent stiffness or damping terms of the forearm system (shoulder and elbow) via altered level of muscle activations.

In summary, the results of this study suggest that damping behavior during object transport during locomotion is achieved by continuous adjustments of phasic muscle activations in the shoulder, elbow, and wrist/hand joints in connection with gait events, in combination with constant tonic activations of involved muscles to generate more flexible muscular control to stabilize the upper arm joints as well as hand-held object. Elbow flexion angle with rhythmical pattern and earlier muscle activation before both heel contacts support an anticipatory control of CNS to stabilize the arm and hand-held object against gait-induced IFs while walking. Stabilization of proximal joints before the distal joints is consistent with the hypothesis of time-ordered proximal-to-distal activation of muscles. Among three muscle synergies identified during object transport, two of them are shared with the no-object condition, suggesting the same motor control strategy

of CNS. One additional synergy mainly consists of wrist/hand muscles as they are involved in grasping the object. Identification of basic muscle synergy patterns using methods outlined here might provide further information on the understanding of neuromuscular control strategies during the object transport with increased demands on control of object orientation.

CHAPTER 5. THE EFFECT OF DIFFERENT PRECISION DEMAND AND VISUAL INFORMATION ON UPPER LIMB JOINT KINEMATICS AND MUSCLE SYNERGY DURING OBJECT TRANSPORT WHILE WALKING: STUDY 3

INTRODUCTION

In the last study of the dissertation, the influence of increased stability requirements on the upper limb muscle synergies during object transport was examined. It has been reported that young healthy individuals successfully adjust fingertip forces to the object's physical properties and to gait-induced IFs acting on the object in an anticipatory manner (Diermayr et al., 2008; Gysin et al., 2003a). Ground reaction and GFs are closely related in time (Diermayr et al., 2008), and grip and IFs of the transporting hand were highly coupled in an anticipatory fashion to ensure object stability (Gysin et al., 2003a). While there've been studies examining the effects of increased task constraint on GF and walking dynamics (Gysin et al., 2003a), upper limb synergy adaptations are not understood, and one may still ask the question of how do people alter the upper limb control as opposed for finger forces and gait cycle adjustments.

A human's ability to remain stable requires precise motor control using sensory integration from proprioception, visual, and vestibular inputs to inform people about the state of the body with respect to the environment. During object transport while walking, the sensory information from visual and proprioceptive systems is critical to complete this task. Proprioception provides information about the body's position, movement velocity of the limbs, the amount of load weighted by the object. The sensory structures involved in proprioception are muscle spindles, GTOs, and sensory structures such as the vestibular system, sensory receptors found in skin, bones, or joints also play an important role in completing the motor task successfully. The perception of the object's mass and moment of inertia properties obtained from joints and muscles are also essential to gauge the proper level of GF to counteract the IFs. In addition, visual information

about the carried object's location relative to the trunk and the upper limb enables the CNS to determine the movement trajectory of the upper limbs and the object's orientation. The CNS integrates the sensory information from these two systems to generate a more accurate motor command to accomplish this particular goal of the task (Sarlegna & Sainburg, 2009; van Beers et al., 1999). However, the relative contributions of these sensory systems for object stabilization during walking have not been thoroughly examined, and the focus has been on the GF alterations, not on muscle synergies of the upper limb that position the arm in space.

The purpose of this study was to examine the effect of task difficulty and visual information of the carried object on the neuromuscular control strategy during object transport while walking. More specifically, this study was aimed at answering the question of how CNS can maintain stability in object manipulation by regulating kinematic parameters, including limb stiffness, when the task involves greater difficulty with an unpredictable object system (ball-cup system). A 3D-printed cup-shaped object with a curved top surface was used to provide different levels of task difficulty (Figure 5.1). Participants were required to maintain the small ball on the cup's surface for higher precision demand. For lower precision, participants simply carried the curved cup without the ball. To examine the relative contribution of sensory and proprioceptive inputs on this task, participants were required to look forward vs. look at the cup and the ball. In the looking forward condition, participants had to rely on the proprioceptive information primarily with the limitation of using central vision and using only peripheral visual information, while in the looking at the cup condition, both sensory systems were used for concurrent correction of the object and body's movement.

Hypotheses

It was hypothesized that transporting a shallow cup with a ball (Figure 5.1) would increase

kinematic damping behavior and decrease relative angular displacement of the shoulder and elbow motion compared to natural walking and walking with the cup and no-ball. These kinematic alterations would be accompanied by increased upper limb muscle activations, especially when the central visual information about the cup-ball system and hand is not available.

In terms of upper limb muscle synergies, it was expected that task constraint with central visual information about the object would result in additional synergies as the task continuously requires the adaptation of the upper limb kinematics and muscle activations to stabilize the object. Compared to the conditions where the central visual information is available, when central visual information is limited, a smaller number of muscle synergies would be identified as the co-contraction level increases to stabilize the entire upper limb segment by overall increased stiffness rather than real-time modulation throughout the gait cycle.

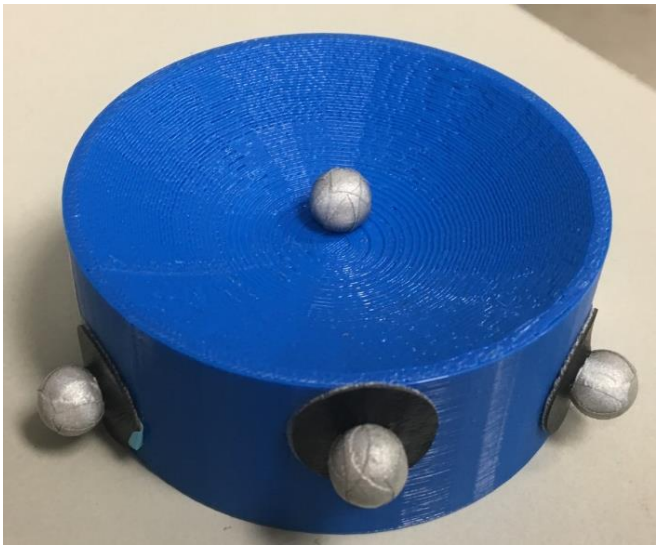

Figure 5.1. The object used in this study was 3D-printed cylinder with curved top surface (1.2 cm depth at apex) with radius of 3.75 cm, weight of 100g (+5g of the ball).

METHODS

Participants

Nine healthy right-handed adults free of orthopedic, cardiovascular, and neuromuscular

deficits participated in this study (three males, 26.11±6.07 years, 172.01±9.82 cm, 69.53±11.49 kg). Edinburgh Handedness Inventory score was +87.53±12.22 on average ranged between 70 and 100. The Edinburgh Handedness Inventory was performed to identify each participant's dominant hand. If a participant scored greater than +40, the participant was determined as right-handed, if a participant scored between -40 and +40, then the participant was classified as ambidextrous, and if a participant scored less than -40, then the participant was determined as a left-handed. All participants signed a written informed consent document approved by the Institutional Review Board at Louisiana State University.

Experimental protocol

The experimental protocol was similar to that of studies 1 and 2, with the following modifications: only the dominant arm was used for carrying, and the transported object was the 3D-printed cylinder with a curved top surface (1.2 cm depth at apex) with a radius of 3.75 cm. Participants were asked to keep their elbow at approximately 90° of flexion and maintain the object's vertical orientation while walking.

For the lower precision demand, participants were required to carry the cup without the ball while walking (NOBALL). For the higher precision demand, they were required to carry the same object, but there was a small ball on the surface, and participants were asked to keep the ball in the cup and not to drop it to the ground (BALL). The object transport task was also performed with two different visual information conditions: participants were instructed to 1) look forward directly and not to look at the object in their hand (looking forward, LF), and 2) look at the cup and a ball (looking at the object, LO). Therefore, the procedure consisted of participants walking on a split-belt treadmill under five conditions: 1) holding a cup while looking forward (NOBALL LF), 2) holding a cup while looking at the cup (NOBALL LO), 3) holding a cup with a ball while

looking forward (BALL LF), 4) holding a cup with a ball while looking at the cup and a ball (BALL LO), 5) treadmill walking without any object transport (TW). Five experimental conditions were presented in randomized blocks consisting of two trials, each with at least 30 strides.

Participants were instructed to walk on the treadmill at their preferred walking speed determined before experiments. Self-selected treadmill walking speed was determined by asking participants to walk on the same treadmill as naturally as possible before attaching any equipment. To find the most comfortable walking speed, an investigator gradually increased the treadmill's velocity from 0.5 m/s to 1.5 m/s in steps of 0.1 m/s until the participant verbally indicated they were walking at a comfortable speed.

Data collection and analysis

3D kinematics were acquired using a Qualisys motion capture system (Göteborg, Sweden). Retro-reflective markers were placed at the spine of the C7 vertebrae, at the front head (mid-point between left and right eyebrows), and right clavicle. Twenty markers were placed bilaterally on the side of the head (mandibular notch around the articulation between temporal and mandible bone), the acromion process (shoulder), medial and lateral epicondyle of the humerus (medial and lateral elbow), ulna- and radius-styloid processes (medial and lateral wrists, respectively), MCP joint of a middle finger, lateral malleolus of the tibia (ankle), posterior surface of the calcaneus (heel), and head of first metatarsus (hallux). All markers were placed on the skin, except for the heel, and hallux, which were placed on the participants' shoes. Missing data segments of less than 100 ms were interpolated using a cubic spline algorithm (spline.m in Matlab 2020b). All kinematic data were sampled at 100 Hz and were low-pass filtered using dual-pass, second-order, Butterworth filter with a cut-off frequency of 7 Hz.

A gait cycle was defined based on heel strikes. Heel contact was determined using a vertical

velocity threshold of 120 mm/frame. All gait cycles of each marker's data were then time-normalized to 100 data points, with each data point representing 1% of the gait cycle. To ensure the consistency of walking in terms of speed and stride or step length, the first three and the last two gait cycles of each trial were excluded from the analysis. Kinematics and EMG of the dominant side of the body were analyzed based on the ipsilateral gait cycle.

Damping ratio (DR)

The quantification of the DR was the same as described in study 2.

Angular displacement of shoulder and elbow joints

The quantification of the angular displacement of the shoulder and elbow joints was exactly the same as described in study 1. The shoulder joint angle in the sagittal plane was defined with respect to the absolute vertical line. Elbow joint angle was defined as the 3D angle between the upper arm segment and forearm segment.

Ball motion

The amount of ball motion within the cup was quantified using the 95% ellipse area (Schubert & Kirchner, 2014) of the ball's x-y coordinates in the local coordinate frame of the cup. To obtain the local coordinates, the ball trajectories in the x and y direction were subtracted from the x and y coordinates of the center of the object. Eigenvectors of the x-y covariance values were used to determine the principal axes of variation of the ball's motion. The distribution of distances ($\sqrt{x^2 + y^2}$) to the center of the cup were fit with a Rayleigh distribution and the value accounting for 95% of the distance values captured the boundary of the area covered by the ball's motion (for full details, see Schubert & Kirchner, 2014). The area was calculated for each gait stride for individual participants, and then the averaged area from an individual participant was used for statistical analysis.

Surface electromyography (EMG)

Data collection and post-processing procedures were the same as described in studies 1 and 2. However, in study 3, pectoralis major (PM) and latissimus dorsi (LD) were additionally recorded. The mean muscle activation from time- and amplitude-normalized EMG during each gait cycle was calculated across participants. Similar to study 2, since the anticipatory muscular activity was expected with the maximum activation before or around heel contacts as reported earlier in previous studies (Gysin et al., 2003b; Johann P. Kuhtz-Buschbeck & Antoniz Frendel, 2015; Kuhtz-Buschbeck & Jing, 2012), the timing of the activation peak of each individual muscle was determined as the time when the peak amplitude of the linear envelope curve occurred (Akashi et al., 2008) in three different sub-regions of a gait cycle (region 1: 1-25%, region 2: 26-75%, region 3: 76-100%) which are related to contra- and ipsilateral heel contacts, respectively.

Muscle synergy analysis

The muscle synergy was identified by using the same method (NNMF) and data processing as described in study 2.

Statistical analysis

A two-way within-subject ANOVA with Ball (BALL vs. NOBALL) and Vision (LF vs. LO) was performed to identify statistically significant differences in relative angular displacement of shoulder joint in both sagittal and transverse planes, the relative angular displacement of elbow joint, DR, group-averaged EMG activation level of individual muscle, and peak timing of muscle activation in three different regions of the gait cycle (region 1, 2, and 3). To directly test the hypothesis about the change in the movement amplitude, a one-sample repeated-measures *t*-test was used to determine whether the relative angular displacement during object transport condition was significantly different from the 0% during TW. One sample *t*-test was also used to determine

whether the DR is significantly different from 1.0 for each condition. Statistical difference in 95% ellipse area of the ball on the cup surface between two visual conditions (BALL LF vs. BALL LO) was examined by performing a one-sample repeated-measures *t*-test. All statistical analyses were performed using SAS (version 9.4, SAS Institute Inc., Cary, NC, USA), and statistically significant differences was determined at a p-value<0.05.

RESULTS

Across all participants, the mean walking speed was 0.89±0.11 m/s ranged between 0.8 and 1.1 m/s. The mean preferred walking stride time was 1.17±0.07 s ranged between 1.01 and 1.31 s, with the mean timing of contralateral heel contact occurring at 50.33±0.90% of the gait cycle across all participants. Ipsilateral toe-off occurred at 68.00±3.08% of the gait cycle. Mean stride time and timing of gait cycles did not significantly differ across participants (p>0.05).

Angular displacement of the shoulder joint in sagittal plane

Group averaged relative angular displacement of the shoulder joint in the sagittal plane with respect to TW was presented in Figure 5.2A. There was no main effect of Ball and Vision (p>0.05). When compared to the angular displacement during TW, the angular displacement during the object transport task was significantly decreased for all four experimental conditions (p<0.01).

Angular displacement of the shoulder joint in transverse plane

There was a main effect of Ball (BALL vs. NOBALL) in relative angular displacement of the shoulder joint in the transverse plane ($F_{(1,32)}$=6.86, p=0.0133) (Figure 5.2B), indicating that participants decreased the angular change in transverse plane when they carried the object with a ball when compared to the conditions when they only carried the object without a ball on the surface. Except for the condition of NOBALL LO, there were significant differences with respect

to 0% (p<0.05).

Angular displacement of the elbow joint

There was no main effect of Ball (BALL vs. NOBALL) and the main effect of Vision (LF vs. LO) in the 3D elbow joint angular displacement (p>0.05, Figure 5.2C). For all conditions, the angular displacement was significantly decreased when compared to 0% during TW (p<0.001).

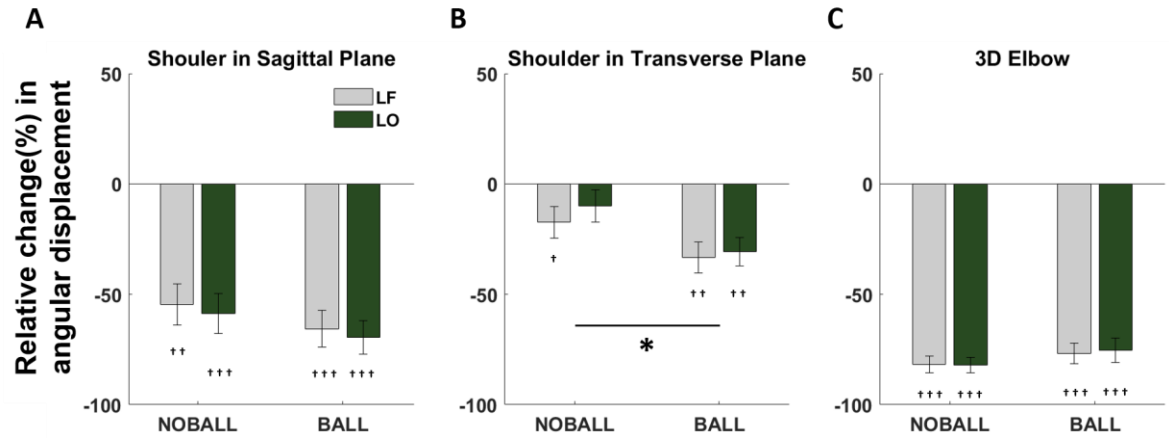

Figure 5.2. Group averaged relative angular displacement with standard error of shoulder joint in sagittal plane (A), in transverse plane (B), and elbow joint (C). The angular displacements during all conditions were normalized by the angular displacement during TW (0%). Main effect of the ball is displayed with asterisk (p = 0.01). Statistical difference with respect to 0% is displayed with cross (†p <0.05, ††p<0.01, †††p<0.001**).**

Damping ratio (DR)

There was a main effect of Ball (BALL vs. NOBALL) (F(1,32)=5.96, p=0.02) in DR. The DR during BALL LO was significantly different from 1 (p=0.003) (Figure 5.3). Mean DRs for individual participants were presented in Table 5.1.

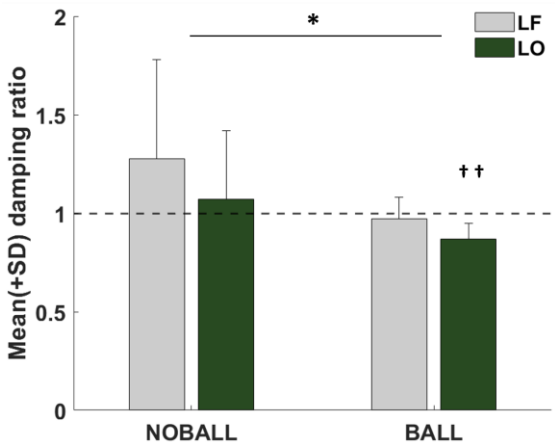

Figure 5.3. Mean damping ratio (DR). Error bars depict standard deviation (+SD) across participants. The main effect of the ball is presented with an asterisk (p = 0.02). Statistical difference with respect to 1 is displayed with cross (†p <0.05, ††p<0.01, †††p<0.001**).**

Table 5.1. Mean damping ratio (DR) across gait strides of individual participant and group averaged DR across participants (±SD).

	NOBALL LF	NOBALL LO	BALL LF	BALL LO
SUB1	1.22 (0.24)	0.87 (0.16)	0.83 (0.16)	0.82 (0.14)
SUB2	0.94 (0.21)	0.79 (0.16)	0.79 (0.22)	0.79 (0.16)
SUB3	1.12 (0.20)	1.10 (0.15)	1.08 (0.26)	1.00 (0.37)
SUB4	1.18 (0.18)	1.02 (0.14)	0.96 (0.16)	0.87 (0.18)
SUB5	0.96 (0.22)	0.93 (0.17)	0.99 (0.28)	0.95 (0.30)
SUB6	1.09 (0.12)	0.94 (0.12)	0.98 (0.41)	0.93 (0.17)
SUB7	0.96 (0.15)	0.80 (0.18)	0.93 (0.24)	0.84 (0.34)
SUB8	2.53 (0.23)	1.90 (0.24)	1.12 (0.21)	0.75 (0.19)
SUB9	1.50 (0.34)	1.30 (0.30)	1.06 (0.25)	0.89 (0.26)
Average	1.28 (0.50)	1.07 (0.35)	0.97 (0.11)	0.87 (0.08)

95% Ellipse area of the ball

During the experiments, there was no participant who dropped the ball from the cup. The 95% ellipse area of the ball within the surface of the cup (object) was not statistically different between two different visual conditions (LF vs. LO), even though the group averaged area was smaller during the BALL LO condition. The mean areas of the ball for the individual participant were presented in Table 5.2.

Table 5.2. Mean 95% ellipse area of the ball across gait cycles for individual participant (±SD).

	BALL LF	BALL LO
SUB1	208.24 (152.89)	329.04 (179.11)
SUB2	202.20 (120.70)	201.30 (145.24)
SUB3	281.83 (180.17)	302.02 (183.18)
SUB4	246.66 (180.76)	152.14 (101.80)
SUB5	183.34 (95.47)	225.25 (120.62)
SUB6	1099.32 (649.73)	856.85 (513.14)
SUB7	1448.34 (720.00)	391.68 (451.59)
SUB8	554.36 (313.85)	202.22 (122.19)
SUB9	383.46 (253.78)	343.00 (194.21)
Average	511.97 (455.47)	333.72 (211.45)

*Unit: mm^2

Surface electromyography (EMG)

The group averaged (N=9) amplitude- and time-normalized EMG profiles during walking with different object transport conditions are shown in Figure 5.4, and the estimated timings of muscle activation peaks in three regions of the gait cycle are shown in Table 5.3. Similar to the result of study 2, most of the muscles during the object transport task showed a biphasic pattern with the maximum amplitudes around or slightly prior to the heel contact of the lower limbs. Group averaged EMG activation for each condition is shown in Figure 5.5. The muscles that showed significant changes in mean EMG activation compared to TW were TRAP, AD, BB, BR, FCR,

ECU, FDS, and EDC. There was a main effect of Ball in the wrist flexor and extensor muscles which are FCR ($F_{(1,32)}$=6.70, p=0.01), ECU ($F_{(1,32)}$=8.00, p=0.008), FDS ($F_{(1,32)}$=8.67, p=0.006), and EDC ($F_{(1,32)}$=4.19, p=0.04), showing the greater mean EMG activation when participants carried the object with the ball on the surface for both visual conditions. There were no main effects of Ball and Vision in activation peak timing for all three regions of the gait cycle for all twelve muscles except for TB in region 3 ($F_{(1,32)}$=4.55, p=0.04).

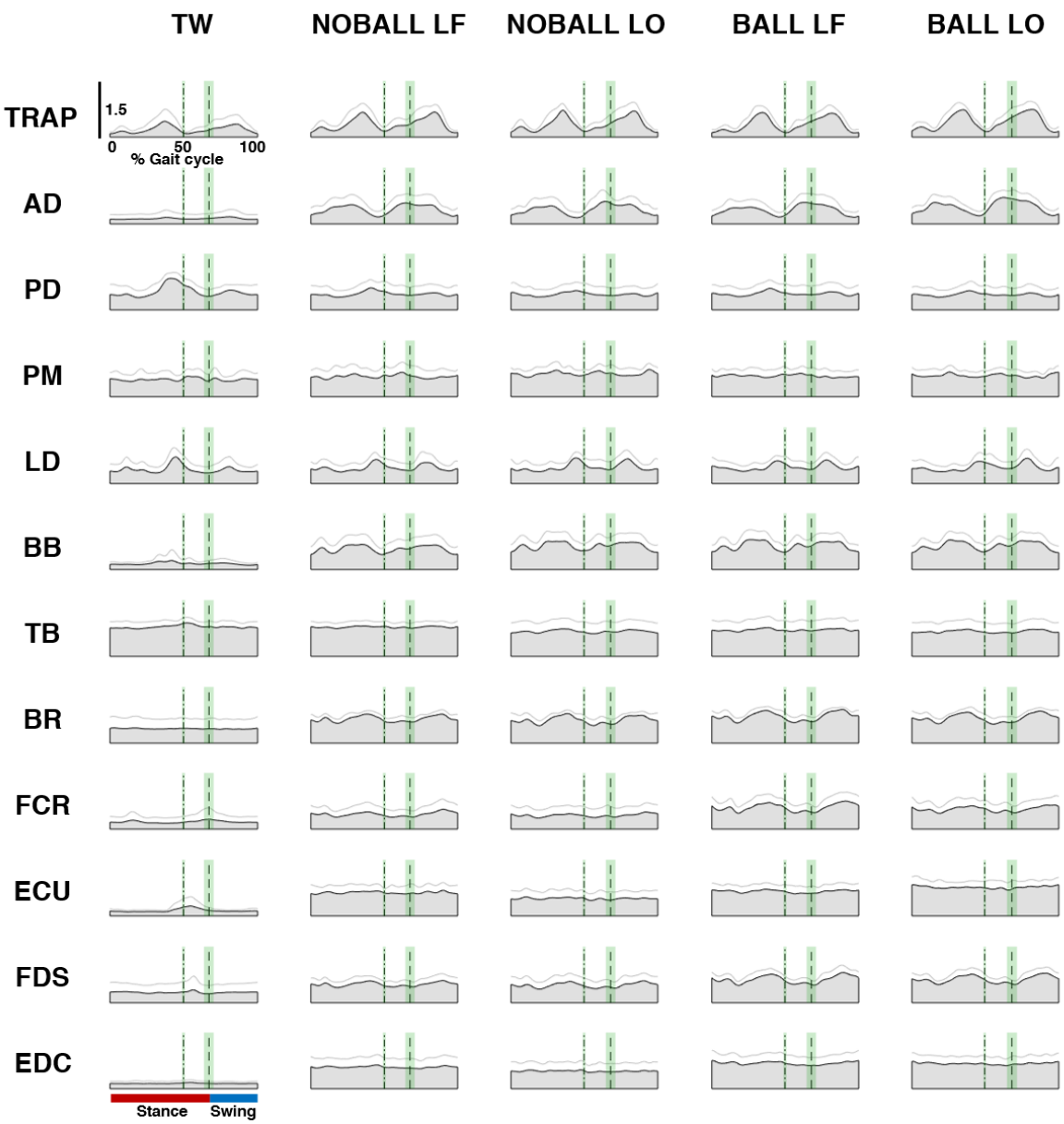

Figure 5.4. Group averaged (n=9) amplitude- and time-normalized EMG (see method) during walking with different arm conditions. A gray area with black edge represents the mean EMG across participants, and a light gray line above the filled area in each plot represents standard deviation (+SD). The first vertical line in each graph represents the group mean timing of contra-lateral heel contacts, and the second vertical line represents that of ipsilateral toe-off. SD for both timings was displayed with a green area. Muscles recorded: trapezius (TRAP), anterior deltoid (AD), posterior deltoid (PD), pectoralis major (PM), latissimus dorsi (LD), biceps brachii (BB), triceps brachii (TB), brachioradialis (BR), flexor carpi radialis (FCR), extensor carpi ulnaris (ECU), flexor digitorum superficialis (FDS), and extensor digitorum communis (EDC).

Table 5.3. Group mean timings of activation peak (+SD, % gait cycle) of individual muscles for the regions of gait cycle 1, 2, and 3 across all conditions and *p* values for main effects of the ball (BALL vs. NOBALL) and vision (looking forward vs. looking at an object).

Muscle	Region 1 (1-25% of Gait Cycle)						
	TW	NOBALL LF	NOBALL LO	BALL L	BALL LO	*p* value	
						BALL	VISION
TRAP	10.67 (6.36)	13.67 (8.65)	14.22 (8.70)	20.44 (8.59)	15.11 (9.24)	NS	NS
AD	12.33 (8.47)	20.00 (7.57)	21.67 (4.44)	18.78 (7.97)	18.56 (4.19)	NS	NS
PD	8.67 (7.87)	8.11 (7.74)	5.78 (4.97)	8.11 (7.77)	8.22 (7.79)	NS	NS
PM	10.78 (10.83)	14.11 (9.60)	12.44 (9.49)	14.56 (9.22)	14.11 (11.11)	NS	NS
LD	10.78 (8.30)	9.00 (4.24)	10.67 (9.18)	5.33 (4.58)	9.56 (7.91)	NS	NS
BB	12.33 (8.49)	19.89 (7.70)	18.22 (8.21)	21.33 (7.07)	17.11 (7.77)	NS	NS
TB	12.67 (10.23)	10.33 (9.73)	13.11 (5.97)	15.11 (9.17)	19.00 (6.69)	NS	NS
BR	10.56 (7.23)	11.78 (5.93)	12.33 (5.79)	8.89 (7.61)	9.78 (7.60)	NS	NS
FCR	9.67 (9.04)	6.00 (4.72)	7.33 (8.38)	9.67 (7.86)	6.56 (7.57)	NS	NS
ECU	6.00 (8.17)	10.67 (8.03)	13.56 (7.49)	6.89 (7.52)	8.78 (9.64)	NS	NS
FDS	9.00 (6.91)	11.67 (5.96)	9.00 (8.14)	9.00 (8.09)	7.56 (7.21)	NS	NS
EDC	5.67 (6.36)	9.89 (8.61)	13.33 (6.16)	8.67 (8.20)	7.56 (8.08)	NS	NS
	Region 2 (26-75% of Gait Cycle)						
	TW	NOBALL LF	NOBALL LO	BALL LF	BALL LO	*p* value	
						BALL	VISION
TRAP	46.78 (15.73)	43.33 (17.63)	49.00 (18.17)	46.11 (19.74)	46.22 (18.87)	NS	NS
AD	57.11 (16.03)	60.67 (15.92)	64.33 (10.44)	64.22 (10.26)	64.33 (5.96)	NS	NS
PD	43.11 (4.23)	50.22 (14.74)	47.44 (11.62)	47.44 (11.18)	47.89 (14.21)	NS	NS
PM	56.89 (14.03)	44.78 (13.49)	52.22 (14.45)	53.89 (11.13)	39.67 (14.82)	NS	NS
LD	49.33 (8.65)	57.44 (13.67)	50.33 (15.39)	53.33 (12.61)	54.89 (12.42)	NS	NS
BB	52.00 (18.23)	37.89 (14.69)	42.78 (15.06)	32.44 (4.33)	43.11 (21.51)	NS	NS
TB	44.89 (9.78)	42.89 (9.94)	35.44 (7.04)	38.56 (8.52)	40.22 (13.41)	NS	NS
BR	53.33 (12.04)	38.67 (3.84)	39.22 (2.22)	38.78 (5.26)	41.56 (10.99)	NS	NS
FCR	50.44 (15.43)	39.44 (6.84)	43.67 (13.08)	37.56 (6.27)	38.89 (7.87)	NS	NS
ECU	57.11 (6.92)	45.44 (11.59)	42.67 (12.21)	44.89 (12.14)	51.78 (12.17)	NS	NS
FDS	46.78 (13.10)	40.11 (6.09)	40.78 (5.56)	40.00 (5.02)	39.11 (4.86)	NS	NS

EDC	51.89 (9.44)	45.89 (7.15)	47.78 (9.93)	44.11 (8.99)	50.56 (17.30)	NS	NS
	Region 3 (76-100% of Gait Cycle)						
	TW	NOBALL LF	NOBALL LO	BALL LF	BALL LO	*p* value	
						BALL	VISION
TRAP	84.33 (3.74)	82.89 (4.17)	84.11 (3.41)	82.33 (3.08)	82.00 (2.87)	NS	NS
AD	83.67 (7.47)	81.33 (5.41)	82.00 (5.17)	78.56 (6.02)	79.00 (6.14)	NS	NS
PD	86.11 (8.02)	88.56 (9.14)	90.44 (10.04)	90.44 (9.42)	86.22 (8.61)	NS	NS
PM	86.44 (9.44)	91.22 (8.64)	92.67 (6.73)	86.89 (9.99)	90.89 (9.61)	NS	NS
LD	86.89 (8.19)	85.00 (9.45)	83.89 (7.39)	83.56 (9.21)	83.67 (9.08)	NS	NS
BB	84.11 (9.71)	81.78 (4.84)	81.22 (4.63)	82.33 (4.90)	80.00 (4.27)	NS	NS
TB	86.67 (9.50)	86.67 (7.92)	82.67 (3.71)	87.89 (8.12)	83.00 (3.74)	NS	0.04
BR	89.11 (10.58)	84.44 (5.68)	87.67 (6.12)	88.22 (5.40)	90.00 (7.16)	NS	NS
FCR	91.67 (10.19)	90.33 (3.97)	90.56 (5.48)	91.56 (4.50)	92.22 (5.36)	NS	NS
ECU	88.00 (8.70)	86.67 (7.16)	89.11 (8.27)	90.44 (8.83)	91.33 (8.90)	NS	NS
FDS	89.33 (7.91)	89.67 (4.33)	90.56 (6.27)	90.33 (3.28)	88.78 (4.58)	NS	NS
EDC	90.11 (7.74)	88.56 (7.84)	87.56 (10.01)	92.44 (6.89)	89.33 (9.00)	NS	NS

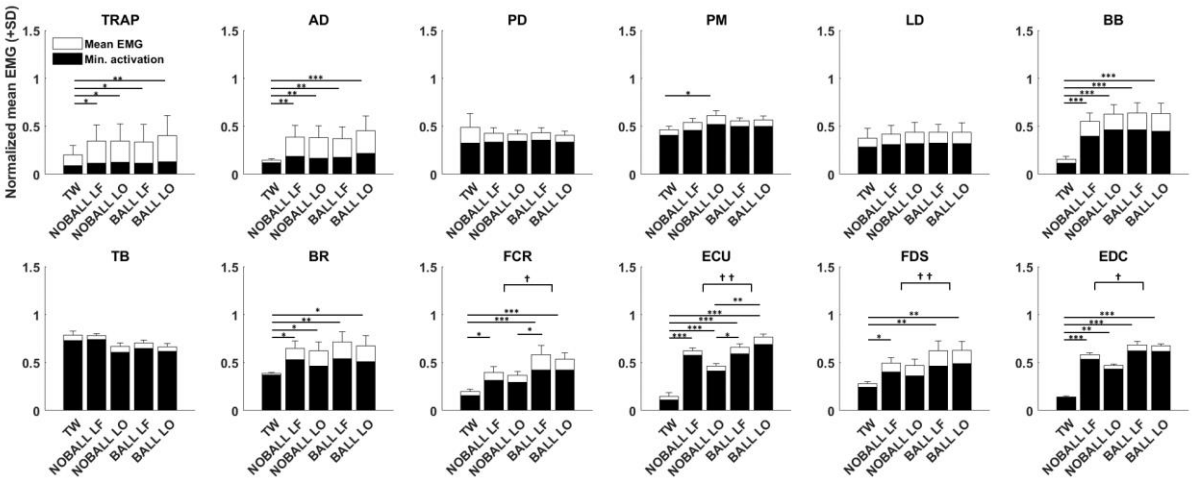

Figure 5.5. Group averaged (N=9) mean EMG magnitude of individual muscle throughout the gait cycle for each condition. In addition, the group averaged minimal level of muscle activation across participants is presented (black bar). Statistical difference with respect to the EMG amplitude during TW is presented with asterisk (p<0.05: *, p<0.01: **, and p<0.001: ***). The main effect of ball is displayed with cross (p<0.05: †, p<0.01: ††, and p<0.001: †††).

Muscle synergy analysis

The group averaged weighting coefficients from the extracted muscle synergies are shown in Figure 5.6. The clustering analysis identified six synergy patterns across conditions that appeared in greater than 50% of participants in each condition. The mean scalar product of the weighting coefficient vectors between individual participants and the group mean was 0.87 (range from 0.77 to 0.95). SYN1 and SYN2 were identified in all five experimental conditions, mainly related to the activation of LD and PD (SYN1) and TRAP, BB, and BR (SYN2). SYN3 was identified during TW and NOBALL LO conditions mainly consisted of the activities of PM. SYN4 was only identified for TW, consisting of the activation of PD. SYN5 identified during object transport task was primarily related to wrist and finger flexor and extensors (FCR, ECU, FDS, and EDC). SYN6 identified during object transport task except for NOBALL LF was associated with the activation of AD and BB. Figure 5.7 presents the temporal pattern of change in the weighting coefficients for identified synergies over a gait cycle. The group averaged activation peaks of

temporal muscle activation patterns from identified synergies are presented in Table 5.4. SYN1 and SYN4, which are mainly related to the activation of LD and PD, showed the activation peak around the contralateral heel contact and prior to ipsilateral heel contact. SYN2, mainly associated with the activation of TRAP, showed the activation peak prior to both contralateral and ipsilateral heel contacts. SYN5 associated with wrist and finger muscles also showed the activation peak prior to both heel contacts. SYN6 related to the activation of AD and BB showed the first activation peak around 20% of the gait cycle and then the second peak around the ipsilateral toe-off (60% of the gait cycle).

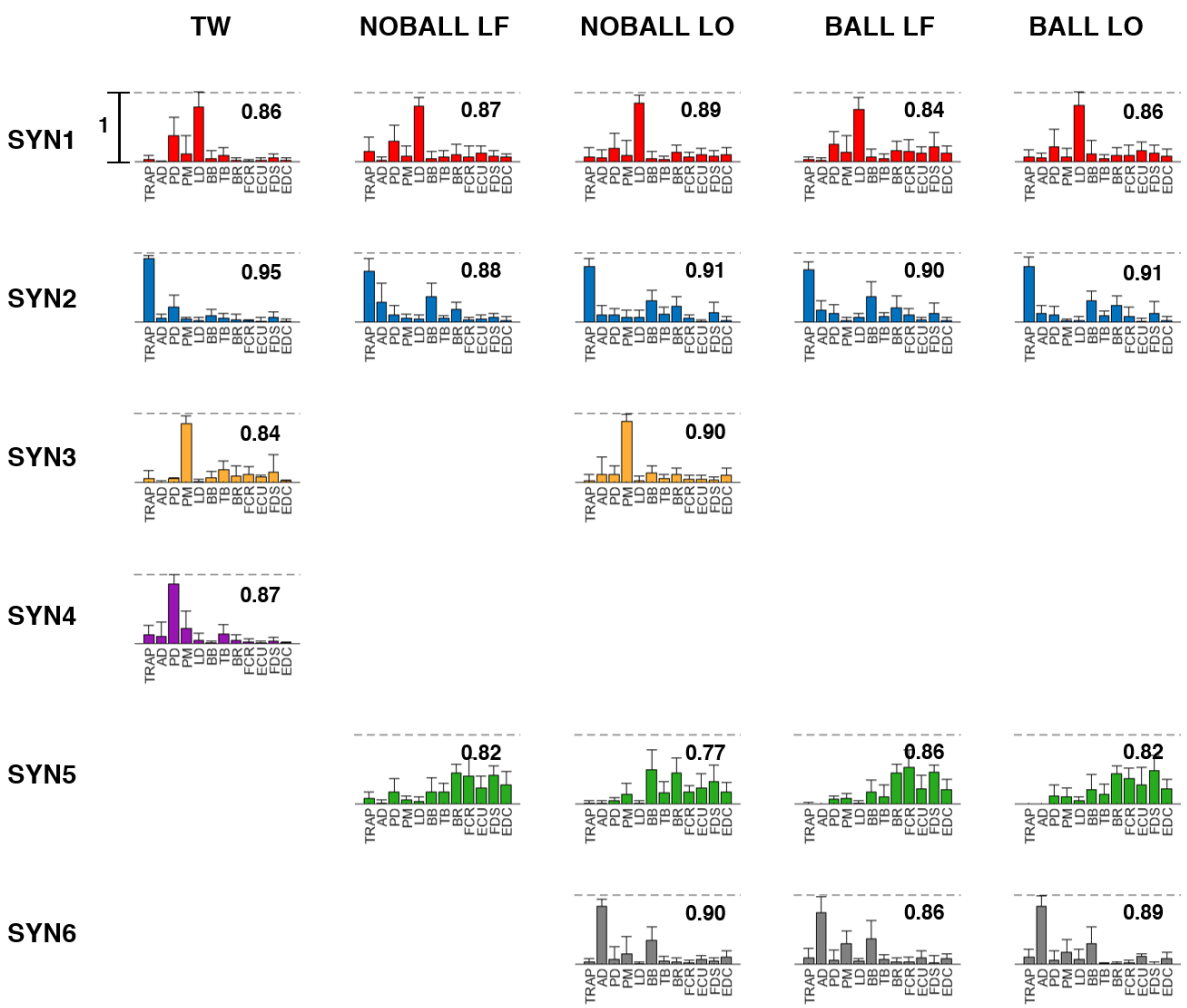

Figure 5.6. Group averaged weighting coefficients (W) and standard deviation (+SD) of extracted muscle synergies for all experimental conditions. The mean scalar product between individual participants and the group averaged weighting coefficients are presented on each graph on the top right. Synergies depicted in the same color between conditions indicate the same synergies with the mean scalar product greater than 0.6.

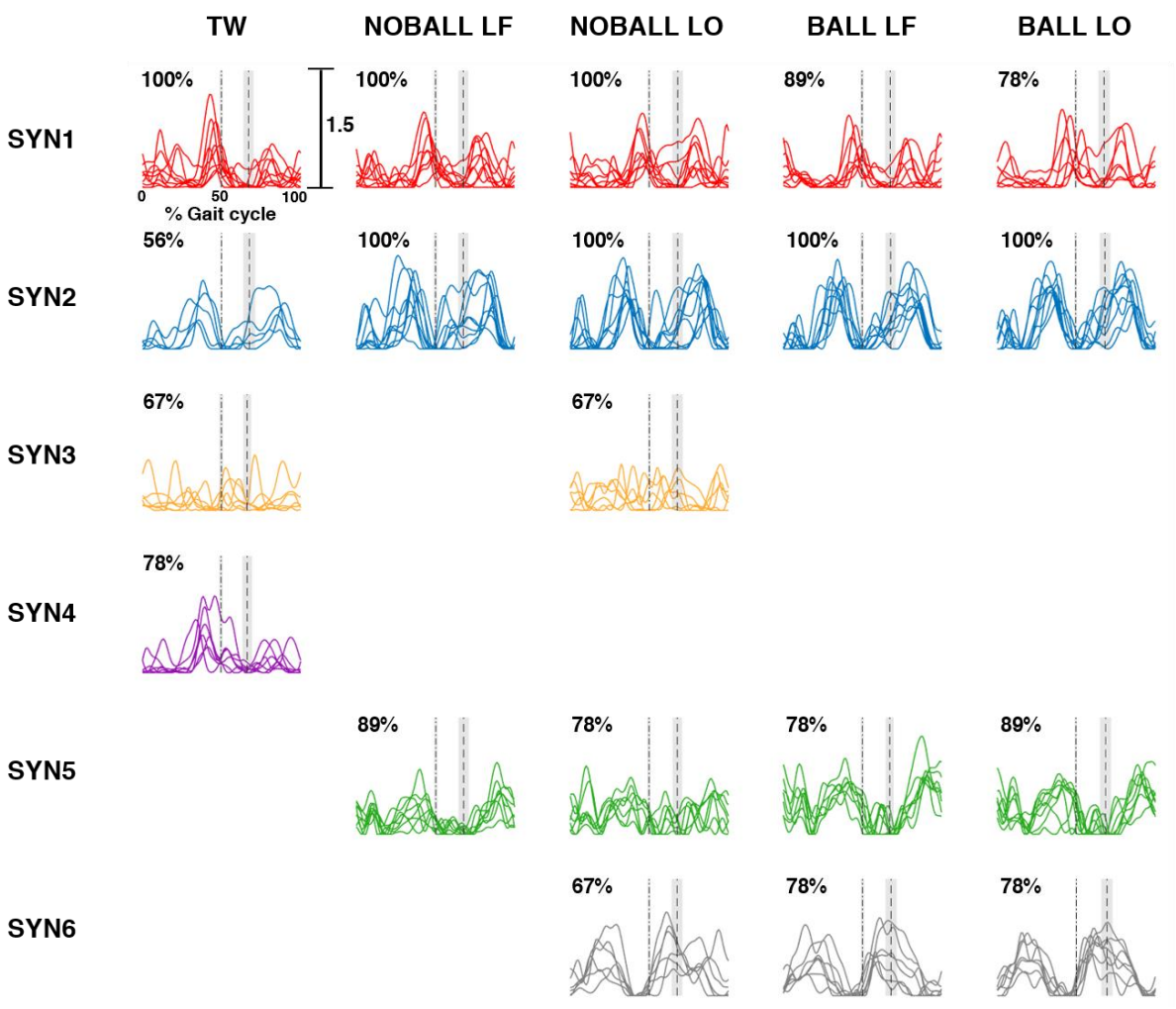

Figure 5.7. Temporal activation pattern (H) of extracted muscle synergies. Each line indicates the activation pattern from the individual participant who showed the muscle synergy. The number on each graph indicates the % of participants showed the specific muscle synergy pattern. The first vertical line (-.) indicates the mean timing of contralateral heel contact and the second vertical line (--) indicates the mean timing of toe-off across participants who presented each pattern. SDs for both timings were presented in light gray areas, calculated from those participants who presented that specific muscle synergy pattern.

Table 5.4**.** Group mean timings of activation peak (+SD, % gait cycle) of identified synergies for the regions of gait cycle 1, 2, and 3 across all conditions. Each group mean and SD were calculated from the participants who displayed that specific muscle synergy pattern.

Synergy	Region 1 (1-25% of Gait Cycle)				
	TW	NOBALL LF	NOBALL LO	BALL LF	BALL LO
SYN1	14.56 (7.72)	8.56 (6.15)	6.78 (8.91)	6.50 (5.50)	6.71 (4.68)
SYN2	12.60 (7.23)	18.00 (8.29)	14.33 (8.90)	15.22 (9.55)	19.78 (7.48)
SYN3	13.33 (9.93)		14.50 (8.31)		
SYN4	11.43 (7.52)				
SYN5		7.50 (5.53)	15.14 (9.87)	12.71 (9.84)	8.38 (8.25)
SYN6			20.83 (4.54)	20.57 (3.78)	19.00 (4.16)
	Region 2 (26-75% of Gait Cycle)				
	TW	NOBALL LF	NOBALL LO	BALL LF	BALL LO
SYN1	52.33 (12.14)	57.22 (13.85)	50.44 (15.34)	53.88 (13.39)	54.86 (14.30)
SYN2	44.80 (16.45)	42.22 (15.76)	43.67 (16.43)	46.33 (19.89)	38.78 (12.53)
SYN3	50.83 (15.93)		54.17 (14.74)		
SYN4	40.57 (3.74)				
SYN5		44.75 (13.37)	47.00 (14.40)	40.14 (2.79)	41.50 (5.63)
SYN6			62.83 (1.94)	59.86 (4.06)	61.71 (4.42)
	Region 3 (76-100% of Gait Cycle)				
	TW	NOBALL LF	NOBALL LO	BALL LF	BALL LO
SYN1	86.78 (8.61)	82.22 (7.93)	83.78 (7.71)	86.75 (10.86)	87.29 (10.24)
SYN2	84.40 (4.39)	83.11 (4.04)	84.89 (4.08)	82.78 (3.46)	83.56 (3.54)
SYN3	86.00 (7.97)		92.33 (8.33)		
SYN4	84.14 (5.90)				
SYN5		91.63 (3.58)	87.14 (7.93)	91.14 (5.08)	93.13 (5.30)
SYN6			84 (5.83)	80.14 (7.54)	79.00 (3.65)

DISCUSSION

This study aimed to investigate the effect of different levels of task difficulty and visual information on object transport tasks while walking in healthy young individuals. Along with the kinematic analysis, this study utilized the muscle synergy analysis to identify the modular organization of upper limb muscle activations when participants were required to transport an object with different precision demands and visual information.

As hypothesized, the highest damping behavior was observed during the ball-in-cup conditions, especially when the participants were asked to look at the cup while walking. The damping ratio (DR) in this condition was significantly smaller than 1, indicating that the vertical displacement of the hand transporting the cup was highly restricted compared to the vertical displacement of the trunk. Overall, there was a main effect of the ball constraint on the DR, suggesting that controlling the ball on the surface of the object during walking induced greater stabilization strategies. A similar damping effect of the task constraint was found in Gysin et al. (2003), where transporting an uncovered water container during overground walking induced a significant decrease in peak-to-peak vertical displacement of the container compared to the trunk (Gysin et al., 2003a). Our results also showed that visual information (looking at the object vs. forward) did not strongly affect DR. This means that the carried object could be stabilized by relying on proprioception. However, it is reasonable to expect that using central visual information about the transported object contributes to a more effective damping effect because there was a slightly smaller DR when looking at the cup in both NOBALL and BALL conditions (although not reaching the statistical significance level).

As opposed to the initial hypotheses, and despite the change in the DR, there was no distinct difference in the number of extracted synergies depending upon the visual condition and the ball constraint. Generally, the same number of synergies (four) were identified in the NOBALL and BALL conditions regardless of the visual information. SYN 1 and SYN 2 appeared in all conditions, mainly responsible for the activation of PD, LD, and TRAP. The additional synergies (SYN 5 and SYN 6) found during all objects transport conditions (with and without the ball) were mainly responsible for the activation of shoulder and elbow flexors and wrist/hand muscles (AD, BB, BR, FCR, ECU, FDS, and EDC). The mean levels of activation of wrist/hand flexors and extensors (FCR, ECU, FDS, and EDC) were increased in the higher precision demand (BALL) to control the ball on the cup continuously.

These results suggest that the CNS uses the same synergy patterns identified from the phasic muscle activation (NNMF analysis) during object transport with lower and higher precision demands (NOBALL and BALL). The main difference between these conditions was the mean level of tonic muscle activation in the wrist/hand muscles. Thus, it is plausible that co-contraction through the tonic activation contributes to stabilizing the cup-ball system during walking, just as observed in other tasks with unpredictable perturbations (Takahashi et al., 2001). At the same time, the phase modulation of EMG contributes to the concurrent and real-time correction when continuous perturbation occurs during the task. Togo et al. (2012) found that the increased velocity of horizontal oscillation when holding a water-filled cup during treadmill walking enhanced the synergy required to stabilize horizontal hand jerk for horizontal dampening of hand vibration (Togo et al., 2012). Using uncontrolled manifold (UCM), the authors in this study quantified joint coordination associated with the motor synergy necessary to decrease the hand jerk and variance of the cup angle. Reduction of hand jerk synergy around the late swing phase might indicate the

anticipatory control of CNS to soften the impact at heel contact. As the authors reported (Togo et al., 2012), the phasic modulation of EMG observed in this dissertation might suggest that the muscular activations contribute to the coordination at certain joints for dampening hand motion.

In addition, the increase in minimal muscle (tonic) activation might contribute to object stabilization by the rise in the co-contraction level of the muscles during the higher task constraint. Gysin et al. (2003) found similar mean GF and safety margins during the unconstrained and increased accuracy constraint conditions. Still, they found a significantly lower amount of peak-to-peak GF with higher accuracy constraints (Gysin et al., 2003a). However, in this study, the muscles that mainly contribute to GF showed greater mean activation when compared to NOBALL (unconstrained) condition. This inconsistency between studies might be due to the difference in task nature of carrying a cup without a lid vs. carrying a cylinder-shaped object and a ball on the surface. If the weight of the water was the same in Gysin's study, carrying the container without a lid (constrained condition) includes less weight of the object; on the other hand, the constrained condition in our study includes greater weight due to the ball compared to unconstrained condition (NOBALL), this might induce the greater mean activation of the EMG of wrist and finger muscles in our study. It is hard to compare the results of these two studies directly due to the different variables and tasks. Given that the GF is continuously modulated throughout the gait cycle, it could also be possible that the GF reaches its high peaks at only some points of the gait cycle, and this could result in a flattening effect of the mean GF, or vice versa.

Lastly, to understand the behavioral change of damping, the angular displacements of the shoulder and elbow joints were examined. The results of the study showed that there were no main effects of the Ball and Vision on the angular displacement of the shoulder joint in the sagittal plane and the angular displacement of the elbow joint. The movement amplitude during transporting task

was not affected by the ball constraint or whether they were given the central or peripheral visual information. In fact, the shoulder joint in the sagittal plane was not significantly affected by the ball existence of visual information; however, there was a greater relative change in amplitude, meaning that when participants carried the object with the ball, they showed a greater decrease in the movement amplitude of the shoulder joint in this plane. Interestingly, the angular displacement of the shoulder in the transverse plane was significantly decreased during higher task constraint (BALL), and this result is supported by the previous study where the significant decrease in pelvis and trunk motion amplitude in the transverse plane was observed during load carriage while walking (LaFiandra et al., 2003). It might be one of the CNS strategies to restrict the movement amplitude about the vertical axis as opposed to natural oscillation caused by the walking so that participants could maintain the stability of the object and the ball. It is also possible that there was no need to generate trunk motion about the vertical axis due to the overall restriction in trunk movement in this plane that led to a reduction in whole-body angular momentum (Siragy et al., 2020). Relative change of angular displacement of the shoulder and elbow joints were significantly different from the 0% during TW except for the shoulder in the transverse plane during NOBALL LO condition. Along with the result of DR, the greater damping behavior during the object transport task with the ball was likely affected by the decrease in angular displacement of the shoulder joint in the transverse plane and partially due to the decrease in angular displacement of the shoulder joint in the sagittal plane, suggesting that the shoulder joint is primarily responsible for object stabilization during walking (Frédéric Danion & Mark L Latash, 2011; Hirashima et al., 2002).

In summary, the results of this study indicate that the damping behavior during the higher task constraint was achieved by the phasic EMG modulation (as indicated by the NNMF analysis)

along with the higher level of tonic activation to control the disturbing ball on the cup surface. There was no change in the number of synergies extracted, indicating that the CNS seems to use a similar type of module strategy for an inherently similar motor task. Similar to study 2, among three to five synergies during object transport tasks, two of them were shared with natural treadmill walking, suggesting a similar motor control strategy by the CNS mainly due to the shared locomotor task. Kinematics analysis showed that the angular displacement of the shoulder joint in the transverse plane was significantly decreased to stabilize the cup-ball system in hand.

CHAPTER 6. CONCLUSIONS

Object transport while waking is one of the most common activities in daily life. The purpose of this dissertation was to examine the underlying neuromuscular control during this task and provide a further understanding of how CNS integrates upper limb movement into gait using kinematic and muscle activation analyses. More specifically, the kinematic coordination pattern of arm swing was examined in study 1, study 2 identified the muscle synergy patterns utilized in upper limb muscles involved in object stabilization during walking, and study 3 examined the effect of different levels of object transport task constraint and relative contributions of visual information (central vs. peripheral) to object stabilization and upper limb muscle synergies. The results of this dissertation could be a foundation for future studies on populations with neurological pathologies with asymmetrical impairments.

KEY RESULTS

Study 1 was designed to examine the interlimb coordination pattern of the upper limbs during object transport tasks while walking where the task constraint is more goal-oriented and functional rather than physically passive and artificial. As hypothesized, the relative angular displacement of flexion-extension of the shoulder joint used for arm placement and object transport significantly decreased compared to natural treadmill walking. However, even though there was a trend to decrease the angular displacement in both shoulder and elbow joints in the non-constrained side during NOBJ and OBJ conditions, there was no statistically significant difference such that the movement amplitude of the contralateral limb did not show the expected increases in amplitude as predicted from the conservation of total angular momentum framework. Transporting an object in one hand also caused the change in the upper limb coordination patterns, showing the decrease

in the relative frequency of anti-phase pattern with NOBJ and OBJ conditions, and this reduction of anti-phase pattern might be compensated by the restriction of movement of the upper limb shoulder joint so that the whole upper body can still deal with the angular momentum from the lower body. Overall, the transporting an object task induced the increase in the phase of the contra-lateral shoulder pattern while the phase of the ipsilateral shoulder remained constant or decreased.

Study 2 was aimed at examining the muscle synergy patterns used by the CNS for controlling the upper limb damping during object transport tasks while walking. The results of study 2 indicate that the damping behavior during object transport tasks while walking can be achieved by continuous adjustments of phasic muscle activations in the shoulder, elbow, and wrist/hand muscles to generate coordinated muscular control for stabilization of the upper limb joints and the hand-held object. Rhythmical modulation of relative elbow flexion angle and earlier muscle activation before both heel contacts support an anticipatory control of CNS to stabilize the arm and hand-held object against gait-induced IFs while walking. Stabilization of the proximal upper limb joints before the distal joints is consistent with the hypothesis of time-ordered proximal-to-distal activation of muscles. Identification of basic muscle synergy patterns using methods outlined here might provide further information on the understanding of neuromuscular control strategies during the object transport with increased demands on control of object orientation.

Study 3 was designed to answer the question of how CNS can maintain stability in object manipulation by regulating kinematic parameters, including limb stiffness when the task involved greater difficulty with an unpredictable object system (ball-cup system) so that participants needed to use sensory feedback to maintain the stability. Higher damping behavior and greater relative change in angular displacement of the shoulder joint in the transverse plane were observed during

the ball constraint (higher precision demand). In addition, the ball constraint also increased the activation of wrist/hand flexors and extensors, suggesting that these distal muscles are primarily responsible for controlling the object transport task against the IFs generated by the gait rather proximal joints were involved. In addition, the overall increase in minimal activation of distal muscles seems to contribute to the object stabilization by higher co-contraction level during the higher task constraint. NNMF synergy analysis found that there was no apparent difference in the number of muscle synergy extracted, indicating that our CNS control this task with the same organization of muscle module (identified from the phasic muscle activation). It could be concluded that co-contraction through the tonic activation contributes to the entire stabilization of the cup-ball system during walking, and at the same time, the phase modulation of EMG contributes to the concurrent and real-time correction when continuous perturbation occurs during the task. There was no significant effect of visual information on this task in regard to upper limb joint kinematics and muscle activation. The results of this dissertation support the idea that the arm swing is affected by active neural control. The results of EMG of AD and PD, which are the muscles mainly responsible for arm swing motion by concentric and eccentric contractions (Kuhtz-Buschbeck & Jing, 2012), showed a similar biphasic pattern and timing of activation peak throughout the gait cycle between natural treadmill walking condition and the conditions where one arm was constrained due to the object transport task as shown in peak timings and temporal muscle activation patterns in studies 2 and 3, though the activation amplitudes were significantly decreased by the passive manipulation due to the task. Similar findings have been reported in the previous study where biphasic modulation of upper limb muscles were observed even the arm movement was restricted (Kuhtz-Buschbeck & Jing, 2012) and where consistent peak timing of PD was observed when additional weight was attached in one or both upper limbs (MacLellan &

Ellis, 2019). Conserved temporal timing of muscle activations with different amounts of activation and arm swing amplitude might support the active neural contribution during the object transport while walking.

SUMMARY

In this dissertation, it has been found that functional and asymmetrical constraints of one arm included the change in upper limb kinematics coordination patterns by decreasing the anti-phase and increase in-phase coordination patterns for stabilization of the upper arm and the object (study 1). The relative change in angular displacement of the shoulder in sagittal and transverse plane differed depending upon the characteristics of the task constraint (transporting a food can vs. ball-cup system), indicating that the CNS altered the kinematic adaptation of upper limb joints depending on how much the movement amplitude should be restricted. Interestingly, with higher precision demand, there was a significant decrease in movement amplitude of the upper trunk (shoulder) in the transverse plane, minimizing the angular momentum. From the study 2 and 3, it has been found that there were always consistent muscle synergies between the natural treadmill walking and object transport task, suggesting the basic motor control strategy of CNS. Upon those basic synergies, additional synergies were identified as the voluntary motor task was added upon an original motor task (walking). In addition, the results of this study provided evidence of stabilization of proximal joints before the distal joints presented with the time-ordered proximal-to-distal activation of muscles. Object transport task with both high or low precision demand was achieved through the co-contraction by the tonic activation contributing to the entire stabilization of the cup-ball system during walking. At the same time, the phase modulation of EMG contributes to the concurrent and real-time correction when continuous perturbation occurs during the task.

FUTURE DIRECTIONS

Though this dissertation was designed to provide a further understanding of the underlying mechanism of neuromuscular control strategy by CNS during object transport task while walking, the damping strategy, especially the kinematic strategy taken by the CNS seems to vary based on the nature of the task, such as carrying a cup of water, ball-cup system, the weight of the object in hand, etc. To further understand this underlying control, it would be beneficial to investigate the different types of object transport tasks, including different objects or walking conditions (treadmill, overground, obstacle clearance). In this dissertation, the damping behavior was quantified by the DR using only the vertical displacement of markers on C7 and the hand (Albert et al., 2010). Since walking generates IFs in all three planes, it would also be interesting to examine the damping behavior in the other two planes, such as horizontal displacement and angular displacement in the transverse plane. Since it is possible that looking forward and looking at an object in hand while walking on a treadmill might impose a cognitive burden on participants, it is reasonable to expect that participants might alter the gait pattern such as step length, width if the experiment were repeated while walking overground. Investigating how participants change their gait patterns along with the muscle activations of the lower limbs during overground walking would provide more information regarding the neuromuscular control strategy during the object transport. In addition, looking at the three upper limb joints (shoulder, elbow, and wrist) simultaneously would provide more information in that how these joints coordinate together to secure the damping behavior, rather examination at an individual joint separately. Further, it could be helpful to examine the kinematic variabilities between experimental conditions or between body segments (joints), which could be beneficial to locate where CNS struggles hard to accommodate or generate more flexible control yet show inconsistent movement patterns with greater variability.

Damping strategy observed with alteration in kinematics and muscle activations in people with neurological pathologies, especially those who suffer from an asymmetrical impairment, could also allow for a deeper understanding of how CNS adapts to complete the object transport task.

LIMITATIONS

One of the limitations of this dissertation was that this dissertation involved only walking on a treadmill. Differences between treadmill and overground walking in kinematics (Alton et al., 1998; Hollman et al., 2016) and kinetics (Parvataneni et al., 2009; White et al., 1998) have been reported. In addition, while the carried object during overground walking has to move horizontally with a person's body, the transported object during treadmill walking remains relatively in place. This difference might pose a difficulty in generalizing the results of this dissertation to overground walking.

Another potential limitation was that the instruction provided to participants by the investigator might affect the control strategy of individuals. For example, in study 3, telling them "try to maintain the ball in the middle of the cup as possible as you can" versus "just try to maintain the ball within the cup surface" would induce a different level of damping behavior. Although too many detailed instructions might restrict eliciting the natural behavior of the participants, too simple instructions could also make the study results too various as it gives so many options for participants to take.

In study 2, the heel contact was determined by using the lowest vertical position of the heel marker, which is actually not accurate because the heel contact occurs before the lowest position due to the due to compression of footwear. This issue was addressed in studies 1 and 3 by using the velocity threshold of the heel marker.

APPENDIX A. IRB APPROVAL FORMS

LSU | Office of Research & Economic Development

TO:	Kuznetsov, Nikita LSUAM | Col of HSE | Kinesiology
FROM:	Alex Cohen Chair, Institutional Review Board
DATE:	30-Oct-2020
RE:	3871
TITLE:	Upper Limb Damping Behavior When Carrying Objects in Young Healthy Individuals
New Protocol/Modification/Continuation:	Modification
Review Type:	Expedited Review
Risk Factor:	Minimal
Review Date:	30-Oct-2020
Status:	Approved
Approval Date:	30-Oct-2020
Approval Expiration Date:	
Re-review frequency:	(annual unless otherwise stated)
Number of subjects approved:	30
By:	Alex Cohen, Chairman

Continuing approval is CONDITIONAL on:

1. Adherence to the approved protocol, familiarity with, and adherence to the ethical standards of the Belmont Report, and LSU's Assurance of Compliance with DHHS regulations for the protection of human subjects*
2. Prior approval of a change in protocol, including revision of the consent documents or an increase in the number of subjects over that approved.
3. Obtaining renewed approval (or submittal of a termination report), prior to the approval expiration date, upon request by the IRB office (irrespective of when the project actually begins); notification of project termination.
4. Retention of documentation of informed consent and study records for at least 3 years after the study ends.
5. Continuing attention to the physical and psychological well-being and informed consent of the individual participants, including notification of new information that might affect consent.
6. A prompt report to the IRB of any adverse event affecting a participant potentially arising from the study.
7. Notification of the IRB of a serious compliance failure.

8. **SPECIAL NOTE: When emailing more than one recipient, make sure you use bcc.**

** All investigators and support staff have access to copies of the Belmont Report, LSU's Assurance with DHHS, DHHS (45 CFR 46) and FDA regulations governing use of human subjects, and other relevant documents in print in this office or on our World Wide Web site at http://www.lsu.edu/research*

Louisiana State University
131 David Boyd Hall
Baton Rouge, LA 70803

O 225-578-5833
F 225-578-5983
http://www.lsu.edu/research

APPENDIX B. CONSENT FORMS

CONSENT TO PARTICIPATE IN A RESEARCH STUDY
INFORMED CONSENT

Study Title:
Upper Limb Damping Behavior When Carrying Objects in Young Healthy Individuals

Performance Site:
School of Kinesiology Biomechanics Laboratory (Gym Armory, B-2)

Investigator:
If you have any questions regarding the study, please contact

Nikita A. Kuznetsov, Ph.D.
Phone: 225-578-3845
Email: nikita@lsu.edu

Purpose of the Study:

The proposed project will be to observe the effects of walking and stepping over an obstacle on the upper limb's damping behavior during object transport with the dominant and non-dominant upper limbs. Further, the damping behavior of the upper limb will also be compared for object transport during over-ground and treadmill walking.

Participant Information:

Thirty healthy young adults (male and female) between the ages of 18 and 40, who are free of any orthopedic, cardiovascular, and neuromuscular health problems, will be recruited for this study. Firstly, participants will be required to complete the COVID-19 related health screening questionnaire to determine whether or not the participant's participation to the study is eligible. The participants must also have the ability to provide informed consent to the study. Participant will complete the Edinburgh Handedness Inventory form to assess and analysis their handedness prior to participation in the study.

Equipment / Study Procedures:

The study will involve the recording of EMG and whole body movements using a 4-sensor Codamotion CX1 optoelectronic system for Experiment 1 and Qaulisys motion capture system for

Experiment 2. The later systems record 3-D positions of infrared markers placed on the anatomical landmarks of the body. These positions will subsequently be used to build a biomechanical model of the participant. Muscle activity will be recorded using two 16-channel MA-300 EMG systems (Motion Lab Systems Inc., Baton Rouge, LA). Using skin surface electrodes, electrical potentials of the various muscles are recorded and stored on a computer. In preparation for EMG electrodes' placements, participants will be shaved (if needed) and cleaned with alcoholic wipes to remove any dry skin or cream around the desired muscle location. These locations will be palpated prior to the placement of the electrode which will be determined by SENIAM guidelines. Self-adhering Ag-AgCl surface electrodes will be placed bilaterally at the upper and lower extremities secured by adhesive tape. In addition, self-adhesive elastic sports bandages will also be used to provide additional security of holding these upper and lower extremity electrodes onto the skin during data collection. Upper extremity muscles are anterior deltoid (AD), posterior deltoid (PD), biceps brachii (BB), triceps brachii (TB), trapezius (TRAP), brachioradialis (BR), extensor carpi ulnaris (ECU), flexor carpi radialis (FCR), flexor digitorum superficialis (FDS), extensor digitorum communis (EDC) whereas lower extremity muscles are gluteus maximus (GMAX), rectus femoris (RECF), vastus lateralis (VASL), biceps femoris (BICF), tibialis anterior (TA), and lateral gastrocnemius (GASTL). As well, infrared markers will be placed bilaterally on the anatomical landmarks of the body using double-sided tape. The positions of these markers will be tracked using a 4-sensor Codamotion CX1 system and Qualisys motion capture system. Markers will be placed at the spine of the C7 vertebrae, shoulder, elbow, medial and lateral side of the wrist, metacarpophalangeal (MCP) joint of the middle finger, distal phalanx (DP) of the middle finger, hip, knee, ankle, heel, fifth toe, and big toe. All the other markers will be placed directly on to the skin, except for the heel, fifth toe, and big toe, which will be placed on the participants' shoes.

Experimental Task:

Experiment 1:

Participants will arrive in the laboratory wearing a short sleeve shirt, shorts, and closed toe shoes. Long hair of the participants will be pulled up to prevent any obstruction of the markers during data collection. They will be further informed about the details of the study. Setup for the experiment consists of using a double-sided hypoallergenic tape to place infrared markers on anatomical landmarks to record body motion along with the Ag-AgCl electrodes which will be

secured by adhesive tape on upper and lower limb muscles to record muscle activity. Once setup is completed, the experiment will begin.

This study will consist of participants walking on a treadmill and over-ground while carrying an object in either their dominant or non-dominant hand. The over-ground walking condition will include trials with an obstacle or with no obstacle present.

Before the experiment, static trials will be recorded while participants stand and hold the object in both the dominant and non-dominant hands while EMG is recorded. As well, the participants over-ground walking speed will be determined. The experimental protocol will consist of three walking conditions (over-ground, obstructed, and treadmill) and five obstacle transport conditions (free arm swing without object or positioning, positioning dominant limb with no object, positioning non-dominant limb with no object, holding object in the dominant hand, and holding object in the non-dominant hand). The obstructed walking conditions will be divided further into 2 additional conditions (leading with the lower limb ipsilateral to dominant hand, and leading with the lower limb contralateral to dominant hand), totaling in 20 experimental conditions which will be presented in randomized blocks. Over-ground and obstructed walking trials will be performed on a 30-foot walkway at the participant's comfortable self-selected speed. The obstructed walking condition will consist of participants stepping over an obstacle measuring 4-inches in height placed in the middle of the walkway. The treadmill condition will be performed at a speed matching the over-ground walking speed determined prior to the start of the experiment. During the object transport conditions, participants will be instructed to pick up and hold an object weighting approximately 300g at elbow level with their dominant or non-dominant hand and carry it to the end of the walkway. During the conditions where the arm will be positioned with no object, the participants will be asked to hold their hand at elbow level throughout the walking task. Each condition will consist of a minimum of 10 strides and 10 obstacle clearances for data analysis. The entire experiment will take approximately 2 hours.

Experiment 2:

The second experiment will have the same experimental procedure with the study 1 described above but involve a different type of transported object instead of the object used for study 1. The cylinder-shaped object that was 3D-printed with curved top surface (1.2 cm depth at apex) with radius of 3.75 cm will be used for object transport task in order to investigate the upper limb damping strategies when different levels of precision demand and visual focus of attention

are required while walking. Participants will be asked to walk on a treadmill while carrying the object (ball-in-cup system) in their dominant and non-dominant hand. Participants will perform the task with high and low precision demands (with vs. without a small ball in cup) and two visual focus of attention conditions (looking forward vs. looking at the cup). Each condition will consist of a minimum of 10 strides and for data analysis and the entire experiment will take approximately 2 hours.

Access to Select Medical Information:

The participants participating in this study should be free of any orthopedic, cardiovascular, and neuromuscular health problems and have normal or corrected to normal vision. Participants cannot present any signs or symptoms of COVID 19.

Covid 19 Health Precautions:

- Masks must be worn by the experimenter the entire time, while masks must be covered by the subject at all times. Gloves will be worn by experimenter when placing markers. Subject and research staff will be required to wash hand before and after the study. Hand sanitizer will also be available to both the research staff and study participant.
- All Equipment will be wiped down before and after experiment.
- Subjects will be presented health-related questions to determine eligibility to participate in the study.
- Primary investigator (PI) and research staff must complete the daily symptom check required to attend campus. This will be added to the coded folder with the subjects coded documents for that experiment session.
- Students must also present confirmation from the daily symptom checker stating that they are allowed to be on campus.
- If subject, research staff, and PI do not pass the daily symptom checker, they will not be allowed on campus until a negative test / doctor's approval is provided.
- PI and research staff will always report to each other and the LSU if traveling greater than 100 miles and follow EOC guidelines on self-quarantine.

- If a positive test is found from PI and research staff post experimentation, information on what subject was in contact previously with the PI and research staff before the test will be reported to LSU to follow EOC procedure on tracing and notification.
- PI and research staff will monitor regulatory agencies (daily) in reference to outbreaks or policy initiated on that day or week regarding in person contact with students for LSU. If LSU designated a policy of no contact due to outbreaks or weather conditions, PI and research staff will let subject know of the current situation and proceed with experimentation if allowed by LSU.

Benefits:

The study does not have any direct benefits. The results of this study will be useful to examine the damping behavior of the upper limb during object transport while walking with and without obstacle clearance condition in healthy young adults. The finding of this study will be further used to develop an experimental protocol for stroke population to examine their upper limb's damping behavior during object transport while walking with and without obstacle clearance.

Risks/Discomfort:

The potential risks involved as a research participant in this study are minimal and may include skin irritation due to the use of tape and fatigue. The risk of skin irritation will be minimized with the use of hypoallergenic tape. As well, rest periods will be provided throughout the experiment to prevent fatigue. The research staff for this study is prepared to make suitable accommodation to all the participants to avoid any kind of injury.

Right to Refuse:

Participants may choose to not participate or withdraw from the study at any time without any penalty.

Privacy:

Every effort will be made to maintain the confidentiality of your study records. Results of the study may be published; however, we will keep your name and other identifying information

private. If you agree, video data of your participation may be used in the scientific presentation of the study, and measures will be taken to keep your participation anonymous. Your identity will remain confidential unless disclosure is required by law.

Signatures:

The study has been discussed with me and all my questions have been answered. I may direct additional questions regarding study specifics to the investigators. If I have questions about participants' rights or other concerns, I can contact Dr. Alex Cohen, Chairman, LSU Institutional Review Board, (225)-578-8692, irb@lsu.edu, www.lsu.edu/irb. I agree to participate in the study described above and acknowledge the researchers' obligation to provide me with a copy of this consent form if signed by me.

Participant Signature: _____

Date: _____ Participant's Date of Birth: _____

The study participant has indicated to me that he/she is unable to read. I certify that I have read this consent form to the participant and explained that by completing the signature line above, the participant has agreed to participate.

Participant Signature: _____

Date: _____ Participant's Date of Birth: _____

APPENDIX C. EDINBURGH HANDEDNESS INVENTORY

Edinburgh Handedness Inventory[1]

Participant ID:_____

Please indicate with a one (1) your preference in using your left or right hand in the following tasks. Where the preference is so strong you would never use the other hand, unless absolutely forced to, put a two (2).

If you are indifferent, put a one in each column (1 | 1).

Some of the activities require both hands. In these cases, the part of the task or object for which hand preference is wanted is indicated in parentheses.

Task / Object	Left Hand	Right Hand
1. Writing		
2. Drawing		
3. Throwing		
4. Scissors		
5. Toothbrush		
6. Knife (without fork)		
7. Spoon		
8. Broom (upper hand)		
9. Striking a Match (match)		
10. Opening a Box (lid)		
Total checks:	LH =	RH =
Cumulative Total	CT = LH + RH =	
Difference	D = RH – LH =	
Result	R = (D / CT) × 100 =	
Interpretation: (Left Handed: R < -40) (Ambidextrous: -40 ≤ R ≤ +40) (Right Handed: R > +40)		

Please stop here

[1] Oldfield, R. C. (1971). The assessment and analysis of handedness: The Edinburgh inventory. *Neuropsychologia*, *9*, 97-113.

APPENDIX D. PUBLICATION REUSE LICENSE

SPRINGER NATURE LICENSE
TERMS AND CONDITIONS

Jul 03, 2021

This Agreement between Louisiana State University -- Ahyoung Song ("You") and Springer Nature ("Springer Nature") consists of your license details and the terms and conditions provided by Springer Nature and Copyright Clearance Center.

License Number	5101440901480
License date	Jul 03, 2021
Licensed Content Publisher	Springer Nature
Licensed Content Publication	Experimental Brain Research
Licensed Content Title	Muscle synergy for upper limb damping behavior during object transport while walking in healthy young individuals
Licensed Content Author	A. Song et al
Licensed Content Date	Apr 4, 2020
Type of Use	Thesis/Dissertation
Requestor type	academic/university or research institute
Format	print and electronic
Portion	full article/chapter
Will you be	no

translating?	
Circulation/distribution	500 - 999
Author of this Springer Nature content	yes
Title	Neuromuscular control strategy during object transport while walking (Ph.D. dissertation)
Institution name	Louisiana State University
Expected presentation date	Aug 2021
Requestor Location	1100 Pulaski Street APT 402 COLUMBIA, SC 29201 United States Attn: Ahyoung Song
Total	0.00 USD

Terms and Conditions

Springer Nature Customer Service Centre GmbH
Terms and Conditions

This agreement sets out the terms and conditions of the licence (the **Licence**) between you and **Springer Nature Customer Service Centre GmbH** (the **Licensor**). By clicking 'accept' and completing the transaction for the material (**Licensed Material**), you also confirm your acceptance of these terms and conditions.

1. Grant of License

1. 1. The Licensor grants you a personal, non-exclusive, non-transferable, world-wide licence to reproduce the Licensed Material for the purpose specified in your order only. Licences are granted for the specific use requested in the order and for no other use, subject to the conditions below.

1. 2. The Licensor warrants that it has, to the best of its knowledge, the rights to license reuse of the Licensed Material. However, you should ensure that the material you are requesting is original to the Licensor and does not carry the copyright of

another entity (as credited in the published version).

1. 3. If the credit line on any part of the material you have requested indicates that it was reprinted or adapted with permission from another source, then you should also seek permission from that source to reuse the material.

2. Scope of Licence

2. 1. You may only use the Licensed Content in the manner and to the extent permitted by these Ts&Cs and any applicable laws.

2. 2. A separate licence may be required for any additional use of the Licensed Material, e.g. where a licence has been purchased for print only use, separate permission must be obtained for electronic re-use. Similarly, a licence is only valid in the language selected and does not apply for editions in other languages unless additional translation rights have been granted separately in the licence. Any content owned by third parties are expressly excluded from the licence.

2. 3. Similarly, rights for additional components such as custom editions and derivatives require additional permission and may be subject to an additional fee. Please apply to Journalpermissions@springernature.com/bookpermissions@springernature.com for these rights.

2. 4. Where permission has been granted **free of charge** for material in print, permission may also be granted for any electronic version of that work, provided that the material is incidental to your work as a whole and that the electronic version is essentially equivalent to, or substitutes for, the print version.

2. 5. An alternative scope of licence may apply to signatories of the STM Permissions Guidelines, as amended from time to time.

3. Duration of Licence

3. 1. A licence for is valid from the date of purchase ('Licence Date') at the end of the relevant period in the below table:

Scope of Licence	Duration of Licence
Post on a website	12 months
Presentations	12 months
Books and journals	Lifetime of the edition in the language purchased

4. Acknowledgement

4. 1. The Licensor's permission must be acknowledged next to the Licenced Material in print. In electronic form, this acknowledgement must be visible at the same time as the figures/tables/illustrations or abstract, and must be hyperlinked to the journal/book's homepage. Our required acknowledgement format is in the Appendix below.

5. Restrictions on use

5. 1. Use of the Licensed Material may be permitted for incidental promotional use and minor editing privileges e.g. minor adaptations of single figures, changes of format, colour and/or style where the adaptation is credited as set out in Appendix 1 below. Any other changes including but not limited to, cropping, adapting, omitting material that affect the meaning, intention or moral rights of the author are strictly prohibited.

5. 2. You must not use any Licensed Material as part of any design or trademark.

5. 3. Licensed Material may be used in Open Access Publications (OAP) before publication by Springer Nature, but any Licensed Material must be removed from OAP sites prior to final publication.

6. Ownership of Rights

6. 1. Licensed Material remains the property of either Licensor or the relevant third party and any rights not explicitly granted herein are expressly reserved.

7. Warranty

IN NO EVENT SHALL LICENSOR BE LIABLE TO YOU OR ANY OTHER PARTY OR ANY OTHER PERSON OR FOR ANY SPECIAL, CONSEQUENTIAL, INCIDENTAL OR INDIRECT DAMAGES, HOWEVER CAUSED, ARISING OUT OF OR IN CONNECTION WITH THE DOWNLOADING, VIEWING OR USE OF THE MATERIALS REGARDLESS OF THE FORM OF ACTION, WHETHER FOR BREACH OF CONTRACT, BREACH OF WARRANTY, TORT, NEGLIGENCE, INFRINGEMENT OR OTHERWISE (INCLUDING, WITHOUT LIMITATION, DAMAGES BASED ON LOSS OF PROFITS, DATA, FILES, USE, BUSINESS OPPORTUNITY OR CLAIMS OF THIRD PARTIES), AND
WHETHER OR NOT THE PARTY HAS BEEN ADVISED OF THE POSSIBILITY OF SUCH DAMAGES. THIS LIMITATION SHALL APPLY NOTWITHSTANDING ANY FAILURE OF ESSENTIAL PURPOSE OF ANY LIMITED REMEDY PROVIDED HEREIN.

8. Limitations

8. 1. ***BOOKS ONLY:*** Where **'reuse in a dissertation/thesis'** has been selected the following terms apply: Print rights of the final author's accepted manuscript (for clarity, NOT the published version) for up to 100 copies, electronic rights for use only on a personal website or institutional repository as defined by the Sherpa guideline (www.sherpa.ac.uk/romeo/).

8. 2. For content reuse requests that qualify for permission under the STM Permissions Guidelines, which may be updated from time to time, the STM Permissions Guidelines supersede the terms and conditions contained in this licence.

9. Termination and Cancellation

9. 1. Licences will expire after the period shown in Clause 3 (above).

9. 2. Licensee reserves the right to terminate the Licence in the event that payment is not received in full or if there has been a breach of this agreement by you.

Appendix 1 — Acknowledgements:

For Journal Content:
Reprinted by permission from [**the Licensor**]: [**Journal Publisher** (e.g. Nature/Springer/Palgrave)] [**JOURNAL NAME**] [**REFERENCE CITATION** (Article name, Author(s) Name), [**COPYRIGHT**] (year of publication)

For **Advance Online Publication papers:**
Reprinted by permission from [**the Licensor**]: [**Journal Publisher** (e.g. Nature/Springer/Palgrave)] [**JOURNAL NAME**] [**REFERENCE CITATION** (Article name, Author(s) Name), [**COPYRIGHT**] (year of publication), advance online publication, day month year (doi: 10.1038/sj.[JOURNAL ACRONYM].)

For Adaptations/Translations:
Adapted/Translated by permission from [**the Licensor**]: [**Journal Publisher** (e.g. Nature/Springer/Palgrave)] [**JOURNAL NAME**] [**REFERENCE CITATION** (Article name, Author(s) Name), [**COPYRIGHT**] (year of publication)

Note: For any republication from the British Journal of Cancer, the following credit line style applies:

Reprinted/adapted/translated by permission from [**the Licensor**]: on behalf of Cancer Research UK: : [**Journal Publisher** (e.g. Nature/Springer/Palgrave)] [**JOURNAL NAME**] [**REFERENCE CITATION** (Article name, Author(s) Name), [**COPYRIGHT**] (year of publication)

For **Advance Online Publication** papers:
Reprinted by permission from The [**the Licensor**]: on behalf of Cancer Research UK: [**Journal Publisher** (e.g. Nature/Springer/Palgrave)] [**JOURNAL NAME**] [**REFERENCE CITATION** (Article name, Author(s) Name), [**COPYRIGHT**] (year of publication), advance online publication, day month year (doi: 10.1038/sj.[JOURNAL ACRONYM])

For Book content:
Reprinted/adapted by permission from [**the Licensor**]: [**Book Publisher** (e.g. Palgrave Macmillan, Springer etc) [**Book Title**] by [**Book author**(s)] [**COPYRIGHT**] (year of publication)

Other Conditions:

Version 1.3

LIST OF REFERENCES

Akashi, P. M., Sacco, I. C., Watari, R., & Hennig, E. (2008). The effect of diabetic neuropathy and previous foot ulceration in EMG and ground reaction forces during gait. *Clin Biomech (Bristol, Avon)*, *23*(5), 584-592. https://doi.org/10.1016/j.clinbiomech.2007.11.015

Albert, F., Diermayr, G., McIsaac, T. L., & Gordon, A. M. (2010). Coordination of grasping and walking in Parkinson's disease. *Exp Brain Res*, *202*(3), 709-721. https://doi.org/10.1007/s00221-010-2179-5

Alton, F., Baldey, L., Caplan, S., & Morrissey, M. C. (1998). A kinematic comparison of overground and treadmill walking. *Clin Biomech (Bristol, Avon)*, *13*(6), 434-440. https://doi.org/10.1016/s0268-0033(98)00012-6

Amado, A. (2019). Walking for Object Transport: An Examination of the Coordinative Adaptations to Locomotor, Perceptual, and Manual Task Constraints.

Ambike, S., Zhou, T., Zatsiorsky, V. M., & Latash, M. L. (2015). Moving a hand-held object: Reconstruction of referent coordinate and apparent stiffness trajectories. *Neuroscience*, *298*, 336-356. https://doi.org/10.1016/j.neuroscience.2015.04.023

Anderson, F. C., & Pandy, M. G. (2003). Individual muscle contributions to support in normal walking. *Gait Posture*, *17*(2), 159-169. https://doi.org/10.1016/s0966-6362(02)00073-5

Arnold, A. S., Anderson, F. C., Pandy, M. G., & Delp, S. L. (2005). Muscular contributions to hip and knee extension during the single limb stance phase of normal gait: a framework for investigating the causes of crouch gait. *J Biomech*, *38*(11), 2181-2189. https://doi.org/10.1016/j.jbiomech.2004.09.036

Aruin, A. S., & Latash, M. L. (1995). Directional specificity of postural muscles in feed-forward postural reactions during fast voluntary arm movements. *Exp Brain Res*, *103*(2), 323-332. https://www.ncbi.nlm.nih.gov/pubmed/7789439

Ayyappa, E. (1997). Normal Human Locomotion, Part 1: Basic Concepts and Terminology. *JPO Journal of Prosthetics and Orthotics*, *9*, 1P 17.

Bagesteiro, L. B., & Sainburg, R. L. (2002). Handedness: dominant arm advantages in control of limb dynamics. *J Neurophysiol*, *88*(5), 2408-2421. https://doi.org/10.1152/jn.00901.2001

Bagesteiro, L. B., & Sainburg, R. L. (2002). Handedness: Dominant Arm Advantages in Control of Limb Dynamics. *J Neurophysiol*, *88*, 2408–2421.

Bagesteiro, L. B., & Sainburg, R. L. (2003). Nondominant arm advantages in load compensation during rapid elbow joint movements. *J Neurophysiol*, *90*(3), 1503-1513. https://doi.org/10.1152/jn.00189.2003

Baldissera, F., & Cavallari, P. (2001). Neural compensation for mechanical loading of the hand during coupled oscillations of the hand and foot. *Exp Brain Res*, *139*(1), 18-29. https://doi.org/10.1007/s002210100762

Baldissera, F., Cavallari, P., & Leocani, L. (1998). Cyclic modulation of the H-reflex in a wrist flexor during rhythmic flexion-extension movements of the ipsilateral foot. *Exp Brain Res*, *118*(3), 427-430. https://doi.org/10.1007/s002210050297

Ballesteros, M. L., Buchthal, F., & Rosenfalck, P. (1965). The Pattern of Muscular Activity during the Arm Swing of Natural Walking. *Acta Physiol Scand*, *63*, 296-310. https://doi.org/10.1111/j.1748-1716.1965.tb04069.x

Barthelemy, D., & Nielsen, J. B. (2010). Corticospinal contribution to arm muscle activity during human walking. *J Physiol*, *588*(Pt 6), 967-979. https://doi.org/10.1113/jphysiol.2009.185520

Behrman, A. L., & Harkema, S. J. (2000). Locomotor training after human spinal cord injury: a series of case studies. *Phys Ther*, *80*(7), 688-700. https://www.ncbi.nlm.nih.gov/pubmed/10869131

Bellinger, G. C., Pickett, K. A., & Mason, A. H. (2019). Interlimb Coordination During a Combined Gait and Prehension Task. *Motor Control*, 1-18. https://doi.org/10.1123/mc.2018-0053

Beloozerova, I., & Sirota, M. (1988). Role of motor cortex in control of locomotion. In *Stance and Motion* (pp. 163-176). Springer.

Bernstein, N. (1966). The co-ordination and regulation of movements. *The co-ordination and regulation of movements*.

Bertram, C., Marteniuk, R., & Wymer, M. (1999). Coordination during a combined locomotion/prehension task. *Journal of Sport Expert Psychology*, *21*, 18.

Bertram, C. P. (2002). *Motor control in compound movements involving prehension* Theses (School of Kinesiology)/Simon Fraser University].

Beurskens, R., Helmich, I., Rein, R., & Bock, O. (2014). Age-related changes in prefrontal activity during walking in dual-task situations: a fNIRS study. *Int J Psychophysiol*, *92*(3), 122-128. https://doi.org/10.1016/j.ijpsycho.2014.03.005

Bishop, N. A., Lu, T., & Yankner, B. A. (2010). Neural mechanisms of ageing and cognitive decline. *Nature*, *464*(7288), 529-535. https://doi.org/10.1038/nature08983

Bizzi, E., Polit, A., & Morasso, P. (1976). Mechanisms underlying achievement of final head position. *J Neurophysiol*, *39*(2), 435-444. https://doi.org/10.1152/jn.1976.39.2.435

Blakemore, S. J., Goodbody, S. J., & Wolpert, D. M. (1998). Predicting the consequences of our own actions: the role of sensorimotor context estimation. *Journal of Neuroscience*, *18*(18), 7511-7518.

Borghese, N. A., Bianchi, L., & Lacquaniti, F. (1996). Kinematic determinants of human locomotion. *J Physiol*, *494 (Pt 3)*, 863-879. https://doi.org/10.1113/jphysiol.1996.sp021539

Brown, T. G. (1911). The intrinsic factors in the act of progression in the mammal. *Proceedings of the Royal Society of London. Series B, containing papers of a biological character*, *84*(572), 308-319.

Bruijn, S. M., Meijer, O. G., van Dieen, J. H., Kingma, I., & Lamoth, C. J. (2008). Coordination of leg swing, thorax rotations, and pelvis rotations during gait: the organisation of total body angular momentum. *Gait Posture*, *27*(3), 455-462. https://doi.org/10.1016/j.gaitpost.2007.05.017

Callaghan, J. P., Patla, A. E., & McGill, S. M. (1999). Low back three-dimensional joint forces, kinematics, and kinetics during walking. *Clin Biomech (Bristol, Avon)*, *14*(3), 203-216. https://doi.org/10.1016/s0268-0033(98)00069-2

Canton, S., & MacLellan, M. J. (2018). Active and passive contributions to arm swing: Implications of the restriction of pelvis motion during human locomotion. *Hum Mov Sci*, *57*, 314-323. https://doi.org/10.1016/j.humov.2017.09.009

Cappozzo, A. (1983). The forces and couples in the human trunk during level walking. *J Biomech*, *16*(4), 265-277. https://doi.org/10.1016/0021-9290(83)90134-3

Carnahan, H., Mcfadyen, B. J., Cockell, D. L., & Halverson, A. H. (1996). The combined control of locomotion and prehension. *Neuroscience Research Communications*, *19*(2), 91-100.

Ceccato, J. C., de Seze, M., Azevedo, C., & Cazalets, J. R. (2009). Comparison of trunk activity during gait initiation and walking in humans. *PLoS One*, *4*(12), e8193. https://doi.org/10.1371/journal.pone.0008193

Chang, R., Van Emmerik, R., & Hamill, J. (2008). Quantifying rearfoot-forefoot coordination in human walking. *J Biomech*, *41*(14), 3101-3105. https://doi.org/10.1016/j.jbiomech.2008.07.024

Chao, E. Y., Laughman, R. K., Schneider, E., & Stauffer, R. N. (1983). Normative data of knee joint motion and ground reaction forces in adult level walking. *J Biomech*, *16*(3), 219-233. https://doi.org/10.1016/0021-9290(83)90129-x

Cheung, V. C., d'Avella, A., Tresch, M. C., & Bizzi, E. (2005). Central and sensory contributions to the activation and organization of muscle synergies during natural motor behaviors. *J Neurosci*, *25*(27), 6419-6434. https://doi.org/10.1523/JNEUROSCI.4904-04.2005

Chiovetto, E., & Giese, M. A. (2013). Kinematics of the coordination of pointing during locomotion. *PLoS One*, *8*(11), e79555. https://doi.org/10.1371/journal.pone.0079555

Choi, J. T., & Bastian, A. J. (2007). Adaptation reveals independent control networks for human walking. *Nat Neurosci*, *10*(8), 1055-1062. https://doi.org/10.1038/nn1930

Cirstea, M. C., Mitnitski, A. B., Feldman, A. G., & Levin, M. F. (2003). Interjoint coordination dynamics during reaching in stroke. *Exp Brain Res*, *151*(3), 289-300. https://doi.org/10.1007/s00221-003-1438-0

Cockell, D. L., Carnahan, H., & McFadyen, B. J. (1995). A preliminary analysis of the coordination of reaching, grasping, and walking. *Percept Mot Skills*, *81*(2), 515-519. https://doi.org/10.2466/pms.1995.81.2.515

Cole, K. J., & Johansson, R. S. (1993). Friction at the digit-object interface scales the sensorimotor transformation for grip responses to pulling loads. *Exp Brain Res*, *95*(3), 523-532. https://doi.org/10.1007/bf00227146

Collins, S., Ruina, A., Tedrake, R., & Wisse, M. (2005). Efficient bipedal robots based on passive-dynamic walkers. *Science*, *307*(5712), 1082-1085. https://doi.org/10.1126/science.1107799

Collins, S. H., Adamczyk, P. G., & Kuo, A. D. (2009). Dynamic arm swinging in human walking. *Proc Biol Sci*, *276*(1673), 3679-3688. https://doi.org/10.1098/rspb.2009.0664

Cordo, P. J., & Nashner, L. M. (1982). Properties of postural adjustments associated with rapid arm movements. *J Neurophysiol*, *47*(2), 287-302. https://doi.org/10.1152/jn.1982.47.2.287

Courtine, G., & Schieppati, M. (2004). Tuning of a basic coordination pattern constructs straight-ahead and curved walking in humans. *J Neurophysiol*, *91*(4), 1524-1535. https://doi.org/10.1152/jn.00817.2003

d'Avella, A., Portone, A., Fernandez, L., & Lacquaniti, F. (2006). Control of fast-reaching movements by muscle synergy combinations. *J Neurosci*, *26*(30), 7791-7810. https://doi.org/10.1523/JNEUROSCI.0830-06.2006

Danion, F., & Latash, M. L. (2011). *Motor control : theories, experiments, and applications* [Bibliographies

Non-fiction]. Oxford University Press. http://libezp.lib.lsu.edu/login?url=https://search.ebscohost.com/login.aspx?direct=true&db=cat00252a&AN=lalu.3538539&site=eds-live&scope=site&profile=eds-main

Danion, F., & Latash, M. L. (2011). *Motor control: theories, experiments, and applications*. Oxford University Press.

de Brouwer, S., Missal, M., & Lefèvre, P. (2001). Role of retinal slip in the prediction of target motion during smooth and saccadic pursuit. *Journal of neurophysiology*, *86*(2), 550-558.

de Rugy, A., Wei, K., Muller, H., & Sternad, D. (2003). Actively tracking 'passive' stability in a ball bouncing task. *Brain Res*, *982*(1), 64-78. https://doi.org/10.1016/s0006-8993(03)02976-7

Della Croce, U., Riley, P. O., Lelas, J. L., & Kerrigan, D. C. (2001). A refined view of the determinants of gait. *Gait Posture*, *14*(2), 79-84. https://doi.org/10.1016/s0966-6362(01)00128-x

Delwaide, P. J., & Crenna, P. (1984). Cutaneous nerve stimulation and motoneuronal excitability. II: Evidence for non-segmental influences. *J Neurol Neurosurg Psychiatry*, *47*(2), 190-196. https://doi.org/10.1136/jnnp.47.2.190

Dettmann, M. A., Linder, M. T., & Sepic, S. B. (1987). Relationships among walking performance, postural stability, and functional assessments of the hemiplegic patient. *American journal of physical medicine & rehabilitation*, *66*(2), 77-90.

Diermayr, G., Gysin, P., Hass, C. J., & Gordon, A. M. (2008). Grip force control during gait initiation with a hand-held object. *Exp Brain Res*, *190*(3), 337-345. https://doi.org/10.1007/s00221-008-1476-8

Diermayr, G., McIsaac, T. L., Kaminski, T. R., & Gordon, A. M. (2011). Aging effects on object transport during gait. *Gait Posture*, *34*(3), 334-339. https://doi.org/10.1016/j.gaitpost.2011.05.021

Dietz, V. (1992). Human neuronal control of automatic functional movements: interaction between central programs and afferent input. *Physiol Rev*, *72*(1), 33-69. https://doi.org/10.1152/physrev.1992.72.1.33

Dietz, V. (2002). Do human bipeds use quadrupedal coordination? *Trends in neurosciences*, *25*(9), 462-467.

Dietz, V., Fouad, K., & Bastiaanse, C. M. (2001). Neuronal coordination of arm and leg movements during human locomotion. *Eur J Neurosci*, *14*(11), 1906-1914. https://doi.org/10.1046/j.0953-816x.2001.01813.x

Dietz, V., & Michel, J. (2009). Human bipeds use quadrupedal coordination during locomotion. *Annals of the New York Academy of Sciences*, *1164*(1), 97-103.

Dietz, V., Zijlstra, W., & Duysens, J. (1994). Human neuronal interlimb coordination during split-belt locomotion. *Exp Brain Res*, *101*(3), 513-520. https://doi.org/10.1007/BF00227344

Donker, S. F., Beek, P. J., Wagenaar, R., & Mulder, T. (2001). Coordination between arm and leg movements during locomotion. *Journal of motor behavior*, *33*(1), 86-102.

Donker, S. F., Daffertshofer, A., & Beek, P. J. (2005). Effects of velocity and limb loading on the coordination between limb movements during walking. *Journal of motor behavior*, *37*(3), 217-230.

Donker, S. F., Mulder, T., Nienhuis, B., & Duysens, J. (2002). Adaptations in arm movements for added mass to wrist or ankle during walking. *Exp Brain Res*, *146*(1), 26-31. https://doi.org/10.1007/s00221-002-1145-2

Dounskaia, N. (2010). Control of human limb movements: the leading joint hypothesis and its practical applications. *Exerc Sport Sci Rev*, *38*(4), 201-208. https://doi.org/10.1097/JES.0b013e3181f45194

Dounskaia, N. V., Swinnen, S. P., Walter, C. B., Spaepen, A. J., & Verschueren, S. M. (1998). Hierarchical control of different elbow-wrist coordination patterns. *Exp Brain Res*, *121*(3), 239-254. https://www.ncbi.nlm.nih.gov/pubmed/9746130

Duthilleul, N., Pirondini, E., Coscia, M., & Micera, S. (2015). Effect of handedness on muscle synergies during upper limb planar movements. *Conf Proc IEEE Eng Med Biol Soc*, *2015*, 3452-3455. https://doi.org/10.1109/EMBC.2015.7319135

[Record #364 is using a reference type undefined in this output style.]

Duysens, J., Clarac, F., & Cruse, H. (2000). Load-regulating mechanisms in gait and posture: comparative aspects. *Physiological reviews*, *80*(1), 83-133.

Duysens, J., & Pearson, K. (1980). Inhibition of flexor burst generation by loading ankle extensor muscles in walking cats. *Brain research*, *187*(2), 321-332.

Duysens, J., & Pearson, K. G. (1998). From cat to man: basic aspects of locomotion relevant to motor rehabilitation of SCI. *NeuroRehabilitation*, *10*(2), 107-118. https://doi.org/10.3233/NRE-1998-10203

Duysens, J., & Van de Crommert, H. W. (1998). Neural control of locomotion; The central pattern generator from cats to humans. *Gait Posture*, *7*(2), 131-141. https://doi.org/10.1016/s0966-6362(97)00042-8

Dyrby, C. O., & Andriacchi, T. P. (2004). Secondary motions of the knee during weight bearing and non-weight bearing activities. *J Orthop Res*, *22*(4), 794-800. https://doi.org/10.1016/j.orthres.2003.11.003

Eberhart, H. (1954). The principal elements in human locomotion. *Human Limbs and Their Substitutes.*, 437-471.

Ebied, A., Kinney-Lang, E., Spyrou, L., & Escudero, J. (2018). Evaluation of matrix factorisation approaches for muscle synergy extraction. *Med Eng Phys*, *57*, 51-60. https://doi.org/10.1016/j.medengphy.2018.04.003

Ebner-Karestinos, D., Thonnard, J.-L., & Bleyenheuft, Y. (2016). Precision grip control while walking down a stair step. *PLoS One*, *11*(11), e0165549.

Ebner-Karestinos, D., Thonnard, J. L., & Bleyenheuft, Y. (2016). Precision Grip Control while Walking Down a Stair Step. *PLoS One*, *11*(11), e0165549. https://doi.org/10.1371/journal.pone.0165549

Eke-Okoro, S. (1994). Evidence of interaction between human lumbosacral and cervical neural networks during gait. *Electromyography and clinical neurophysiology*, *34*(6), 345-349.

Eke-Okoro, S. T., Gregoric, M., & Larsson, L. E. (1997). Alterations in gait resulting from deliberate changes of arm-swing amplitude and phase. *Clin Biomech (Bristol, Avon)*, *12*(7-8), 516-521. https://doi.org/10.1016/s0268-0033(97)00050-8

Elftman, H. (1939a). Forces and energy changes in the leg during walking. *American Journal of Physiology-Legacy Content*, *125*(2), 339-356.

Elftman, H. (1939b). The function of the arms in walking. *Human Biology*, *11*(4), 529.

Eng, J. J., & Winter, D. A. (1995). Kinetic analysis of the lower limbs during walking: what information can be gained from a three-dimensional model? *J Biomech*, *28*(6), 753-758. https://doi.org/10.1016/0021-9290(94)00124-m

Feldman, A. G., & Levin, M. F. (1995). The origin and use of positional frames of reference in motor control. *Behavioral and Brain Sciences*, *18*(4), 723-806. https://doi.org/10.1017/S0140525X0004070X

Ferris, D. P., Huang, H. J., & Kao, P. C. (2006). Moving the arms to activate the legs. *Exerc Sport Sci Rev*, *34*(3), 113-120. https://doi.org/10.1249/00003677-200607000-00005

Flanagan, J. R., King, S., Wolpert, D. M., & Johansson, R. S. (2001). Sensorimotor prediction and memory in object manipulation. *Canadian Journal of Experimental Psychology/Revue canadienne de psychologie expérimentale*, *55*(2), 87.

Flanagan, J. R., & Lolley, S. (2001). The inertial anisotropy of the arm is accurately predicted during movement planning. *Journal of Neuroscience*, *21*(4), 1361-1369.

Flanagan, J. R., Tresilian, J., & Wing, A. M. (1993). Coupling of grip force and load force during arm movements with grasped objects. *Neurosci Lett*, *152*(1-2), 53-56. https://doi.org/10.1016/0304-3940(93)90481-y

Flanagan, J. R., & Tresilian, J. R. (1994). Grip-load force coupling: a general control strategy for transporting objects. *J Exp Psychol Hum Percept Perform*, *20*(5), 944-957. https://www.ncbi.nlm.nih.gov/pubmed/7964530

Flanagan, J. R., Vetter, P., Johansson, R. S., & Wolpert, D. M. (2003). Prediction precedes control in motor learning. *Curr Biol*, *13*(2), 146-150. https://doi.org/10.1016/s0960-9822(03)00007-1

Flanagan, J. R., & Wing, A. M. (1993). Modulation of grip force with load force during point-to-point arm movements. *Exp Brain Res*, *95*(1), 131-143. https://doi.org/10.1007/BF00229662

Flanagan, J. R., & Wing, A. M. (1995). The stability of precision grip forces during cyclic arm movements with a hand-held load. *Exp Brain Res*, *105*(3), 455-464. https://doi.org/10.1007/bf00233045

Flanagan, J. R., & Wing, A. M. (1997). The role of internal models in motion planning and control: evidence from grip force adjustments during movements of hand-held loads. *Journal of Neuroscience*, *17*(4), 1519-1528.

Ford, M. P., Wagenaar, R. C., & Newell, K. M. (2007). Arm constraint and walking in healthy adults. *Gait Posture*, *26*(1), 135-141. https://doi.org/10.1016/j.gaitpost.2006.08.008

Friedli, W. G., Hallett, M., & Simon, S. R. (1984). Postural adjustments associated with rapid voluntary arm movements 1. Electromyographic data. *J Neurol Neurosurg Psychiatry*, *47*(6), 611-622. https://doi.org/10.1136/jnnp.47.6.611

Fukuchi, C. A., Fukuchi, R. K., & Duarte, M. (2018). A public dataset of overground and treadmill walking kinematics and kinetics in healthy individuals. *PeerJ*, *6*, e4640. https://doi.org/10.7717/peerj.4640

Gebo, D. L. (1996). Climbing, brachiation, and terrestrial quadrupedalism: historical precursors of hominid bipedalism. *Am J Phys Anthropol*, *101*(1), 55-92. https://doi.org/10.1002/(SICI)1096-8644(199609)101:1<55::AID-AJPA5>3.0.CO;2-C

Gerasimenko, Y., Gorodnichev, R., Machueva, E., Pivovarova, E., Semyenov, D., Savochin, A., Roy, R. R., & Edgerton, V. R. (2010). Novel and direct access to the human locomotor

spinal circuitry. *J Neurosci*, *30*(10), 3700-3708. https://doi.org/10.1523/JNEUROSCI.4751-09.2010

Gordon, A. M., Quinn, L., Reilmann, R., & Marder, K. (2000). Coordination of prehensile forces during precision grip in Huntington's disease. *Exp Neurol*, *163*(1), 136-148. https://doi.org/10.1006/exnr.2000.7348

Gordon, K. E., Ferris, D. P., & Kuo, A. D. (2009). Metabolic and mechanical energy costs of reducing vertical center of mass movement during gait. *Arch Phys Med Rehabil*, *90*(1), 136-144. https://doi.org/10.1016/j.apmr.2008.07.014

Gore, D. R., Murray, M. P., Sepic, S. B., & Gardner, G. M. (1975). Walking patterns of men with unilateral surgical hip fusion. *J Bone Joint Surg Am*, *57*(6), 759-765. https://www.ncbi.nlm.nih.gov/pubmed/1158910

Gottschall, J. S., & Kram, R. (2005). Energy cost and muscular activity required for leg swing during walking. *J Appl Physiol (1985)*, *99*(1), 23-30. https://doi.org/10.1152/japplphysiol.01190.2004

Goudriaan, M., Jonkers, I., van Dieen, J. H., & Bruijn, S. M. (2014). Arm swing in human walking: What is their drive? *Gait & posture*, *40*(2), 321-326.

Gray, J. (1956). Muscular activity during locomotion. *Br Med Bull*, *12*(3), 203-209. https://doi.org/10.1093/oxfordjournals.bmb.a069551

Gribble, P. L., & Ostry, D. J. (1999). Compensation for interaction torques during single- and multijoint limb movement. *J Neurophysiol*, *82*(5), 2310-2326. https://doi.org/10.1152/jn.1999.82.5.2310

Grillner, S. (1975). Locomotion in vertebrates: central mechanisms and reflex interaction. *Physiol Rev*, *55*(2), 247-304. https://doi.org/10.1152/physrev.1975.55.2.247

Grillner, S. (2011). Control of locomotion in bipeds, tetrapods, and fish. *Comprehensive physiology*, 1179-1236.

Grillner, S., & Dubuc, R. (1988). Control of locomotion in vertebrates: spinal and supraspinal mechanisms. *Adv Neurol*, *47*, 425-453. https://www.ncbi.nlm.nih.gov/pubmed/3278525

Grillner, S., Wallen, P., Saitoh, K., Kozlov, A., & Robertson, B. (2008). Neural bases of goal-directed locomotion in vertebrates--an overview. *Brain Res Rev*, *57*(1), 2-12. https://doi.org/10.1016/j.brainresrev.2007.06.027

Grover, F., Lamb, M., Bonnette, S., Silva, P. L., Lorenz, T., & Riley, M. A. (2018). Intermittent coupling between grip force and load force during oscillations of a hand-held object. *Exp Brain Res*, *236*(10), 2531-2544. https://doi.org/10.1007/s00221-018-5315-2

Grover, F. M., Nalepka, P., Silva, P. L., Lorenz, T., & Riley, M. A. (2019). Variable and intermittent grip force control in response to differing load force dynamics. *Exp Brain Res*, *237*(3), 687-703. https://doi.org/10.1007/s00221-018-5451-8

Grover, F. M., Riehm, C., Silva, P. L., Lorenz, T., & Riley, M. A. (2021). Grip force anticipation of nonlinear, underactuated load force. *J Neurophysiol*, *125*(5), 1647-1662. https://doi.org/10.1152/jn.00616.2020

Gurfinkel, V. S., Levik, Y. S., Kazennikov, O. V., & Selionov, V. A. (1998). Locomotor-like movements evoked by leg muscle vibration in humans. *Eur J Neurosci*, *10*(5), 1608-1612. https://doi.org/10.1046/j.1460-9568.1998.00179.x

Gutnik, B., Mackie, H., Hudson, G., & Standen, C. (2005). How close to a pendulum is human upper limb movement during walking? *Homo*, *56*(1), 35-49.

Györy, A. N., Chao, E., & Stauffer, R. (1976). Functional evaluation of normal and pathologic knees during gait. *Archives of physical medicine and rehabilitation*, *57*(12), 571-577.

[Record #333 is using a reference type undefined in this output style.]

Gysin, P., Kaminski, T. R., & Gordon, A. M. (2003b). Coordination of fingertip forces in object transport during locomotion. *Exp Brain Res*, *149*(3), 371-379. https://doi.org/10.1007/s00221-003-1380-1

Gysin, P., Kaminski, T. R., & Gordon, A. M. (2009). Dynamic grasp control during gait.

Gysin, P., Kaminski, T. R., Hass, C. J., Grobet, C. E., & Gordon, A. M. (2008). Effects of gait variations on grip force coordination during object transport. *J Neurophysiol*, *100*(5), 2477-2485. https://doi.org/10.1152/jn.90561.2008

Haddad, J. M., van Emmerik, R. E., Whittlesey, S. N., & Hamill, J. (2006). Adaptations in interlimb and intralimb coordination to asymmetrical loading in human walking. *Gait Posture*, *23*(4), 429-434. https://doi.org/10.1016/j.gaitpost.2005.05.006

Hadjiosif, A. M., & Smith, M. A. (2015). Flexible Control of Safety Margins for Action Based on Environmental Variability. *J Neurosci*, *35*(24), 9106-9121. https://doi.org/10.1523/JNEUROSCI.1883-14.2015

Hamill, J., & Knutzen, K. M. (2006). *Biomechanical basis of human movement*. Lippincott Williams & Wilkins.

Hamill, J., van Emmerik, R. E., Heiderscheit, B. C., & Li, L. (1999). A dynamical systems approach to lower extremity running injuries. *Clin Biomech (Bristol, Avon)*, *14*(5), 297-308. https://doi.org/10.1016/s0268-0033(98)90092-4

Hejrati, B., Chesebrough, S., Foreman, K. B., Abbott, J. J., & Merryweather, A. S. (2016). Comprehensive quantitative investigation of arm swing during walking at various speed and surface slope conditions. *Human Movement Science*, *49*, 104-115.

Hermens, H. J., Freriks, B., Disselhorst-Klug, C., & Rau, G. (2000). Development of recommendations for SEMG sensors and sensor placement procedures. *J Electromyogr Kinesiol*, *10*(5), 361-374. https://www.ncbi.nlm.nih.gov/pubmed/11018445

Herr, H., & Popovic, M. (2008). Angular momentum in human walking. *J Exp Biol*, *211*(Pt 4), 467-481. https://doi.org/10.1242/jeb.008573

Hewes, G. W. (1961). Food transport and the origin of hominid bipedalism. *American Anthropologist*, 687-710.

Hiebert, G. W., Whelan, P. J., Prochazka, A., & Pearson, K. G. (1996). Contribution of hind limb flexor muscle afferents to the timing of phase transitions in the cat step cycle. *Journal of neurophysiology*, *75*(3), 1126-1137.

Hinrichs, R. N. (1987). Upper extremity function in running. II: Angular momentum considerations. *Journal of Applied Biomechanics*, *3*(3), 242-263.

Hinrichs, R. N. (1990a). Upper extremity function in distance running. *Biomechanics of distance running*, *4*, 107-133.

Hinrichs, R. N. (1990b). Whole body movement: coordination of arms and legs in walking and running. In *Multiple muscle systems* (pp. 694-705). Springer.

Hirashima, M., Kadota, H., Sakurai, S., Kudo, K., & Ohtsuki, T. (2002). Sequential muscle activity and its functional role in the upper extremity and trunk during overarm throwing. *J Sports Sci*, *20*(4), 301-310. https://doi.org/10.1080/026404102753576071

Hirashima, M., Kudo, K., Watarai, K., & Ohtsuki, T. (2007). Control of 3D limb dynamics in unconstrained overarm throws of different speeds performed by skilled baseball players. *J Neurophysiol*, *97*(1), 680-691. https://doi.org/10.1152/jn.00348.2006

Hodder, J. N., & Keir, P. J. (2012). Targeted gripping reduces shoulder muscle activity and variability. *J Electromyogr Kinesiol*, *22*(2), 186-190. https://doi.org/10.1016/j.jelekin.2011.11.011

Hof, A. L. (2008). The 'extrapolated center of mass' concept suggests a simple control of balance in walking. *Human Movement Science*, *27*(1), 112-125.

Hof, A. L., Gazendam, M. G., & Sinke, W. E. (2005). The condition for dynamic stability. *J Biomech*, *38*(1), 1-8. https://doi.org/10.1016/j.jbiomech.2004.03.025

Hollman, J. H., Watkins, M. K., Imhoff, A. C., Braun, C. E., Akervik, K. A., & Ness, D. K. (2016). A comparison of variability in spatiotemporal gait parameters between treadmill and overground walking conditions. *Gait & posture*, *43*, 204-209.

Holt, K. G., Hamill, J., & Andres, R. O. (1990). The force-driven harmonic oscillator as a model for human locomotion. *Human Movement Science*, *9*(1), 55-68.

Hosue, R. E. (1969). Upper-extremity muscular activity at different cadences and inclines during normal gait. *Physical therapy*, *49*(9), 963-972.

Huang, H. J., & Ferris, D. P. (2004). Neural coupling between upper and lower limbs during recumbent stepping. *Journal of Applied Physiology*, *97*(4), 1299-1308.

Huang, H. J., & Ferris, D. P. (2009). Upper and lower limb muscle activation is bidirectionally and ipsilaterally coupled. *Medicine and science in sports and exercise*, *41*(9), 1778.

Hug, F., Turpin, N. A., Couturier, A., & Dorel, S. (2011). Consistency of muscle synergies during pedaling across different mechanical constraints. *J Neurophysiol*, *106*(1), 91-103. https://doi.org/10.1152/jn.01096.2010

Inman, V. T., Ralston, H. J., & Todd, F. (1981). *Human walking*. Williams & Wilkins.

Ivanenko, Y. P., Cappellini, G., Dominici, N., Poppele, R. E., & Lacquaniti, F. (2005). Coordination of locomotion with voluntary movements in humans. *J Neurosci*, *25*(31), 7238-7253. https://doi.org/10.1523/JNEUROSCI.1327-05.2005

Ivanenko, Y. P., Poppele, R. E., & Lacquaniti, F. (2006). Motor control programs and walking. *Neuroscientist*, *12*(4), 339-348. https://doi.org/10.1177/1073858406287987

[Record #540 is using a reference type undefined in this output style.]

Jackson, K. M., Joseph, J., & Wyard, S. J. (1978). A mathematical model of arm swing during human locomotion. *J Biomech*, *11*(6-7), 277-289. https://doi.org/10.1016/0021-9290(78)90061-1

Jackson, K. M., Joseph, J., & Wyard, S. J. (1983). The upper limbs during human walking. Part 2: Function. *Electromyogr Clin Neurophysiol*, *23*(6), 435-446. https://www.ncbi.nlm.nih.gov/pubmed/6641599

Jeka, J. J., & Kelso, J. A. (1995). Manipulating symmetry in the coordination dynamics of human movement. *J Exp Psychol Hum Percept Perform*, *21*(2), 360-374. https://doi.org/10.1037//0096-1523.21.2.360

Jeka, J. J., Kelso, J. A., & Kiemel, T. (1993). Pattern switching in human multilimb coordination dynamics. *Bull Math Biol*, *55*(4), 829-845. https://doi.org/10.1007/BF02460675

Jin, X., Uygur, M., Getchell, N., Hall, S. J., & Jaric, S. (2011). The effects of instruction and hand dominance on grip-to-load force coordination in manipulation tasks. *Neurosci Lett*, *504*(3), 330-335. https://doi.org/10.1016/j.neulet.2011.09.059

Johansson, R. S., & Flanagan, J. R. (2009). Coding and use of tactile signals from the fingertips in object manipulation tasks. *Nature Reviews Neuroscience*, *10*(5), 345-359.

Johansson, R. S., & Westling, G. (1984). Roles of glabrous skin receptors and sensorimotor memory in automatic control of precision grip when lifting rougher or more slippery objects. *Exp Brain Res*, *56*(3), 550-564. https://doi.org/10.1007/bf00237997

Johansson, R. S., Westling, G., Bäckström, A., & Flanagan, J. R. (2001). Eye–hand coordination in object manipulation. *Journal of Neuroscience*, *21*(17), 6917-6932.

Johnston, R. C., & Smidt, G. L. (1969). Measurement of hip-joint motion during walking. Evaluation of an electrogoniometric method. *J Bone Joint Surg Am*, *51*(6), 1082-1094. https://www.ncbi.nlm.nih.gov/pubmed/5805410

Juvin, L., Simmers, J., & Morin, D. (2005). Propriospinal circuitry underlying interlimb coordination in mammalian quadrupedal locomotion. *J Neurosci*, *25*(25), 6025-6035. https://doi.org/10.1523/JNEUROSCI.0696-05.2005

Juvin, L., Simmers, J., & Morin, D. (2007). Locomotor rhythmogenesis in the isolated rat spinal cord: a phase-coupled set of symmetrical flexion extension oscillators. *J Physiol*, *583*(Pt 1), 115-128. https://doi.org/10.1113/jphysiol.2007.133413

Kadaba, M., Ramakrishnan, H., Wootten, M., Gainey, J., Gorton, G., & Cochran, G. (1989). Repeatability of kinematic, kinetic, and electromyographic data in normal adult gait. *Journal of Orthopaedic Research*, *7*(6), 849-860.

Kadaba, M. P., Ramakrishnan, H. K., & Wootten, M. E. (1990). Measurement of lower extremity kinematics during level walking. *J Orthop Res*, *8*(3), 383-392. https://doi.org/10.1002/jor.1100080310

Kam, D. d., Rijken, H., Manintveld, T., Nienhuis, B., Dietz, V., & Duysens, J. (2013). Arm movements can increase leg muscle activity during submaximal recumbent stepping in neurologically intact individuals. *Journal of Applied Physiology*, *115*(1), 34-42.

Kandel, E. R., Schwartz, J. H., Jessell, T. M., Biochemistry, D. o., Jessell, M. B. T., Siegelbaum, S., & Hudspeth, A. (2000). *Principles of neural science* (Vol. 4). McGraw-hill New York.

Kandel, E. R., Schwartz, J. H., Jessell, T. M., Siegelbaum, S., Hudspeth, A. J., & Mack, S. (2000). *Principles of neural science* (Vol. 4). McGraw-hill New York.

Kao, P. C., & Ferris, D. P. (2005). The effect of movement frequency on interlimb coupling during recumbent stepping. *Motor Control*, *9*(2), 144-163. https://doi.org/10.1123/mcj.9.2.144

Kawashima, N., Nozaki, D., Abe, M. O., & Nakazawa, K. (2008). Shaping appropriate locomotive motor output through interlimb neural pathway within spinal cord in humans. *Journal of neurophysiology*, *99*(6), 2946-2955.

Kelso, J. A., & Jeka, J. J. (1992). Symmetry breaking dynamics of human multilimb coordination. *J Exp Psychol Hum Percept Perform*, *18*(3), 645-668. https://doi.org/10.1037//0096-1523.18.3.645

Kelso, J. S. (1995). *Dynamic patterns: The self-organization of brain and behavior*. MIT press.

Kettelkamp, D. B., Johnson, R. J., Smidt, G. L., Chao, E. Y., & Walker, M. (1970). An electrogoniometric study of knee motion in normal gait. *J Bone Joint Surg Am*, *52*(4), 775-790. https://www.ncbi.nlm.nih.gov/pubmed/5479460

Kinoshita, H., Kawai, S., Ikuta, K., & Teraoka, T. (1996). Individual finger forces acting on a grasped object during shaking actions. *Ergonomics*, *39*(2), 243-256. https://doi.org/10.1080/00140139608964455

[Record #182 is using a reference type undefined in this output style.]

Kubo, M., Holt, K. G., Saltzman, E., & Wagenaar, R. C. (2006). Changes in axial stiffness of the trunk as a function of walking speed. *Journal of biomechanics*, *39*(4), 750-757.

Kuhtz-Buschbeck, J. P., & Frendel, A. (2015). Stable patterns of upper limb muscle activation in different conditions of human walking. *Brazilian Journal of Motor Behavior*, *9*(1), 1-10.

Kuhtz-Buschbeck, J. P., & Frendel, A. (2015). Stable patterns of upper limb muscle activation in different conditions of human walking. *Brazilian Journal of Motor Behavior*, *9*(1).

Kuhtz-Buschbeck, J. P., & Jing, B. (2012). Activity of upper limb muscles during human walking. *J Electromyogr Kinesiol*, *22*(2), 199-206. https://doi.org/10.1016/j.jelekin.2011.08.014

Kutch, J. J., & Valero-Cuevas, F. J. (2011). Muscle redundancy does not imply robustness to muscle dysfunction. *J Biomech*, *44*(7), 1264-1270. https://doi.org/10.1016/j.jbiomech.2011.02.014

Lacquaniti, F., Ivanenko, Y. P., & Zago, M. (2012). Patterned control of human locomotion. *J Physiol*, *590*(10), 2189-2199. https://doi.org/10.1113/jphysiol.2011.215137

Lacquaniti, F., Licata, F., & Soechting, J. F. (1982). The mechanical behavior of the human forearm in response to transient perturbations. *Biol Cybern*, *44*(1), 35-46. https://www.ncbi.nlm.nih.gov/pubmed/7093368

LaFiandra, M., Wagenaar, R. C., Holt, K., & Obusek, J. (2003). How do load carriage and walking speed influence trunk coordination and stride parameters? *Journal of biomechanics*, *36*(1), 87-95.

Latash, M. L. (2012). The bliss (not the problem) of motor abundance (not redundancy). *Experimental brain research*, *217*(1), 1-5.

Latash, M. L., & Zatsiorsky, V. M. (1993). Joint stiffness: Myth or reality? *Human Movement Science*, *12*(6), 653-692.

Lee, D. D., & Seung, H. S. (1999). Learning the parts of objects by non-negative matrix factorization. *Nature*, *401*(6755), 788-791. https://doi.org/10.1038/44565

Levangie, P. K., & Norkin, C. C. (2011). Joint structure and function: a comprehensive analysis.

Levens, A. S., Inman, V. T., & Blosser, J. A. (1948). Transverse rotation of the segments of the lower extremity in locomotion. *J Bone Joint Surg Am*, *30A*(4), 859-872. https://www.ncbi.nlm.nih.gov/pubmed/18887290

Li, Y., Wang, W., Crompton, R. H., & Gunther, M. M. (2001). Free vertical moments and transverse forces in human walking and their role in relation to arm-swing. *Journal of Experimental Biology*, *204*(1), 47-58.

Lin, D. C., & Rymer, W. Z. (2000). Damping actions of the neuromuscular system with inertial loads: soleus muscle of the decerebrate cat. *J Neurophysiol*, *83*(2), 652-658. https://doi.org/10.1152/jn.2000.83.2.652

Lin, D. C., & Rymer, W. Z. (2001). Damping actions of the neuromuscular system with inertial loads: human flexor pollicis longus muscle. *J Neurophysiol*, *85*(3), 1059-1066. https://doi.org/10.1152/jn.2001.85.3.1059

Lovejoy, C. O. (1988). Evolution of human walking. *Sci Am*, *259*(5), 118-125. https://doi.org/10.1038/scientificamerican1188-118

MacLellan, M. J. (2017). Modular organization of muscle activity patterns in the leading and trailing limbs during obstacle clearance in healthy adults. *Exp Brain Res*, *235*(7), 2011-2026. https://doi.org/10.1007/s00221-017-4946-z

MacLellan, M. J., & Ellis, S. (2018). Shoulder Muscle Activity Dampens Arm Swing Motion When Altering Upper Limb Mass Characteristics During Locomotion. *J Mot Behav*, *51*(4), 428-437. https://doi.org/10.1080/00222895.2018.1502146

MacLellan, M. J., & Ellis, S. (2019). Shoulder Muscle Activity Dampens Arm Swing Motion When Altering Upper Limb Mass Characteristics During Locomotion. *J Mot Behav*, *51*(4), 428-437. https://doi.org/10.1080/00222895.2018.1502146

Madehkhaksar, F., & Egges, A. (2016). Effect of dual task type on gait and dynamic stability during stair negotiation at different inclinations. *Gait & posture*, *43*, 114-119.

Martino, G., Ivanenko, Y. P., d'Avella, A., Serrao, M., Ranavolo, A., Draicchio, F., Cappellini, G., Casali, C., & Lacquaniti, F. (2015). Neuromuscular adjustments of gait associated with unstable conditions. *J Neurophysiol*, *114*(5), 2867-2882. https://doi.org/10.1152/jn.00029.2015

Massion, J. (1992). Movement, posture and equilibrium: interaction and coordination. *Prog Neurobiol*, *38*(1), 35-56. https://www.ncbi.nlm.nih.gov/pubmed/1736324

Matsuo, T., Hashimoto, M., Koyanagi, M., & Hashizume, K. (2008). Asymmetric load-carrying in young and elderly women: Relationship with lower limb coordination. *Gait & posture*, *28*(3), 517-520.

Mayer, H. C., & Krechetnikov, R. (2012). Walking with coffee: why does it spill? *Phys Rev E Stat Nonlin Soft Matter Phys*, *85*(4 Pt 2), 046117. https://doi.org/10.1103/PhysRevE.85.046117

McIsaac, T. L., Diermayr, G., & Albert, F. (2012). Impaired anticipatory control of grasp during obstacle crossing in Parkinson's disease. *Neurosci Lett*, *516*(2), 242-246. https://doi.org/10.1016/j.neulet.2012.03.096

Meyns, P., Bruijn, S. M., & Duysens, J. (2013). The how and why of arm swing during human walking. *Gait & posture*, *38*(4), 555-562.

Milner, T. E., & Cloutier, C. (1993). Compensation for mechanically unstable loading in voluntary wrist movement. *Exp Brain Res*, *94*(3), 522-532. https://www.ncbi.nlm.nih.gov/pubmed/8359266

Milner, T. E., & Cloutier, C. (1998). Damping of the wrist joint during voluntary movement. *Exp Brain Res*, *122*(3), 309-317. https://www.ncbi.nlm.nih.gov/pubmed/9808304

[Record #1013 is using a reference type undefined in this output style.]

Moglo, K. E., & Shirazi-Adl, A. (2005). Cruciate coupling and screw-home mechanism in passive knee joint during extension--flexion. *J Biomech*, *38*(5), 1075-1083. https://doi.org/10.1016/j.jbiomech.2004.05.033

Murphy, J. T., Wong, Y. C., & Kwan, H. C. (1985). Sequential activation of neurons in primate motor cortex during unrestrained forelimb movement. *J Neurophysiol*, *53*(2), 435-445. https://doi.org/10.1152/jn.1985.53.2.435

Murray, M., Mollinger, L., Gardner, G., & Sepic, S. (1984). Kinematic and EMG patterns during slow, free, and fast walking. *Journal of Orthopaedic Research*, *2*(3), 272-280.

Murray, M. P., Drought, A. B., & Kory, R. C. (1964). Walking Patterns of Normal Men. *J Bone Joint Surg Am*, *46*, 335-360. https://www.ncbi.nlm.nih.gov/pubmed/14129683

Murray, M. P., Sepic, S. B., & Barnard, E. J. (1967). Patterns of sagittal rotation of the upper limbs in walking. *Phys Ther*, *47*(4), 272-284. https://doi.org/10.1093/ptj/47.4.272

Nakazawa, K., Obata, H., & Sasagawa, S. (2012). Neural control of human gait and posture. *The Journal of Physical Fitness and Sports Medicine*, *1*(2), 263-269.

Neptune, R. R., Clark, D. J., & Kautz, S. A. (2009). Modular control of human walking: a simulation study. *J Biomech*, *42*(9), 1282-1287. https://doi.org/10.1016/j.jbiomech.2009.03.009

Nester, C. J., van der Linden, M. L., & Bowker, P. (2003). Effect of foot orthoses on the kinematics and kinetics of normal walking gait. *Gait Posture*, *17*(2), 180-187. https://doi.org/10.1016/s0966-6362(02)00065-6

Nicolas, G., Marchand-Pauvert, V., Burke, D., & Pierrot-Deseilligny, E. (2001). Corticospinal excitation of presumed cervical propriospinal neurones and its reversal to inhibition in humans. *J Physiol*, *533*(Pt 3), 903-919. https://doi.org/10.1111/j.1469-7793.2001.t01-1-00903.x

Niemitz, C. (2010). The evolution of the upright posture and gait—a review and a new synthesis. *Naturwissenschaften*, *97*(3), 241-263.

Nordin, M., & Frankel, V. H. (2001). *Basic biomechanics of the musculoskeletal system*. Lippincott Williams & Wilkins.

Nowak, D. A., & Hermsdorfer, J. (2006). Predictive and reactive control of grasping forces: on the role of the basal ganglia and sensory feedback. *Exp Brain Res*, *173*(4), 650-660. https://doi.org/10.1007/s00221-006-0409-7

O'Neill, M. C., Lee, L. F., Demes, B., Thompson, N. E., Larson, S. G., Stern, J. T., Jr., & Umberger, B. R. (2015). Three-dimensional kinematics of the pelvis and hind limbs in chimpanzee (Pan troglodytes) and human bipedal walking. *J Hum Evol*, *86*, 32-42. https://doi.org/10.1016/j.jhevol.2015.05.012

Oatis, C. A. (2017). *Kinesiology: the mechanics and pathomechanics of human movement*. Wolters Kluwer.

Ortega, J. D., Fehlman, L. A., & Farley, C. T. (2008). Effects of aging and arm swing on the metabolic cost of stability in human walking. *J Biomech*, *41*(16), 3303-3308. https://doi.org/10.1016/j.jbiomech.2008.06.039

Partridge, L. D. (1966). Signal-handling characteristics of load-moving skeletal muscle. *Am J Physiol*, *210*(5), 1178-1191. https://doi.org/10.1152/ajplegacy.1966.210.5.1178

Parvataneni, K., Ploeg, L., Olney, S. J., & Brouwer, B. (2009). Kinematic, kinetic and metabolic parameters of treadmill versus overground walking in healthy older adults. *Clin Biomech (Bristol, Avon)*, *24*(1), 95-100. https://doi.org/10.1016/j.clinbiomech.2008.07.002

Perry, J., & Burnfield, J. M. (2010). Gait analysis. Normal and pathological function 2nd ed. *California: Slack*.

Pilon, J. F., De Serres, S. J., & Feldman, A. G. (2007). Threshold position control of arm movement with anticipatory increase in grip force. *Exp Brain Res*, *181*(1), 49-67. https://doi.org/10.1007/s00221-007-0901-8

Pontzer, H., Holloway, J. H. t., Raichlen, D. A., & Lieberman, D. E. (2009). Control and function of arm swing in human walking and running. *Journal of Experimental Biology*, *212*(Pt 4), 523-534. https://doi.org/10.1242/jeb.024927

Przybyla, A., Good, D. C., & Sainburg, R. L. (2012). Dynamic dominance varies with handedness: reduced interlimb asymmetries in left-handers. *Exp Brain Res*, *216*(3), 419-431. https://doi.org/10.1007/s00221-011-2946-y

Quinn, L., Reilmann, R., Marder, K., & Gordon, A. M. (2001). Altered movement trajectories and force control during object transport in Huntington's disease. *Mov Disord*, *16*(3), 469-480. https://doi.org/10.1002/mds.1108

Racic, V., Pavic, A., & Brownjohn, J. (2009). Experimental identification and analytical modelling of human walking forces: Literature review. *Journal of Sound and Vibration*, *326*(1-2), 1-49.

Rack, P. M. (1966). The behaviour of a mammalian muscle during sinusoidal stretching. *J Physiol*, *183*(1), 1-14. https://doi.org/10.1113/jphysiol.1966.sp007848

Ranganathan, R., & Krishnan, C. (2012). Extracting synergies in gait: using EMG variability to evaluate control strategies. *J Neurophysiol*, *108*(5), 1537-1544. https://doi.org/10.1152/jn.01112.2011

Reisman, D. S., Block, H. J., & Bastian, A. J. (2005). Interlimb coordination during locomotion: what can be adapted and stored? *Journal of neurophysiology*, *94*(4), 2403-2415.

Rinaldi, N. M., & Moraes, R. (2015). Gait and reach-to-grasp movements are mutually modified when performed simultaneously. *Human Movement Science*, *40*, 38-58.

Rinaldi, N. M., van Emmerik, R., & Moraes, R. (2017). Changes in interlimb coordination during walking and grasping task in older adult fallers and non-fallers. *Human Movement Science*, *55*, 121-137.

Robertson, D. G. E., Caldwell, G. E., Hamill, J., Kamen, G., & Whittlesey, S. (2013). *Research methods in biomechanics*. Human kinetics.

Roerdink, M., de Jonge, C. P., Smid, L. M., & Daffertshofer, A. (2019). Tightening Up the Control of Treadmill Walking: Effects of Maneuverability Range and Acoustic Pacing on Stride-to-Stride Fluctuations. *Front Physiol*, *10*, 257. https://doi.org/10.3389/fphys.2019.00257

Roh, J., Rymer, W. Z., Perreault, E. J., Yoo, S. B., & Beer, R. F. (2013). Alterations in upper limb muscle synergy structure in chronic stroke survivors. *J Neurophysiol*, *109*(3), 768-781. https://doi.org/10.1152/jn.00670.2012

Rose, J., & Gamble, J. G. (1994). *Human walking* (Vol. 3). Williams & Wilkins Baltimore.

Rossignol, S. (2010). Neural control of stereotypic limb movements. *Comprehensive physiology*, 173-216.

Ruina, A. L., & Pratap, R. (2002). *Introduction to statics and dynamics*. Pre-print for Oxford University Press.

Sainburg, R. L. (2002). Evidence for a dynamic-dominance hypothesis of handedness. *Exp Brain Res*, *142*(2), 241-258. https://doi.org/10.1007/s00221-001-0913-8

Sainburg, R. L. (2005). Handedness: differential specializations for control of trajectory and position. *Exerc Sport Sci Rev*, *33*(4), 206-213. https://doi.org/10.1097/00003677-200510000-00010

Saito, A., Tomita, A., Ando, R., Watanabe, K., & Akima, H. (2018). Similarity of muscle synergies extracted from the lower limb including the deep muscles between level and uphill treadmill walking. *Gait Posture*, *59*, 134-139. https://doi.org/10.1016/j.gaitpost.2017.10.007

Sakamoto, M., Tazoe, T., Nakajima, T., Endoh, T., Shiozawa, S., & Komiyama, T. (2007). Voluntary changes in leg cadence modulate arm cadence during simultaneous arm and leg cycling. *Exp Brain Res*, *176*(1), 188-192. https://doi.org/10.1007/s00221-006-0742-x

Salimi, I., Hollender, I., Frazier, W., & Gordon, A. M. (2000). Specificity of internal representations underlying grasping. *J Neurophysiol*, *84*(5), 2390-2397. https://doi.org/10.1152/jn.2000.84.5.2390

Sarlegna, F. R., & Sainburg, R. L. (2009). The roles of vision and proprioception in the planning of reaching movements. *Adv Exp Med Biol*, *629*, 317-335. https://doi.org/10.1007/978-0-387-77064-2_16

Saunders, J. B., Inman, V. T., & Eberhart, H. D. (1953). The major determinants in normal and pathological gait. *J Bone Joint Surg Am*, *35-A*(3), 543-558. https://www.ncbi.nlm.nih.gov/pubmed/13069544

Schiehlen, W., & García-Vallejo, D. (2011). Walking dynamics from mechanism models to parameter optimization. *Procedia IUTAM*, *2*, 199-211.

Schmitt, D. (2003). Insights into the evolution of human bipedalism from experimental studies of humans and other primates. *Journal of Experimental Biology*, *206*(9), 1437-1448.

Schubert, P., & Kirchner, M. (2014). Ellipse area calculations and their applicability in posturography. *Gait & posture*, *39*(1), 518-522.

Schwarz, M., Block, F., Töpper, R., Sontag, K. H., & Noth, J. (1992). Abnormalities of somatosensory evoked potentials in the quinolinic acid model of Huntington's disease: evidence that basal ganglia modulate sensory cortical input. *Annals of Neurology:*

Official Journal of the American Neurological Association and the Child Neurology Society, *32*(3), 358-364.

Serrien, D. J., & Swinnen, S. P. (1998). Load compensation during homologous and non-homologous coordination. *Exp Brain Res*, *121*(3), 223-229. https://doi.org/10.1007/s002210050455

Shiratori, T., & Latash, M. (2000). The roles of proximal and distal muscles in anticipatory postural adjustments under asymmetrical perturbations and during standing on rollerskates. *Clin Neurophysiol*, *111*(4), 613-623. https://www.ncbi.nlm.nih.gov/pubmed/10727912

Shirota, C., Jansa, J., Diaz, J., Balasubramanian, S., Mazzoleni, S., Borghese, N. A., & Melendez-Calderon, A. (2016). On the assessment of coordination between upper extremities: towards a common language between rehabilitation engineers, clinicians and neuroscientists. *Journal of neuroengineering and rehabilitation*, *13*(1), 80.

Sigholm, G., Herberts, P., Almstrom, C., & Kadefors, R. (1984). Electromyographic analysis of shoulder muscle load. *J Orthop Res*, *1*(4), 379-386. https://doi.org/10.1002/jor.1100010406

Silva, J. J., Rinaldi, N. M., & Moraes, R. (2019). Asymmetrical load-carrying while stepping down a curb in young adults. *Gait & posture*, *73*, 202-208.

Simpson, K. J., & Jiang, P. (1999). Foot landing position during gait influences ground reaction forces. *Clin Biomech (Bristol, Avon)*, *14*(6), 396-402. https://doi.org/10.1016/s0268-0033(98)00112-0

Siragy, T., Mezher, C., Hill, A., & Nantel, J. (2020). Active arm swing and asymmetric walking leads to increased variability in trunk kinematics in young adults. *J Biomech*, *99*, 109529. https://doi.org/10.1016/j.jbiomech.2019.109529

Smets, M. P., Potvin, J. R., & Keir, P. J. (2009). Constrained handgrip force decreases upper extremity muscle activation and arm strength. *Ergonomics*, *52*(9), 1144-1152. https://doi.org/10.1080/00140130902919113

Solopova, I. A., Selionov, V. A., Kazennikov, O. V., & Ivanenko, Y. P. (2014). Effects of transcranial magnetic stimulation during voluntary and non-voluntary stepping movements in humans. *Neurosci Lett*, *579*, 64-69. https://doi.org/10.1016/j.neulet.2014.07.015

Song, A., Kuznetsov, N. A., Winges, S. A., & MacLellan, M. J. (2020). Muscle synergy for upper limb damping behavior during object transport while walking in healthy young individuals. *Exp Brain Res*, *238*(5), 1203-1218. https://doi.org/10.1007/s00221-020-05800-3

Sporrong, H., Palmerud, G., & Herberts, P. (1995). Influences of handgrip on shoulder muscle activity. *Eur J Appl Physiol Occup Physiol*, *71*(6), 485-492. https://www.ncbi.nlm.nih.gov/pubmed/8983914

Springer, S., Giladi, N., Peretz, C., Yogev, G., Simon, E. S., & Hausdorff, J. M. (2006). Dual-tasking effects on gait variability: the role of aging, falls, and executive function. *Mov Disord*, *21*(7), 950-957. https://doi.org/10.1002/mds.20848

Stein, P. (1997). Neural and biomechanical control strategies for different forms of vertebrate hindlimb motor tasks. *Neurons, networks, and motor behavior*, 61-73.

Stevenson, A. (2010). *Oxford dictionary of English*. Oxford University Press, USA.

Stokes, V. P., Andersson, C., & Forssberg, H. (1989). Rotational and translational movement features of the pelvis and thorax during adult human locomotion. *J Biomech*, *22*(1), 43-50. https://doi.org/10.1016/0021-9290(89)90183-8

Sutherland, D. H. (2001). The evolution of clinical gait analysis part l: kinesiological EMG. *Gait Posture*, *14*(1), 61-70. https://doi.org/10.1016/s0966-6362(01)00100-x

Swinnen, S. P., Serrien, D. J., Walter, C. B., & Philippaerts, R. (1995). The organization of patterns of multilimb coordination as revealed through reaction time measures. *Experimental brain research*, *104*(1), 153-162.

Sylos-Labini, F., Ivanenko, Y. P., Maclellan, M. J., Cappellini, G., Poppele, R. E., & Lacquaniti, F. (2014). Locomotor-like leg movements evoked by rhythmic arm movements in humans. *PLoS One*, *9*(3), e90775. https://doi.org/10.1371/journal.pone.0090775

Takahashi, C., Scheidt, R. A., & Reinkensmeyer, D. (2001). Impedance control and internal model formation when reaching in a randomly varying dynamical environment. *Journal of neurophysiology*, *86*(2), 1047-1051.

Tesio, L., & Rota, V. (2019). The Motion of Body Center of Mass During Walking: A Review Oriented to Clinical Applications. *Front Neurol*, *10*, 999. https://doi.org/10.3389/fneur.2019.00999

Tesio, L., Rota, V., Chessa, C., & Perucca, L. (2010). The 3D path of body centre of mass during adult human walking on force treadmill. *J Biomech*, *43*(5), 938-944. https://doi.org/10.1016/j.jbiomech.2009.10.049

Ting, & Chvatal. (2010). Decomposing muscle activity in motor tasks. *Motor control: theories, experiments, and applications*, 102-138.

Ting, L. H., & Chvatal, S. A. (2010). Decomposing muscle activity in motor tasks: methods and interpretation. In *Motor Control: Theories, Experiments, and Applications* (pp. 102-138). Oxford University Press.

Ting, L. H., & McKay, J. L. (2007). Neuromechanics of muscle synergies for posture and movement. *Curr Opin Neurobiol*, *17*(6), 622-628. https://doi.org/10.1016/j.conb.2008.01.002

Togo, S., Kagawa, T., & Uno, Y. (2012). Motor synergies for dampening hand vibration during human walking. *Exp Brain Res*, *216*(1), 81-90. https://doi.org/10.1007/s00221-011-2909-3

Tresch, M. C., & Jarc, A. (2009). The case for and against muscle synergies. *Curr Opin Neurobiol*, *19*(6), 601-607. https://doi.org/10.1016/j.conb.2009.09.002

Turvey, M. T., Schmidt, R. C., Rosenblum, L. D., & Kugler, P. N. (1988). On the time allometry of co-ordinated rhythmic movements. *J Theor Biol*, *130*(3), 285-325. https://doi.org/10.1016/s0022-5193(88)80031-6

Umberger, B. R. (2008). Effects of suppressing arm swing on kinematics, kinetics, and energetics of human walking. *J Biomech*, *41*(11), 2575-2580. https://doi.org/10.1016/j.jbiomech.2008.05.024

van Beers, R. J., Sittig, A. C., & Gon, J. J. (1999). Integration of proprioceptive and visual position-information: An experimentally supported model. *J Neurophysiol*, *81*(3), 1355-1364. https://doi.org/10.1152/jn.1999.81.3.1355

Van de Crommert, H. W., Mulder, T., & Duysens, J. (1998). Neural control of locomotion: sensory control of the central pattern generator and its relation to treadmill training. *Gait Posture*, *7*(3), 251-263. https://doi.org/10.1016/s0966-6362(98)00010-1

Van Emmerik, R., Miller, R., Hamill, J., & Robertson, D. (2014). Dynamical systems analysis of coordination. *Research methods in biomechanics*, 291-315.

Van Emmerik, R. E., Wagenaar, R. C., & Van Wegen, E. E. (1998). Interlimb coupling patterns in human locomotion: are we bipeds or quadrupeds? *Annals of the New York Academy of Sciences*, *860*(1), 539-542.

Vaughan, C., Davis, B., & O'connor, J. (1999). Dynamics of human gait. *Cape Town: Kiboho Publishers*.

Wagenaar, R. C., & Beek, W. (1992). Hemiplegic gait: a kinematic analysis using walking speed as a basis. *Journal of biomechanics*, *25*(9), 1007-1015.

Wagenaar, R. C., & van Emmerik, R. E. (2000). Resonant frequencies of arms and legs identify different walking patterns. *J Biomech*, *33*(7), 853-861. https://doi.org/10.1016/s0021-9290(00)00020-8

Wakeling, J. M., & Horn, T. (2009). Neuromechanics of muscle synergies during cycling. *J Neurophysiol*, *101*(2), 843-854. https://doi.org/10.1152/jn.90679.2008

Wannier, T., Bastiaanse, C., Colombo, G., & Dietz, V. (2001). Arm to leg coordination in humans during walking, creeping and swimming activities. *Experimental brain research*, *141*(3), 375-379.

White, O., McIntyre, J., Augurelle, A.-S., & Thonnard, J.-L. (2005). Do novel gravitational environments alter the grip-force/load-force coupling at the fingertips? *Experimental brain research*, *163*(3), 324-334.

White, S. C., Yack, H. J., Tucker, C. A., & Lin, H. Y. (1998). Comparison of vertical ground reaction forces during overground and treadmill walking. *Med Sci Sports Exerc*, *30*(10), 1537-1542. https://doi.org/10.1097/00005768-199810000-00011

Wiesendanger, M., & Serrien, D. J. (2001). Neurological problems affecting hand dexterity. *Brain Res Brain Res Rev*, *36*(2-3), 161-168. https://doi.org/10.1016/s0165-0173(01)00091-1

Wing, A. M., & Lederman, S. J. (1998). Anticipating load torques produced by voluntary movements. *J Exp Psychol Hum Percept Perform*, *24*(6), 1571-1581. https://www.ncbi.nlm.nih.gov/pubmed/9861711

Wing, A. M., & Lederman, S. J. (1998). Anticipatory load torques produced by voluntary movements. *Journal of Experimental Psychology: Human Perception and Performance*, *24*(6), 1571.

Winter, D. A., & Yack, H. J. (1987). EMG profiles during normal human walking: stride-to-stride and inter-subject variability. *Electroencephalogr Clin Neurophysiol*, *67*(5), 402-411. https://doi.org/10.1016/0013-4694(87)90003-4

Witte, H., Preuschoft, H., & Recknagel, S. (1991). Human body proportions explained on the basis of biomechanical principles. *Z Morphol Anthropol*, *78*(3), 407-423. https://www.ncbi.nlm.nih.gov/pubmed/1887666

Xiang, C., Xiaocong, N., De, W., Yi, Y., & Xu, Z. (2017). Investigation of the Intra- and Inter-Limb Muscle Coordination of Hands-and-Knees Crawling in Human Adults by Means of Muscle Synergy Analysis [Article]. *Entropy*, *19*(5), 229. https://doi.org/10.3390/e19050229

Yadav, V., & Sainburg, R. L. (2014). Limb dominance results from asymmetries in predictive and impedance control mechanisms. *PLoS One*, *9*(4), e93892. https://doi.org/10.1371/journal.pone.0093892

Yang, H. S., Atkins, L. T., Jensen, D. B., & James, C. R. (2015). Effects of constrained arm swing on vertical center of mass displacement during walking. *Gait Posture*, *42*(4), 430-434. https://doi.org/10.1016/j.gaitpost.2015.07.010

Yizhar, Z., Boulos, S., Inbar, O., & Carmeli, E. (2009). The effect of restricted arm swing on energy expenditure in healthy men. *International journal of rehabilitation research*, *32*(2), 115-123.

Yokoyama, H., Ogawa, T., Kawashima, N., Shinya, M., & Nakazawa, K. (2016). Distinct sets of locomotor modules control the speed and modes of human locomotion. *Sci Rep*, *6*, 36275. https://doi.org/10.1038/srep36275

Zatsiorsky, V. M., Gao, F., & Latash, M. L. (2005). Motor control goes beyond physics: differential effects of gravity and inertia on finger forces during manipulation of hand-held objects. *Exp Brain Res*, *162*(3), 300-308. https://doi.org/10.1007/s00221-004-2152-2

Zehr, E. P., Carroll, T. J., Chua, R., Collins, D. F., Frigon, A., Haridas, C., Hundza, S. R., & Thompson, A. K. (2004). Possible contributions of CPG activity to the control of rhythmic human arm movement. *Can J Physiol Pharmacol*, *82*(8-9), 556-568. https://doi.org/10.1139/y04-056

Zehr, E. P., & Haridas, C. (2003). Modulation of cutaneous reflexes in arm muscles during walking: further evidence of similar control mechanisms for rhythmic human arm and leg movements. *Experimental brain research, 149*(2), 260-266.

Zhang, L. Q., & Rymer, W. Z. (1997). Simultaneous and nonlinear identification of mechanical and reflex properties of human elbow joint muscles. *IEEE Trans Biomed Eng, 44*(12), 1192-1209. https://doi.org/10.1109/10.649991

VITA

Ahyoung Song earned a Bachelor of Health Science degree in Physical Therapy from Korea University in Seoul, Korea. Following her undergraduate study, she earned a Master of Science degree in Rehabilitation Science from Korea University in Seoul, Korea. Upon completion of her master's degree, she worked as a physical therapist in National Health Insurance Service (NHIS) Ilsan Hospital, Goyang, Korea, for three years. She also worked as an instructor in Daewon University College, Jecheon, Korea, and in Kyungbuk College, Yeongju, Korea, teaching medical terminology, motor control, and diagnosis and evaluation in physical therapy for musculoskeletal disease. In 2016, She started her Ph.D. study in the School of Kinesiology, Louisiana State University, with an emphasis on biomechanics. While at LSU, Ahyoung worked as a graduate assistant teaching Biomechanical Basis of Kinesiology and a teaching assistant for Principles of Conditioning. She is scheduled to graduate from Louisiana State University with her Doctor of Philosophy degree in Kinesiology in August 2021. Ahyoung begins her career as a post-doctoral research fellow in Arnold School of Public Health at the University of South Carolina, Columbia, South Carolina.